

Road noise prediction

2 -Noise propagation computation method
including meteorological effects (NMPB 2008)



Ressources, territoires et habitats
Énergie et climat Développement durable
Prévention des risques Infrastructures, transports et mer

Présent
pour
l'avenir



RÉPUBLIQUE FRANÇAISE



Technical Department of the Ministry of Ecology, Energy Sustainable Development and the Sea, Sétra, is an engineering and expertise reference in the fields of transport, road infrastructure and engineering structures.

The Sétra supports the public owner

The Sétra supplies State agencies and local communities (counties, large cities and urban communities) with informations, methodologies and tools suited to the specificities of the networks in order to:

- improve the projects quality;
- help with the asset management;
- define, apply and evaluate the public policies;
- guarantee the coherence of the road network and state of the art;
- put forward the public interests, in particular within the framework of European standardization;
- bring an expertise on complex projects.

The Sétra, producer of the state of the art

Within a very large scale, beyond the road and engineering structures, in the field of transport, intermodality, sustainable development, the Sétra:

- takes into account the needs of project owners and prime contractors, managers and operators;
- fosters the exchanges of experience;
- evaluates technical progress and the scientific results;
- develops knowledge and good practices through technical guides, softwares;
- contributes to the training and information of the technical community.

The Sétra, a work in partnership

- The Sétra associates all the players of the French road community to its action: operational services; research organizations; Scientific and Technical Network (Réseau Scientifique et Technique de l'Équipement – RST), in particular the **Public Works Regional Engineering Offices (Centres d'Études Techniques de l'Équipement – CETE)**, companies and professional organizations; motorway concessionary operators; other organizations such as French Rail Network Company (Réseau Ferré de France – RFF) and French Waterways Network (Voies Navigables de France - VNF); Departments like the department for Ecology and Sustainable Development...
- The Sétra regularly exchanges its experience and projects with its foreign counterparts, through bilateral co-operations, presentations in conferences and congresses, by welcoming delegations, through missions and expertises in other countries. It takes part in the European standardization commissions and many authorities and international working groups. The Sétra is an organization for technical approval, as an EOTA member (European Organisation for Technical Approvals).

Methodologic guide

Road noise prediction

2 -Noise propagation computation method
including meteorological effects (NMPB2008)





This methodological guide to calculating road noise propagation including the meteorological effects has been written by a working group led by Francis Besnard then Emmanuel Le Duc (SETRA). The members of the group are:

- François Abbaléa (CSTB)
- Savine Andry (Cete Nord Picardie – LRPC, Lille)
- Marine Baulac (CSTB)
- Michel Bérengier (LCPC)
- Bernard Bonhomme (Cete Normandie Centre – LRPC, Blois)
- Jérôme Defrance (CSTB)
- Jean Pierre Deparis (Cete Nord Picardie – LRPC, Lille)
- Guillaume Dutilleux (CETE, Est - LRPC, Strasbourg - Noise Resource Team)
- David Ecotière (CETE, Est - LRPC, Strasbourg - Noise Resource Team)
- Benoît Gauvreau (LCPC)
- Vincent Guizard (SETRA)
- Fabrice Junker (EDF)
- Hubert Lefèvre (CETE, Lyon - LRPC, Clermont-Ferrand)
- Vincent Steimer (CETE, Est - LRPC, Strasbourg - Noise Resource Team, then CERTU)
- Dirk Van Maercke (CSTB)
- Vadim Zouboff (CETE Ouest – LRPC, Angers)

This guide has been reviewed and validated by the following Central Administration Departments of the Ministry of Ecology, Energy, Sustainable Development and Regional Development:

- General Risk Prevention Department (DGPR/Noise Mission and Physical Agents),
- the Transport Infrastructure Division of the General Infrastructure, Transport and Sea Division (DGITM/DIT).

We should like to thank everyone whose remarks and comments have helped finalise this document.

Contents

Foreword	6
1 Introduction	7
1.1 Purpose	7
1.2 Scope	7
1.3 Document structure	8
2 Definitions and notations	9
2.1 General	9
2.2 Definitions	9
2.3 Notations	10
3 Method overview	12
3.1 Sound level in downward-refraction conditions ($L_{i,F}$) for the path (S_i, R)	12
3.2 Sound level in homogeneous conditions ($L_{i,H}$) for the path (S_i, R)	13
3.3 Long-term sound level for the path (S_i, R)	13
3.4 Long-term sound level at point R for all trajectories	14
3.5 Long-term sound level at point R ($dB(A)$)	14
4 Description of the source	15
4.1 Breakdown of sources	15
4.2 Sound emission data on entry	16
5 Taking the micrometeorology into account	18
5.1 Method for estimating the ‘long-term sound level’	18
5.2 Determining meteorological occurrence values	19
6 Propagation analysis	22
6.1 Receiver	22
6.2 Elementary propagation trajectories	22
7 Calculations in an elementary path	27
7.1 Geometrical spreading	27
7.2 Atmospheric absorption	27
7.3 Ground effect	27
7.4 Diffraction	31
7.5 Vertical edges	37
7.6 Reflections in the vertical obstacles	37
7.7 Special elements	38

8 Bibliography	39
8.1 Articles	39
8.2 Standards	39
8.3 Notes	39
8.4 Books	40
8.5 Reports	40
8.6 PhD theses	41
A Calculation method flow chart	43
B Occurrence values and maps of downward-refraction conditions for France	46
B.1 Occurrences over two periods	48
B.2 Occurrences over three periods	50
B.3 Occurrence roses	53
B.4 Maps	60
C Meteorology and sound propagation	64
C.1 Atmospheric absorption	64
C.2 Effects of wind and temperature	64
D Meteorological analysis of an acoustic situation	72
D.1 Opening remarks	72
D.2 Spatio-temporal averages and scales	72
D.3 Meteorological analysis of an acoustic situation	75
E Geometric aspects	80
E.1 Fermat's principle	80
E.2 Ellipsoid and weighting by Fresnel zone	81
F Dealing with special elements	83
G Validation elements	100
H Description of the sites of the experimental campaigns	103
H.1 Mulhouse	103
H.2 Massiac	103
H.3 Mer	104
H.4 Couvron	104
H.5 Molsheim	105
H.6 Saint Omer	105
I Sample NMPB-Roads-2008 applications	107

I.1	Site in slight cut	107
I.2	Site in large cut	119
I.3	Site in fill with low screen	127
I.4	Site with multiple diffraction	133
J	From the NMPB-Roads-96 to the NMPB-Roads-2008	136

Foreword

The new version of the noise prediction method, 'NMPB 2008', is the calculation method dealing with the propagation of sound emissions that updates the 1996 version. It is intended for departments responsible for the sound part of studies for development projects or projects to correct what already exists (resorption of noise black spots).

The method published in 1996 was already an attempt at a compromise between accuracy, calculation time and data collection efforts. It was also adopted as a reference method to be used under Directive 2002/49/EC relating to the assessment and management of environmental noise in anticipation of a harmonised European method.

The aim of this document is to present the new method and its improvements.

The NMPB 2008 is the result of work by Sétra, the *Laboratoire Régional des Ponts et Chaussées* at Strasbourg, Clermont Ferrand, Lille and Blois, the *Laboratoire Central des Ponts et Chaussées* (Central Highways Laboratory), the *Centre Scientifique et Technique du Bâtiment* (Scientific and Technical Building Centre) and EDF. It attempts to answer questions left hanging by the previous method whilst incorporating technical and scientific progress. The main changes lie in seeking greater consistency in the ground effect calculations and in taking the meteorology into account by exploiting data collected over long periods.

The new version has undergone rigorous testing and adjustment based on very complete measurement campaigns over a wide range of actual cases representative of the majority of situations encountered by the highway engineers. The highly-significant advances and improvements contribute to new, decisive progress; the support of the design and research departments has been essential to this progress.

Although major in terms of method reliability, these changes do not raise usage problems for the departments involved, the acoustic design offices or software program publishers, as the spirit of the previous version has been maintained.

This document on noise propagation supplements the recently-updated emission calculation methods published in 1981 and thus completes the revision of road noise prediction methods. A further publication will cover a railway section.

So that the highways departments can take immediate advantage of this progress, I have asked that the road section be published and be considered henceforth as the reference tool for road traffic noise prediction within the Ministry departments. This method should also help improve the future European Commission tools.

Transport Infrastructure Director



Marc Papinutti

1-Introduction

The Road Noise Prediction Method is broken down into two documents:

- The first entitled ‘Calculation of sound emissions from road traffic’, used to associate sound power with traffic in an infrastructure [[Abaques 2008](#)];
- The second entitled ‘NMPB 2008 - Noise propagation method included meteorological effects’. It is used to calculate the long-range noise level generated by an infrastructure represented by its sound emissions. This is the document presented here.

1.1-Purpose

This methodological guide describes an updated calculation method for the propagation of road noise outdoors which can be used, in accordance with the requirements of the French regulations, to calculate the sound level of roads far away and take the effects of meteorological conditions into account. This involves revising the NMPB-Roads-96, which becomes known as NMPB-Roads-2008.

The NMPB-Roads-2008 does not question the principle of a detailed calculation of long-term sound levels in two, clearly distinct types of meteorological conditions:

- downward-refraction conditions
- homogeneous conditions.

The final result is always obtained by an energy accumulation of the sound levels noted in these two types of condition, weighted by the probability of occurrence of downward-refraction conditions on the site in question and its counterpart. This comes down to reconstructing a variation profile for atmospheric conditions over a long period, by assimilating the upward-refraction conditions to propagation (where the least noise is received) with homogeneous conditions, which tend to protect local residents better.

The calculation method described here, therefore, is not intended to simulate all meteorological conditions potentially observed on a site but to get close by representing them by two conventional atmospheric situations.

1.2-Scope

The calculation method described here was basically developed to offer Design Offices, motorway companies and the MEEDDM¹ departments (SIR, SMO, CETE, LRPC) a forecasting tool for sound levels which takes the effects of meteorological conditions into account.

The calculation distance validity limit is 800 m perpendicular to the infrastructure and a receiver more than 2 m above the ground. The distance validity field increases when the receiving point is higher off the ground

This document explains a detailed calculation method. The calculations are made by third-octave bands, from 100 Hz to 5 kHz. The method is based on breaking down sources into point sources. Its manual, non-computerised use will therefore be extremely limited.

The method is used to calculated sound levels L_{Aeq} over two periods, Day (06.00-22.00) and Night (22.00-06.00), or over three periods, Day (06.00-18.00), Evening (18.00-22.00) and Night (22.00-06.00), depending on the application.

As its French name indicates, the NMPB-Roads-2008 only deals with road noise. Nevertheless, the method can easily be adapted subsequently to railway and industrial noise.

¹ Ministère de l’Ecologie, de l’Energie, du Développement Durable et de la Mer (*Ministry of Ecology, Energy, Sustainable Development and the Sea*).

1.3 - Document structure

The document's contents are structured as follows:

- Chapter 2 assembles the general definitions, vocabulary, parameters and physical entities used in the NMPB-Roads-2008;
- Chapter 3 gives an overview of the method. The detailed flow chart for the method is given in Appendix A;
- Chapter 4 explains how to represent an infrastructure by one or more source lines and how to break a road source line down into point sources. Secondly, this chapter gives the parameters required to calculate the power in accordance with [Abaques 2008];
- Chapter 5 describes taking the micrometeorology of the site to be processed into account. Various means of estimating probabilities of occurrence of downward-refraction conditions are proposed. This chapter is supplemented by Appendix B which assembles the tabulated occurrences for 41 meteorological stations spread across the whole of France. The reader will find additional information on the effects of micrometeorology on sound propagation in Appendix C. For greater detail or ‘advanced’ use, Appendix D provides additional information on analysing a meteorological situation;
- Chapter 6 addresses the notion of elementary path between source and receiver and identifies elementary trajectories in 3D. Additional information on the geometric aspects of the propagation is given in Appendix E;
- Chapter 7, which specifies the attenuation calculation in an elementary path, is the core of the NMPB-Roads-2008. It is supplemented by Appendix F which deals with particular elements;
- Appendix G analyses statistically the results of the comparison between the NMPB-Roads-2008 and experimental campaigns on sites with complex topography;
- Appendix H describes the sites chosen for the measurement campaigns;
- For those who wish it, either to test their understanding of the NMPB-Roads-2008 or to implement the method, Appendix I provides sample applications for different cross sections;
- Users already familiar with the NMPB-Roads-96 will find a list of changes introduced by the NMPB-Roads-2008 in Appendix J.

2-Definitions and notations

2.1-General

All distances, heights, dimensions and elevations used in this document are expressed in metres (m).

The notation MN stands for the distance between the points M and N , measured along the straight line joining them.

The notation \widehat{MN} stands for the length of the curve path between the points M and N , in downward-refraction conditions (*Cf.* Section C.2.1.2).

It is customary for heights measured vertically in relation to the ground to be noted with the letter h ; the equivalent heights measured orthogonally in relation to the mean ground plane (*Cf.* Section 7.3.1) are noted with the letter z .

The sound levels, noted by the capital letter L , are expressed in dB by third-octave band when index A is omitted. The sound levels in dB(A) are given with the subscript A.

2.2-Definitions

The sum of sound levels due to mutually incoherent sources is noted by the sign \oplus in accordance with the following definition:

$$L_1 \oplus L_2 = 10 \log_{10} \left(10^{L_1/10} + 10^{L_2/10} \right) \quad (2.1)$$

Homogenous atmospheric conditions (or ‘homogeneous conditions’): all atmospheric conditions resulting in a homogenous atmosphere in terms of sound propagation. In these conditions, the acoustic energy propagates in a straight line (*Cf.* Section C.2.1.3 for a physical explanation).

Atmospheric conditions favouring sound propagation (or ‘downward-refraction conditions’): all atmospheric conditions causing a drop in acoustic energy towards the ground and producing sound levels at the receiver higher than those noted in homogeneous conditions (*Cf.* Section C.2.1.2 for a physical explanation).

Atmospheric conditions unfavourable to sound propagation (or ‘upward-refraction conditions’): all atmospheric conditions causing a rise in acoustic energy towards the sky and producing sound levels at the receiver lower than those noted in homogeneous conditions (*Cf.* Section C.2.1.1 for a physical explanation).

Direct path: straight line linking the source S and the receiver R (*Cf.* Figure 7.1).

2.3-Notations

α	Coefficient of atmospheric attenuation (dB/km).
α_r	Coefficient of acoustic absorption of the wall of an obstacle.
δ	Path length difference (m) occurring in the diffraction calculations.
δz_s	Source height correction in downward-refraction conditions (m).
δz_r	Receiver height correction in downward-refraction conditions (m).
δz_T	Height correction due to turbulence in downward-refraction conditions (m).
λ	Wavelength (m) at the nominal median frequency f_m of a given third-octave band: $\lambda = c/f_m$.
Γ	Radius of curvature (m) of the propagation path in downward-refraction conditions.
Δ_{dif}	Attenuation due the pure diffraction (<i>i.e.</i> without taking the ground effects into account) (dB).
A_{atm}	Attenuation due to the atmospheric absorption in a given third-octave band (dB).
$A_{dif,F}$	Attenuation due to the diffraction in downward-refraction conditions in a given third-octave band (dB).
$A_{dif,H}$	Attenuation due to the diffraction in homogeneous conditions in a given third-octave band (dB).
A_{div}	Attenuation due to the geometric divergence (dB).
$A_{i,F}$	Attenuation due to the propagation between S_i and R in downward-refraction conditions in a given third-octave band (dB).
$A_{i,H}$	Attenuation due to the propagation between S_i and R in homogeneous conditions in a given third-octave band (dB).
$A_{sol,F}$	Attenuation due to the ground effect in downward-refraction conditions in a given third-octave band (dB).
$A_{sol,H}$	Attenuation due to the ground effect in homogeneous conditions in a given third-octave band (dB).
A_{talus}	Attenuation due to the embankment (dB).
c	Celerity of the sound in the air, taken equal to 340 m/s.
d	Direct distance between two points, without taking into account potential obstacles between these two points (m). Without reflection, it is the length of the direct path (<i>Cf.</i> Figure 7.1). When an obstacle is reflected, it is the total length of the path with no diffracting obstacles.
d_p	Propagation distance between two points (m). This is the projection length of the SR segment in the mean ground plane perpendicular to it (see Figure 7.1).
e	Distance between the extreme diffraction points under multiple diffractions (m).
f_m	Nominal median frequency of a given third-octave band (Hz). Possible values: {100, 125, 160, 200, 250, 315 400, 500, 630, 800, 1000, 1250, 1600, 2000, 2500, 3150, 4000, 5000}.
G	Dimensionless ground coefficient between 0 and 1. Characterises the acoustic absorption of a ground.
G_{talus}	Average ground coefficient of embankment at the edge of the road.
G_{trajet}	Ground coefficient along a propagation path.
G'_{trajet}	Equivalent ground coefficient along a propagation path.
h_0	Pgreatest of two heights of the diffraction edge compared with each of two mean ground planes source side and receiver side.
h_r	Height of R above the ground (m) (see Figure 7.1).
h_s	Height of S above the ground (m) (see Figure 7.1).
I	Reflection point on the bank (see Figure 7.3).
k	Wave number for a given octave band (m^{-1}): $k = 2\pi f_m/c$
L_{AeqLT}	Global long-term sound level L_{Aeq} due to all sources and image sources at point R (dB(A)).
$L_{eq,LT}$	Long-term sound level L_{eq} due to all sources and image sources at point R in a given third-octave band (dB(A)).
$L_{i,F}$	Sound level L_{eq} due to source S_i at point R in downward-refraction conditions in a given third-octave band (dB).

$L_{i,H}$	Sound level L_{eq} due to source S_i at point R in homogeneous conditions in a given third-octave band (dB).
L_{Awi}	Sound power level of a source S_i in a given third-octave band (dB(A)).
$L_{W/mVL}$	Sound power level per unit of length for a flow rate of one light vehicle/hour (dB/m).
$L_{W/mPL}$	Sound power level per unit of length for a flow rate of one HGV/hour (dB/m).
O	Diffraction point.
p	Probability of occurrence of downward-refraction conditions over a long-term period in a given direction, $p \in [0, 1]$.
p_i	Probability of occurrence of downward-refraction conditions in a long-term period in the direction of the direct path between S_i and R .
Q_{PL}	Hourly HGV flow rate, in vehicles/hour.
Q_{VL}	Hourly light vehicle flow rate, in vehicles/hour.
R	Receiving point.
R'	Image receiver.
S	Point source.
S_i	Point source of index i in a source line.
S'	Image source in relation to the mean ground plane.
S''	Image source in relation to the bank plane.
$z_{o,r}$	Equivalent height of O measured perpendicular to the mean ground plane receiver side (m) (see Figure 7.4).
$z_{o,s}$	Equivalent height of O measured perpendicular to the mean ground plane source side (m) (see Figure 7.4).
z_r	Equivalent height of R measured perpendicular to the mean ground plane (m) (see Figure 7.1).
z_s	Equivalent height of S measured perpendicular to the mean ground plane (m) (see Figure 7.1).

3-Method overview

For a receiver R , the calculations are performed according to the following steps (*Cf.* Figure A.1):

1. breakdown of the noise sources into sound point sources (*Cf.* Section 4.1);
2. determination of the sound power level of each source (*Cf.* Section 4.2);
3. calculation of the probability of occurrence of downward-refraction conditions for each direction (S_i, R) (*Cf.* Chapter 5);
4. search for propagation trajectories between each source and the receiver - direct, reflected and/or diffracted paths - (*Cf.* Chapter 6);
5. in each propagation path (*Cf.* Chapter 7):
 - calculation of the attenuation in downward-refraction conditions;
 - calculation of the attenuation in homogeneous conditions;
 - calculation of the long-term sound level for each path and the occurrence of downward-refraction conditions;
6. accumulation of long-term sound levels for each path, used therefore to calculate the total sound level at the receiving point (*Cf.* Section 3.3).

It will be accepted that only the attenuations from the ground effect (A_{sol}) and the diffraction (A_{dif}) are affected by the meteorological conditions (*Cf.* Figure A.1).

When this method is used for legal purposes, such as applying the French order of 5 May 1995, the calculation hypotheses adopted must be representative of an average annual situation (traffic, ground, atmosphere).

For a *sound point source* S_i of power L_{Awi} and for a *given third-octave band*, the equivalent continuous sound level in a receiving point R in *given atmospheric conditions* will be obtained with the following formulae.

3.1-Sound level in downward-refraction conditions ($L_{i,F}$) for the path (S_i, R)

$$L_{i,F} = L_{Awi} - A_{i,F} \quad (3.1)$$

The term $A_{i,F}$ represents the total attenuation along the propagation path in downward-refraction conditions and is broken down as follows:

$$A_{i,F} = A_{div} + A_{atm} + A_{front,F} \quad (3.2)$$

where

- A_{div} is the attenuation due to the geometrical spreading (*div* stands for divergence);
- A_{atm} is the attenuation due to the *atmospheric* absorption;
- $A_{front,F}$ is the attenuation due to the *boundary*¹ of the propagation medium in downward-refraction conditions. It can contain the following terms:
 - $A_{sol,F}$ which is the attenuation due to the *ground*¹ in downward-refraction conditions;
 - $A_{dif,F}$ which is the attenuation due to the *diffraction* in downward-refraction conditions;
 - A_{talus} which is the attenuation due to the reflection on the cut *bank*¹.

¹ *front* is a short-cut for *frontière* which means boundary, *sol* means ground, *talus* is the French word for embankment.

The following two scenarios are possible for a given path and third-octave:

- $A_{sol,F}$ and A_{talus} ($A_{dif,F}=0$ dB) are calculated with no diffraction:
 - if there is no bank (*Cf.* Section 7.3.5), then $A_{talus}=0$ dB and $A_{front,F}=A_{sol,F}$;
 - otherwise $A_{sol,F}$ and A_{talus} must be calculated and $A_{front,F}=A_{sol,F}+A_{talus}$;
- or $A_{dif,F}$ ($A_{sol,F}=0$ dB and $A_{talus}=0$ dB) are calculated. The ground effect and any embankment are taken into account in the formula of $A_{dif,F}$ itself. This therefore gives $A_{front,F}=A_{dif,F}$.

3.2 - Sound level in homogeneous conditions ($L_{i,H}$) for the path (S_i, R)

The approach is strictly identical to the downward-refraction conditions case presented in the previous section.

$$L_{i,H} = L_{Awi} - A_{i,H} \quad (3.3)$$

The term $A_{i,H}$ represents the total attenuation along the propagation path in homogeneous conditions and is broken down as follows:

$$A_{i,H} = A_{div} + A_{atm} + A_{front,H} \quad (3.4)$$

where

- A_{div} is the attenuation due to the geometric *divergence*;
- A_{atm} is the attenuation due to the *atmospheric* absorption;
- $A_{front,H}$ is the attenuation due to the *boundary* of the propagation medium in homogeneous conditions. It can contain the following terms:
 - $A_{sol,H}$ which is the attenuation due to the *ground* in homogeneous conditions;
 - $A_{dif,H}$ which is the attenuation due to the *diffraction* in homogeneous conditions;
 - A_{talus} which is the attenuation due to the reflection on the cut *bank*.

The following two scenarios are possible for a given path and third-octave:

- $A_{sol,H}$ and A_{talus} ($A_{dif,H}=0$ dB) are calculated with no diffraction:
 - if there is no bank (*Cf.* Section 7.3.5), then $A_{talus}=0$ dB and $A_{front,H}=A_{sol,H}$;
 - otherwise $A_{sol,H}$ and A_{talus} must be calculated and $A_{front,H}=A_{sol,H}+A_{talus}$;
- or $A_{dif,H}$ ($A_{sol,H}=0$ dB and $A_{talus}=0$ dB) are calculated. The ground effect and any embankment are taken into account in the formula of $A_{dif,H}$ itself. This therefore gives $A_{front,H}=A_{dif,H}$.

3.3 - Long-term sound level for the path (S_i, R)

The ‘long-term’ sound level due to the point source i is obtained by energy summing of the sound level in homogeneous conditions and the sound level in downward-refraction conditions. These sound levels are weighted by the average occurrence p_i of downward-refraction conditions in the direction of the path (S_i, R) (*Cf.* Section 5.1):

$$L_{i,LT} = 10 \log_{10} \left(p_i 10^{L_{i,F}/10} + (1-p_i) 10^{L_{i,H}/10} \right) \quad (3.5)$$

Determining average occurrences p_i is described in Section 5.2.

3.4-Long-term sound level at point R for all trajectories

The total sound level at the receiver for a given third-octave band is obtained by summing sound contributions from all the point sources and their potential image sources:

$$L_{eq,LT} = 10 \log_{10} \left(\sum_i 10^{0.1L_{i,LT}} + \sum_{i'} 10^{0.1L_{i',LT}} \right) \quad (3.6)$$

where:

- i represents all the point sources;
- i' all the image sources corresponding to reflections in vertical obstacles.

Taking reflections into account through image sources is described in Section 7.6. The percentage of occurrences of downward refraction conditions for a path reflected in a vertical obstacle will be taken as identical to the direct path: if S_i is the image source of p_i , then the occurrence (S'_i, R) of the path p_i is taken as equal to the occurrence (S_i, R) of the path (S_i, R) .

3.5-Long-term sound level at point R (dB(A))

The total sound level in dB(A) is obtained by summing levels in each third-octave band² :

$$L_{Aeq,LT} = 10 \log_{10} \left(\sum_{j=1}^{18} 10^{0.1L_{eq,LT}(j)} \right) \quad (3.7)$$

where j is the index of eighteen third-octave bands from 100 to 5000 Hz.

This level $L_{Aeq,LT}$ constitutes the final result, i.e. the *long-term sound level* at the receiving point.

² The weighting A is taken into account directly in the power level L_{Awi} .

4-Description of the source

A surface transport infrastructure considered as a source of noise presents specific features due to:

- its linear geometry - the term used is ‘source line’ - and the distribution of the sound power over the width of the traffic lanes;
- the variability in its sound emission over the length of the itinerary.

The source has to be modelled to calculate the sound level generated by such an infrastructure. The model adopted here is based on breaking down the infrastructure into sound point sources.

4.1- Breakdown of sources

4.1.1 - Notion of acoustically-homogenous section

In the first instance, the sections (or ‘arcs’ in geomeric terms) must be determined, where it can be considered that:

1. there is no or little variation in the sound emission [[Abaques 2008](#)];
2. the geometry of the road cross section does not vary. The same model can therefore be used as for breaking down the source line into elementary sources.

The infrastructure studied is thus broken down into as many acoustically-homogenous sections as necessary.

4.1.2 - Extent of source lines

The infrastructure is represented by source lines. Each source line must comply with the following constraints for each receiver:

- the ratio between the distance to the furthest point source and the distance to the nearest point source must be greater than or equal to 10;
- the distance to the furthest point source must be greater than or equal to 200 m.

4.1.3 - Position of source lines

The infrastructure is represented by a certain number of source lines. The number and position of these source lines depends on the accuracy sought. When there is no limitation to the number of calculations to be performed, a source line will be positioned in the centre of each traffic lane (*Cf. Figure 4.1*).

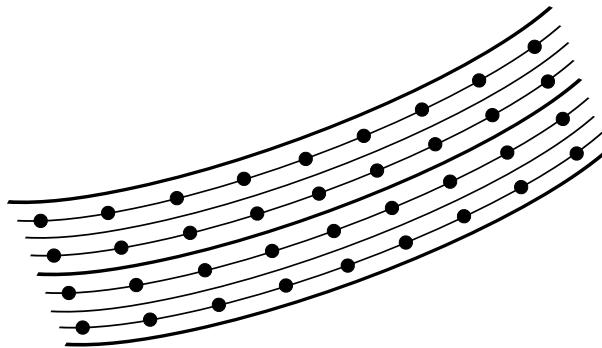


Figure 4.1: Optimum position of source lines for a dual-carriageway.

Depending on the distance to the road and the propagation conditions, each traffic direction can also be represented by a source line placed in the centre of the roadway in each direction, or the entire infrastructure can even be represented by a single source line placed in the road axis. This option is only valid if the road platform is not too wide and if the receiving point is sufficiently far from the road.

It is advisable in all cases to place a source line in the centre of each traffic lane; this becomes mandatory when there is diffraction or when the traffic is highly assymetric between the two traffic directions.

4.1.4 - Breakdown of source lines into elementary point sources

Each source line defined beforehand is broken down into a set of sound point sources. Each point source is placed 0.05 above the roadway. This breakdown can be achieved in several ways:

Equiangular breakdown: the site is swept from the receiving point in question by a set of rays spaced at a constant angle. A source point is placed every time one of these rays intersects a source line¹. With this method, the breakdown of a source line depends on the receiving point in question. In all cases, the angular pitch of the sweeping will be less than 10° (*Cf. Figure 4.2*). When there is a source line segment non-symmetrical to the perpendicular passing through the receiver, the angular pitch must be lower than or equal to 5° . When there is a source segment which does not cut the perpendicular passing through the receiver, the angular pitch must be lower than or equal to 2° .

Equidistant breakdown: each source line is broken down into point sources at regular intervals. To maintain accuracy, the pitch between two consecutive sources must not be greater than half the orthogonal distance between the road and the closest receiving point, without however exceeding 20 m. Here, the same breakdown is valid for all the receivers considered.

Variable breakdown: in some circumstances, particularly when receiving points are close to the road in partially masked view, it may be necessary to modify the breakdown into point sources locally by tightening the pitch between two consecutive sources¹.

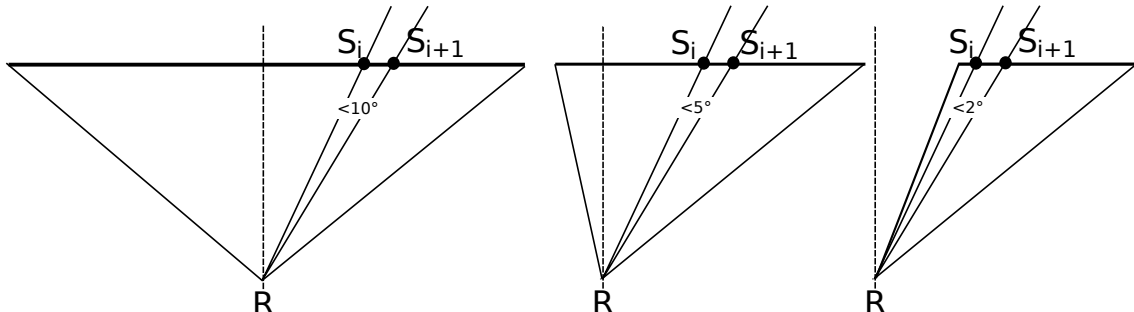


Figure 4.2: Equiangular breakdown - maximum angle of discretisation based on the angle of view.

4.2 - Sound emission data on entry

The sound power level L_{Awi} in dB(A) of an elementary point source i for a given third-octave band is obtained from values provided in [Abaques 2008] by applying the following formula:

$$L_{Awi} = [(L_{W/m VL} + 10 \log_{10} Q_{VL}) \oplus (L_{W/m PL} + 10 \log_{10} Q_{PL})] + 10 \log_{10} l_i + R(j) \quad (4.1)$$

where

- $L_{W/m VL}$ and $L_{W/m PL}$ are power levels per unit of length, as defined in [Abaques 2008], for light vehicles and HGV respectively. These levels depend on the formulation of the roadway surface, its age, the gradient and the speed of vehicles;

¹ In the case of equiangular or variable pitch breakdown, the sound power level of each source L_{Awi} varies.

- Q_{VL} and Q_{PL} are the hourly flow rates for light vehicles and HGV respectively, representative of the period considered;
- l_i is the length in metres of the portion of source line represented by the point source i (*Cf.* Figure 4.3):

$$l_i = 1/2(S_{i-1}S_i + S_iS_{i+1}) \quad (4.2)$$

- $R(j)$ is the value of the road noise spectrum standardised at 0 dB and A-weighted, as defined in [Abaques 2008]. The spectrum should be chosen based on the roadway surface, between ‘Drainage’ and ‘non-Drainage’.

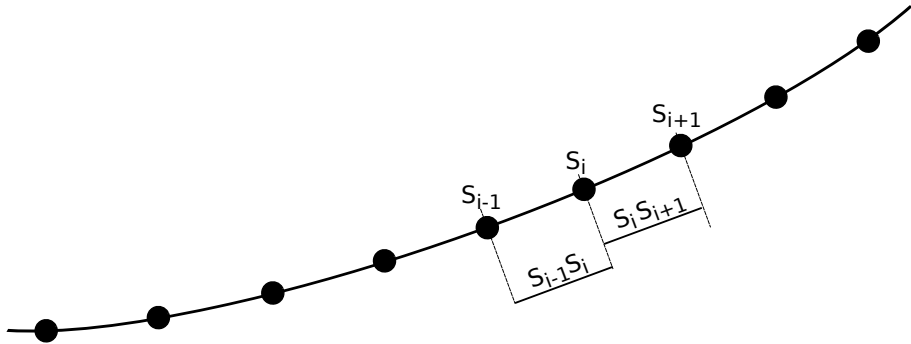


Figure 4.3: Notations for calculating the length of the source represented by a point source.

5-Taking the micrometeorology into account

5.1-Method for estimating the ‘long-term sound level’

The method involves calculating the sound levels in two typical propagation conditions (defined in Appendix C):

- *downward-refraction conditions*: levels noted L_F . These calculated levels are not ‘extreme’ levels, but correspond in a way to an average of levels observed in conditions tending to favour propagation. In the NMPB-Roads-2008, these downward-refraction conditions relate to a vertical sound speed gradient of 0.07/s;
- *homogeneous conditions*: levels noted L_H . Although rarely encountered in reality, these conditions are the simplest to model as the sound rays are therefore straight. Road noise was normally calculated assuming a homogeneous atmosphere before the order of 5 May 1995 was published.

No simple operational model currently exists to calculate the sound levels in ‘upward’ refraction conditions. To assess the long-term sound levels, taking into account all the meteorological conditions encountered on the site, the current method replaces the sound levels in ‘upward-refraction conditions’ by an upper bound represented by sound levels in ‘homogeneous conditions’. This initial assumption overestimates the actual sound levels obtained in these propagation conditions, but tends to protect local residents better.

The long-term level is therefore calculated through the energy sum of levels L_F and L_H , weighted respectively by the probability of occurrence of downward-refraction conditions on the site and the complementary probability:

$$L_{LT} = 10 \log_{10} \left(p 10^{L_F/10} + (1-p) 10^{L_H/10} \right) \quad (5.1)$$

where p is the probability of occurrence of downward-refraction conditions in the long term. p is therefore between 0 and 1. This formula is illustrated by the Figure 5.1, where it is considered that the level L_F reigns during the fraction p of the time and the level L_H during the complementary fraction $1-p$ of the time.

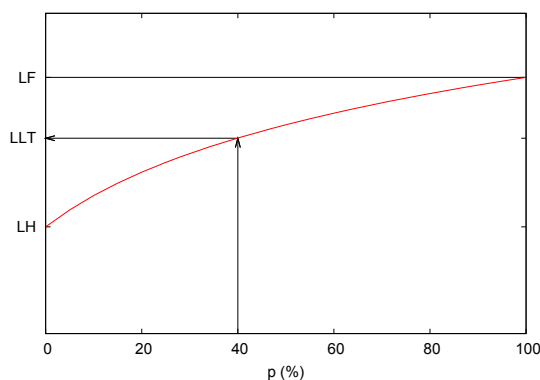


Figure 5.1: Calculation principle for the long-term sound level according to the probability of occurrence p (%). For example, the level L_{LT} obtained for an occurrence of downward-refraction conditions equal to 40% is shown.

On a given site, this probability of occurrence of downward-refraction conditions depends on the receiver-source direction, as these conditions depend in particular on wind direction. The formula above must therefore be applied for each ‘elementary source-receiver’ pair, the global long-term level at the receiver being the energy sum of long-term contributions from each elementary source (*Cf. Section 3.4*).

The probability of occurrence of downward-refraction conditions is therefore required, on the studied site, for all the source-receiver propagation directions for the calculation.

5.2 - Determining meteorological occurrence values

5.2.1 - Possible simplifications

Before embarking on certain particularly onerous actions to determine the probabilities of occurrence of downward-refraction conditions, it may prove judicious to evaluate the issue of accuracy with which these values must be known. For example:

- if it transpires that the projected road complies, in downward-refraction conditions, with the targeted thresholds, this guarantees that these thresholds will also be respected in ‘long-term’ conditions;
- if the sound levels in downward refraction and homogenous conditions are hardly different, the inaccuracies in the knowledge of values of meteorological occurrences have little influence on the ‘long-term’ sound level.

There is no need to fine tune the meteorological analysis of the studied site in either of these cases.

Such simplifications are however only appropriate when the geometric characteristics of the projected road (path, longitudinal section, cross section) are sufficiently stable. If necessary, several options can be simulated.

5.2.2 - Occurrences calculated for Metropolitan France

Readings from 41 meteorological stations across Metropolitan France were analysed using a micrometeorological model (*Cf.* [Bru1996] and [LRS2008]). They were used to calculate the hourly series of vertical gradients for wind speed and temperature over a period of seventeen to twenty years depending on the station (1987-2007). These meteorological gradients were then used to access a statistical description of the vertical gradient of hourly sound speed and to calculate in particular the values of occurrence of downward-refraction conditions in each direction for a long-term period. The results are presented in Appendix B in three forms:

- two series of tables defining, for each meteorological station, the probabilities of occurrence (percentages) of downward-refraction conditions by 20° sectors of receiver-source direction and for different periods (06.00-22.00, 22.00-06.00) and (06.00-18.00, 18.00-22.00 and 22.00-06.00);
- 41 polar diagrams (occurrence roses) which represent for each meteorological station the probabilities of occurrence of downward-refraction conditions as a function of the receiver-source direction for four legal periods, 06.00-18.00, 18.00-22.00, 06.00-18.00 and 22.00-06.00 (*Cf.* Section B.3) ;
- 4 maps, for two receiver-source directions (0° and 90°), the lines ‘of iso-occurrence’ of downward-refraction conditions for the periods 06.00-22.00 and 22.00-06.00. These maps have been obtained by interpolation between the closest stations. They are given for information to illustrate the spatial distribution of occurrences in the region (*Cf.* Section B.4).

Reading these tables shows that overall, for a given station, the value of occurrence does not vary tremendously between two separate directions of 20°, except for sites where a prevailing wind is extremely marked. The variations based on the direction are smoothed out especially given the isotropic effect of thermal factors.

In practice, for a random elementary source-receiver path, the value of occurrence of the closest angular direction will be used, whether selected from the maps or the tables.

5.2.3 - Scope

These values can only be used for sites meeting the installation criteria for meteorological stations set by Météo-France and the assumptions required by the micrometeorological model (*Cf.* [Bru1996]) used to establish these values:

- flat, horizontal site free of trees and shrubs;
- ground covered with grass (optimum vegetation height: 10 cm);

- no large water masses (lakes, rivers);
- clear site (only obstacles less than $r/10$ are permitted in a radius r around the meteorological mast);
- site elevation less than 500 metres.

The criterion of well-clear propagation area cannot be accurately supplied. Its guiding principle is that the obstacles in the propagation area must not modify the wind speed or wind direction significantly. Major water masses are excluded given their very high thermal inertia. Sites over 500 metres altitude are excluded because the influence of the relief on the meteorological characteristics is very decisive and it is impossible to get away with extrapolating values measured in an official meteorological station on far away sites.

5.2.4 - Other cases

When a site does not meet the criteria defined in Section 5.2.3, the designer can have recourse to the various meteorological analysis options listed below:

- using local meteorological data collected specially for the needs of the project;
- using existing local meteorological data;
- adopting the values given in Appendix B;
- adopting the values pre-defined ‘by excess’.

These approaches are listed in increasing order of ease of implementation but decreasing order in terms of accuracy of results obtained.

5.2.4.1 - Using local meteorological data collected for the project

Where there is no local meteorological station representative of the studied site, experimental compilation of meteorological data can be envisaged over a far shorter time than for the ‘meteorological long term’, provided they are re-set with data from an existing station. The approach is thus as follows:

- Local simultaneous measuring of thermal (temperature, sunshine, cloud cover) and aerodynamic (wind speed and direction) characteristics of the site (*Cf.* [Zou1998] and [prNFS31110]). Ideally the measurement is taken over a minimum period in the order of two to three years. In practice, measurements over one year could be enough.
- Compilation at the closest official meteorological station, or the most representative of the studied site, of analogue information corresponding to:
 - the same period, firstly;
 - a long-term period in the meteorological sense, secondly (*i.e.* at least ten years, thirty being the optimum);
- Resetting of data measured on the site based on long-term data collected at the permanent station, to estimate the long-term meteorological characteristics specific to the studied site;
- Analysis of these characteristics (*Cf.* Section D.3.2), to estimate the occurrences of long-term downward-refraction conditions on the studied site.

This is a long and complex approach, but it provides the most accurate results of all four approaches presented here. It can only be applied in very special cases. It also, of course, requires the joint cooperation of specialists in micrometeorology and acoustics and must be planned very much in advance of the studies on the projected road. They must detail and justify the choices made for the meteorological analysis (choice of meteorological station, duration of the measuring period for meteorological magnitudes, duration of the data acquisition period of the official meteorological station, resetting method), *etc.*).

5.2.4.2 - Using existing meteorological data

There are several meteorological station networks providing usable data. The approach described here assumes that there is a meteorological station representative of the studied site. Using a station far from the studied site as a basis represents an approximation which is not without an effect on the spatial representativeness of results (*Cf.* Section D.2.1).

Collecting micrometeorological information can therefore provide access to an order of magnitude of "downward" occurrences as follows:

- The thermal (temperature, sunshine, cloud cover) and aerodynamic (wind speed and direction) characteristics are collected from a local meteorological station simultaneously for a long-term period in the meteorological sense (*i.e.* at least ten years, with thirty as the optimum). To achieve this, regional or quantitative data must be available, (*e.g.* data provided by Météo-France, *Cf.* Section D.3.2);
- Calculation of occurrences of downward-refraction conditions (*Cf.* [Zou1998] and [prNFS31110]).

This complex approaches requires assistance from specialists in micrometeorology and acoustics. They must detail and justify the choices made for the meteorological analysis (choice of meteorological station, duration of the data acquisition period of the official meteorological station, *etc.*).

5.2.4.3 - Using tabulated pre-defined values

Even if a site does not comply with the criteria given in Section 5.2.3, the values provided in Appendix B can be used. In this case, the quality of the estimated pre-defined values of occurrences of downward-refraction conditions will depend to what extent the studied site complies with these criteria. An exact description of the site listing the points of difference with these criteria is therefore necessary. In these conditions, a deliberate commitment is made to using pre-defined values which do not correspond exactly to the local 'downward refraction' conditions.

5.2.4.4 - Using values pre-defined 'by excess'

The principle here is to maximise by precaution the probability of occurrence of downward-refraction conditions, which will over-estimate the long-term levels and therefore protect the local residents better as well as over-dimension the protections with respect to legal requirements.

Metropolitan pre-defined value: for a given period, the values given in Table 5.1 will be considered as the pre-defined value, regardless of the site (metropolis) and the direction.

Period	06.00-22.00	06.00-18.00	18.00-22.00	22.00-06.00
Pre-defined occurrence	65	67	82	94

Table 5.1: Pre-defined values of probability of occurrence of downward-refraction conditions (%).

Regional pre-defined value: for a metropolitan site, a more subtle approach could be to consider, for each period and regardless of the direction, the maximum value of occurrences of downward-refraction conditions of values provided in Appendix B by the meteorological station(s) the closest to the site.

Example 5.1 Application to the town of Niort

For a site near Niort, the regional pre-defined value is obtained by taking the maximum of values of occurrences of all directions from stations in Poitiers and La Rochelle, *i.e.* $p(06.00-22.00)=52$ and $p(22.00-06.00)=71$.

6 - Propagation analysis

6.1 - Receiver

The receiving points must not be placed less than 2 m from the ground. This height must be known to the nearest 0.10 m at least to limit the uncertainty over the results, especially if diffraction is present.

By default, the method calculates sound levels ‘in a free field’, *i.e.* without taking the most recent reflection into account for a facade-mounted receiver.

To satisfy the application needs for regulations in force in terms of noise thresholds, the receivers must be placed 2 m in front of building facades. The facade effect can then be calculated:

- either by adding a pre-defined correction of + 3 dB(A) to the calculated L_{AeqLT} ;
- or by calculating the reflection using the method described in Section 7.6.

6.2 - Elementary propagation trajectories

The calculation method described here, like standard ISO 9613-2 and most official methods in Europe, is a member of the geometric method family [ISO9613p2]. These methods are based on seeking propagation trajectories between the source and the receiver. The trajectories represent the sound energy propagation trajectories.

The search for 3D propagation trajectories can become very costly, especially when reflections are produced on random sloping surfaces. Most of the time the method is preferably applied in ‘two-and-a-half dimension’ (2D1/2) mode.

The expression ‘2D1/2’ means that existing propagation trajectories between a point source and a receiver are sought in a projection of the site in a horizontal plane. Once all the propagation trajectories are identified, each one is processed in two dimensions in a vertical plane. For trajectories with reflections, the vertical planes are flattened, like an unfolding Chinese screen.

The search focuses firstly therefore on the trajectories in a plane passing through the source and the receiver. This plane is defined by the two unit orthogonal vectors \mathbf{u} and \mathbf{v} defined by:

$$\begin{cases} \mathbf{u} = \frac{1}{\|\vec{SR}\|} \vec{SR} = (u_x, u_y, u_z) \\ \mathbf{v} = (-u_y, u_x, 0) \end{cases} \quad (6.1)$$

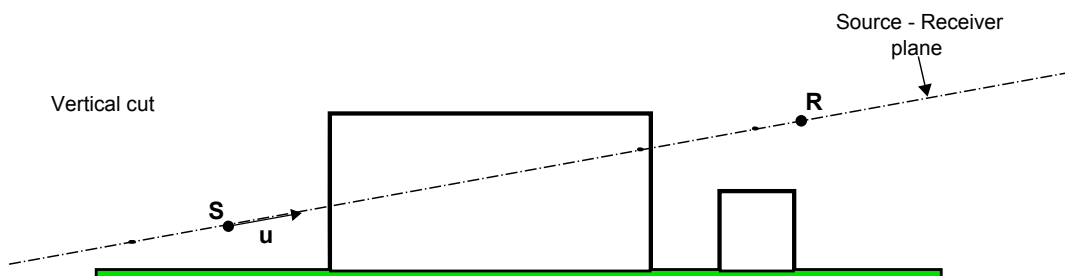


Figure 6.1: Construction of the cut plane containing the source and the receiver.

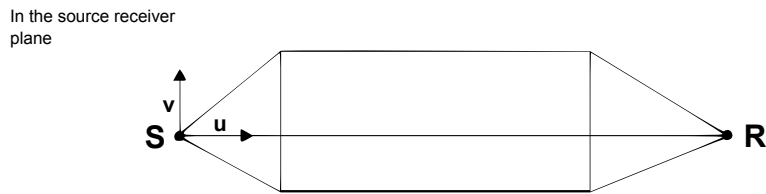


Figure 6.2: Overview of three trajectories detected in the source-receiver plane

Four types of path are normally observed. These are described in the next paragraphs.

6.2.1 - Type 1 trajectories

These are ‘direct’ trajectories from the source to the receiver - straight trajectories in plane view - which can nevertheless include diffractions in the horizontal edges of obstacles (*Cf. Figure 6.3*). These are the easiest cases to deal with.

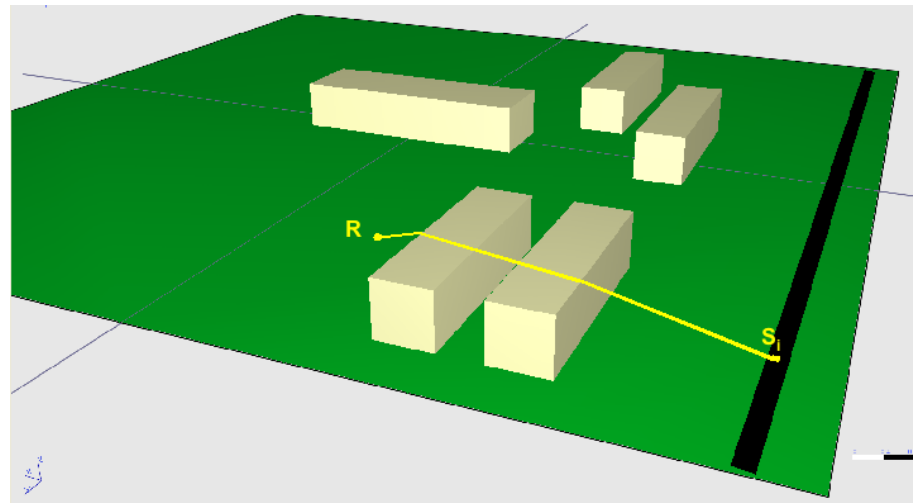


Figure 6.3: Type 1 path.

The 2D section is created in the geometry in a vertical plane passing through the identified path and is calculated in accordance with the indications in Chapter 7.

6.2.2 - Type 2 trajectories

These are trajectories reflected in vertical or slightly sloping ($<15^\circ$) obstacles, as in Figure 6.4. which can also include diffractions in the horizontal edges of obstacles (*Cf. Figure 6.5*).

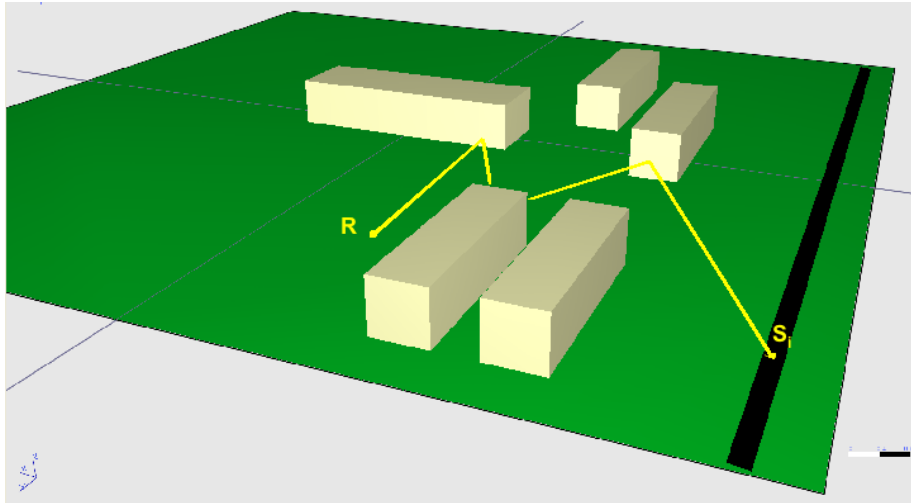


Figure 6.4: Type 2 path.

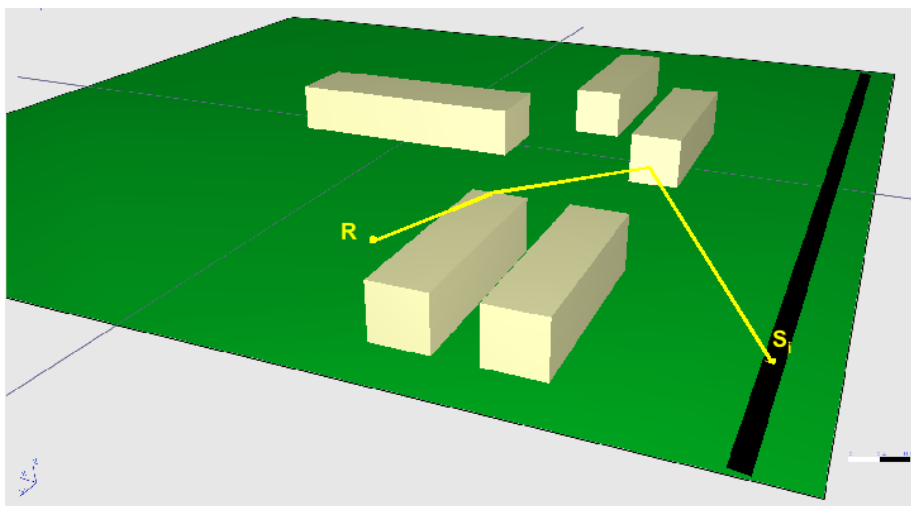


Figure 6.5: Type 2 path with diffraction on horizontal edge.

The principle is to apply the image method (*Cf. Section 7.6*). A 2D section of the geometry is produced in a succession of vertical planes passing through the straight segments located between two reflections. The section is obtained by folding these planes like a Chinese screen and the reflections are taken into account by allocating a term to the sound power which takes into account the coefficient of reflection of each vertical surface encountered. If the order equals 1, the power L'_w to be considered is obtained in accordance with formula 7.21. If the order equals 2, the power L''_w to be considered is obtained by applying formula 7.21, where L_w is replaced by L'_w and L'_w by L''_w . This continues in this fashion until the target order n is reached. The calculation is then made in the vertical 2D section in accordance with the indications in Section 7.6.

6.2.3 - Type 3 trajectories

These are trajectories diffracted by the side edges of obstacles (*Cf. Figure 6.6*).

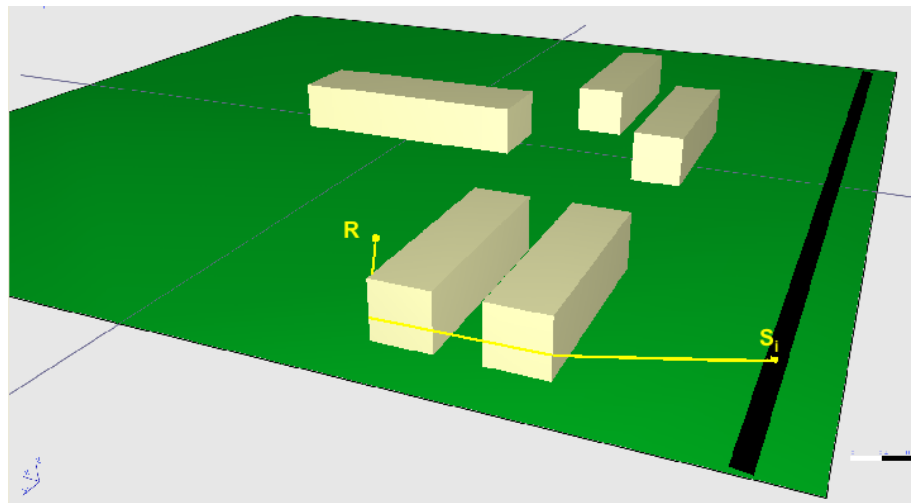


Figure 6.6: Type 3 path.

The principle is to determine each term in formula 7.17:

- The term $\Delta_{dif}(S,R)$ is obtained by calculating the path difference δ_F between the direct path and the envelope convex path of side edges in the horizontal plane;
- The terms $\Delta_{dif}(S',R)$ and $\Delta_{dif}(S,R')$ are assumed equal to $\Delta_{dif}(S,R)$
- The term $A_{sol}(S,O)$ is calculated in a vertical plane between the source and the first point O of the convex envelope of diffracting side edges;
- The term $A_{sol}(O,R)$ is calculated in a vertical plane between the source and the last point O of the convex envelope of diffracting side edges.

6.2.4 - Type 4 trajectories

These are mixed trajectories which are both diffracted by the side edges of obstacles and reflected by vertical surfaces, *i.e.* an off-vertical slope of less than 15° (*Cf.* Figure 6.7). The calculation is therefore the same as for the type 3 trajectories, with a simple correction of the source power as for the type 2 trajectories.

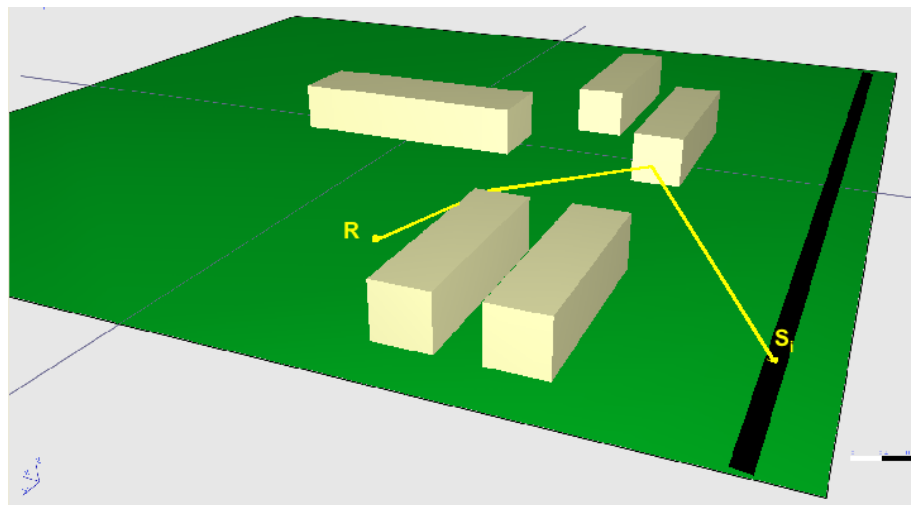


Figure 6.7: Type 4 path.

6.2.5 - Comments

- Seeking the propagation trajectories in plane view does not deal with reflections in the very sloping obstacles. Here it is no longer possible to assume that the plane-view reflection remains specular. This last hypothesis can only be considered valid up to 15° off vertical. Conversely, the reflections on the ground are taken into account in A_{front} , regardless of the gradient of the land.
- The fundamental difference between the homogeneous and upward refraction conditions is the ray bending, which are straight in homogeneous conditions and curving down towards the ground in downward refraction conditions. When seeking propagation paths in this method, especially when determining ‘points of impact’ on the ground or obstacles, the rays are taken as straight in all circumstances. Ray bending is taken into account in the formulae for calculating the ground effect and diffraction. This way of doing things complies with standard ISO 9613-2 [ISO9613p2].
- The order of multiple diffraction can be restricted consistent with the limitation of Δ_{dif} to 25 dB for the diffraction on the horizontal edges and by comparing the path difference between the side path and the ‘direct’ path (type 1) passing over obstacles.

When standardising the calculation method for complex situations, the following must be specified:

- The types of path taken into account and those ignored;
- The order of reflection taken into account based on the type of path and any related criteria;
- The order of diffraction based on the type of path and any related criteria.

It is *impossible* to compare two calculation results without this type of information.

7-Calculations in an elementary path

This chapter applies when the euclidean distance between the source and the receiver is no more than 2000 m. The other trajectories should be ignored.

7.1 - Geometrical spreading

The attenuation from the geometric divergence A_{div} takes into account the reduced sound level due to the propagation distance. For a sound point source in free field, the attenuation in dB is given by:

$$A_{div} = 20 \log_{10} d + 11 \quad (7.1)$$

where d is the direct distance in metres between the source and the receiver, *i.e.* the distance disregarding the land and any obstacles.

7.2 - Atmospheric absorption

The attenuation from atmospheric absorption A_{atm} during propagation over a distance d is given in dB by the formula:

$$A_{atm} = \alpha d / 1000 \quad (7.2)$$

where:

- d is the direct distance between the source and the receiver in metres;
- α is the coefficient of atmospheric attenuation in dB/km at the nominal median frequency of each third-octave band, in accordance with Table 7.1.

Nominal median frequency (Hz)	100	125	160	200	250	315
α (dB/km)	0.25	0.38	0.57	0.82	1.13	1.51
Nominal median frequency (Hz)	400	500	630	800	1000	1250
α (dB/km)	1.92	2.36	2.84	3.38	4.08	5.05
Nominal median frequency (Hz)	1600	2000	2500	3150	4000	5000
α (dB/km)	6.51	8.75	12.2	17.7	26.4	39.9

Table 7.1: Coefficient of atmospheric absorption per third-octave band.

The values of the α coefficient are given for a temperature of 15°C and a relative humidity of 70%. They comply with [ISO9613p1]. Using other temperature and humidity values is not allowed in the NMPB-Roads-2008 framework.

7.3 - Ground effect

The attenuation from the ground effect is mainly the result of interference between the reflected sound and the sound which propagates directly from the source towards the receiver. It is physically linked to the acoustic absorption of grounds above which the sound is propagated. But it also depends extensively on atmospheric conditions during propagation, as ray bending alters the height of the path above the ground and makes the ground effects and lands located near the source more or less significant.

7.3.1 - Significant heights above the ground

To take into account the actual topography of the land along a propagation path in the best way possible, the notion of 'equivalent height' is introduced as a substitute for real heights in the ground effect formulae.

It is customary to note the real heights above the ground h and the equivalent heights z . Remember that $h_s=0.05$ m (*Cf. Section 4.1.4*). The equivalent heights are obtained from the mean ground plane between the source and the receiver. This replaces the actual ground with a fictitious plane representing the average profile of the land (*Cf. Figure 7.1*).

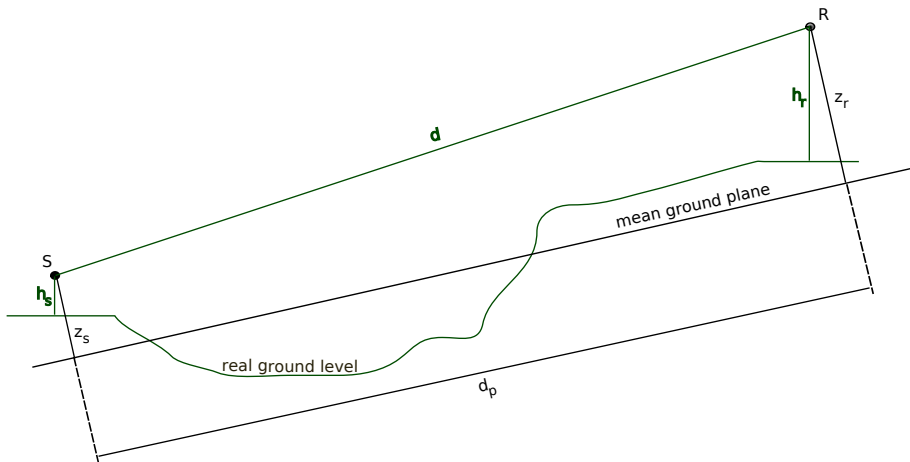


Figure 7.1: Equivalent heights in relation to the ground.

The equivalent height of a point is its orthogonal height in relation to this mean ground plane. The equivalent height z_s and the equivalent height of the receiver z_r can thus be defined. The distance between the source and receiver in projection in the mean ground plane is noted d_p (*Cf. Figure 7.1*).

The mean ground plane can be obtained by regression using the least squares method applied to the ground profile included between the source and the receiver.

Where the equivalent height of a point becomes negative, *i.e.* when the point is located below the mean ground plane, a nil height is adopted and the equivalent point is then combined with its possible image point if there is diffraction.

7.3.2 - Acoustic characterisation of grounds

The acoustic absorption properties of grounds relate basically to their porosity. Compact grounds are general reflective and porous grounds are absorbent.

Type of ground	G (dimensionless)
Lawn, meadow, field of cereals	1
Undergrowth (resinous or deciduous)	1
Non-compacted earth	0.7
Compacted earth, track	0.3
Road surface	0
Smooth concrete	0

Table 7.2: Values of G for different grounds.

For operational calculation needs, the acoustic absorption of a ground is represented by a dimensionless coefficient G between 0 and 1. G is frequency-independent. Table 7.2 gives the value of G for the surrounding grounds. The average of the coefficient G in a path normally takes intermediate values between 0 and 1. Here the average G represents the absorbent fraction along the path. See Figure 7.2 for an example.

G_{trajet} is defined as the fraction of absorbent ground present in the whole of the path covered.

When the source and the receiver are close $d_p \leq 30(z_s + z_r)$, the distinction between the type of grounds located near the source and those near the receiver no longer means anything. If the receiver is very close to the edge of the platform, an absorbent ground receiver side should not be considered. To take this comment into account, the ground factor G_{trajet} is ultimately corrected as follows:

$$G'_{trajet} = \begin{cases} \frac{d_p}{30(z_s+z_r)} G_{trajet} & \text{si } d_p \leq 30(z_s + z_r) \\ G_{trajet} & \text{sinon} \end{cases} \quad (7.3)$$

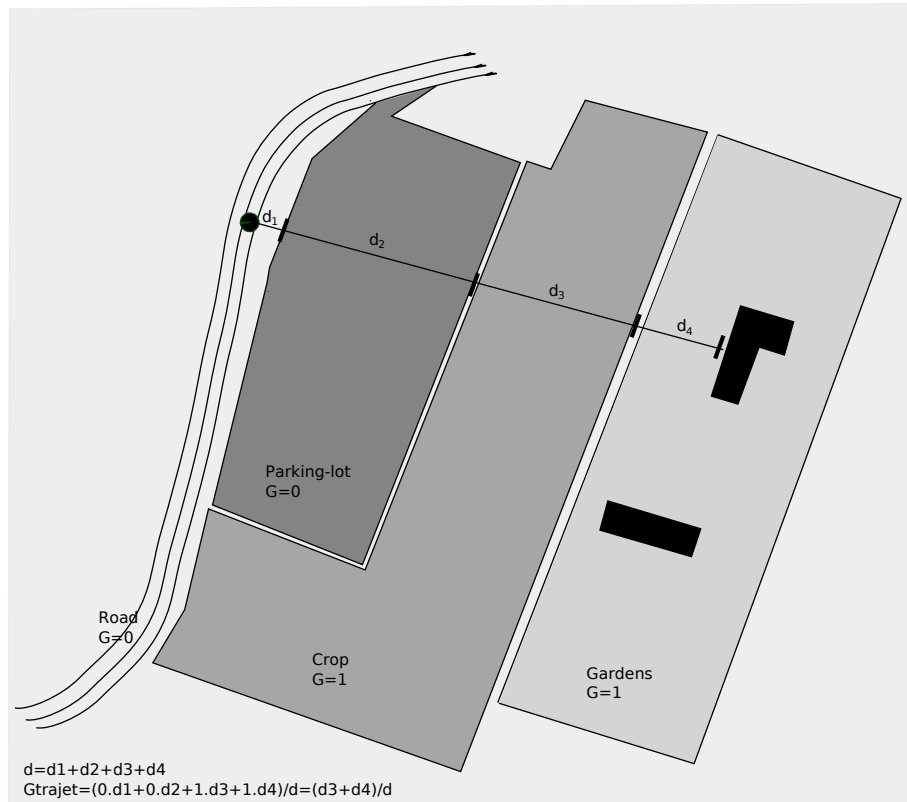


Figure 7.2: Determination of the ground coefficient G_{trajet} in a propagation path.

7.3.3 - Calculation in homogeneous conditions

The attenuation from the ground effect in homogeneous conditions is calculated according to the following formulae:

- if $G_{trajet} \neq 0$

$$A_{sol,H} = \max \left(-10 \log_{10} \left[4 \frac{k^2}{d_p^2} \left(z_s^2 - \sqrt{\frac{2C_f}{k}} z_s + \frac{C_f}{k} \right) \left(z_r^2 - \sqrt{\frac{2C_f}{k}} z_r + \frac{C_f}{k} \right) \right], A_{sol,H,min} \right) \quad (7.4)$$

where $k = 2\pi f_m / c$, f_m is the nominal median frequency of the third-octave band considered in Hz, c is the speed of sound through the air, taken as equal to 340 m/s and C_f is defined by

$$C_f = d_p \frac{1 + 3w d_p e^{-\sqrt{w d_p}}}{1 + w d_p} \quad (7.5)$$

where the values of w are given by the formula below based on f_m and G_{trajet} :

$$w = 0.0185 \frac{f_m^{2.5} G_{trajet}^{2.6}}{f_m^{1.5} G_{trajet}^{2.6} + 1.3 \times 10^3 f_m^{0.75} G_{trajet}^{1.3} + 1.16 \times 10^6} \quad (7.6)$$

$A_{sol,H,min} = -3(1 - G'_{trajet})$ is the lower bound¹ of $A_{sol,H}$.

- if $G_{trajet}=0 : A_{sol,H} = -3$ dB

7.3.4 - Calculation in downward-refraction conditions

The ground effect in downward-refraction conditions (*Cf.* Appendix C) is calculated with the formula of $A_{sol,H}$, provided the following modifications are made:

1. In the formula of $A_{sol,H}$, the heights z_s and z_r are replaced by $z_s + \delta z_s + \delta z_T$ and $z_r + \delta z_r + \delta z_T$ respectively, where

- $\delta z_s = a_0 \left(\frac{z_s}{z_s + z_r} \right)^2 \frac{d_p^2}{2};$
- $\delta z_r = a_0 \left(\frac{z_r}{z_s + z_r} \right)^2 \frac{d_p^2}{2};$
- $a_0 = 2 \times 10^{-4} m^{-1}$ is the reverse of the radius of curvature;
- $\delta z_T = 6 \times 10^{-3} \frac{d_p}{z_s + z_r}.$

2. The lower bound of $A_{sol,F}$ depends on the geometry of the path:

$$A_{sol,F,min} = \begin{cases} -3(1 - G'_{trajet}) & \text{si } d_p \leq 30(z_s + z_r) \\ -3(1 - G'_{trajet})(1 + 2(1 - 30(z_s + z_r)/d_p)) & \text{sinon} \end{cases} \quad (7.7)$$

The height corrections δz_s and δz_r convey the effect of the bending of sound rays. δz_T accounts for the effect of the turbulence.

7.3.5 - Reflection on an embankment slope

In this section, it is assumed that the plane is oriented trigonometrically.

The notion of embankment slope is restricted here to the edges of the road platform which is the source of noise. This type of bank prompts a calculation of A_{talus} only if:

1. the bank is a straight segment in a vertical section. The piecewise profiles or those with non-nil bending are therefore excluded;
2. the gradient of the bank ($\vec{O_1x}, \vec{O_1O_2}$) is strictly between 15° and 45° (*Cf.* Figure 7.3);
3. the foot of the bank and the receiver are in direct view;
4. the foot of the bank is at a maximum distance of 10 metres from the edge of the closest platform;
5. the foot of the bank is lower than or at the same height as the edge of the closest platform.

¹ The term $-3(1 - G'_{trajet})$ takes into account the fact that when the source and the receiver are far apart, the first reflection source side is no longer on the road platform but on the natural land.

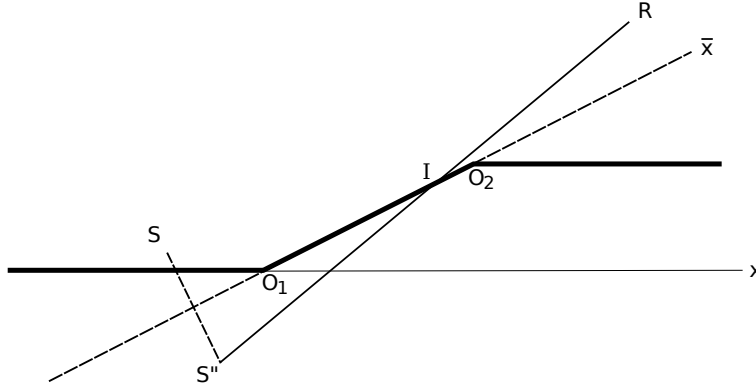


Figure 7.3: Notations used to calculate A_{talus} .

If the previous conditions are satisfied, A_{talus} is calculated as follows, in the vertical plane containing the source and the receiver (*Cf.* Figure 7.3):

1. search for the image source S'' in relation to the tangent at the bank;
2. search for the intersection point I with the path (S'', R) with the tangent at the bank;
3. calculation of the half-length e of the Fresnel ellipsoid intersection (*Cf.* Section E.2) with the tangent at the bank:

$$e = \frac{1}{\cos \theta} \sqrt{\frac{\lambda}{2} \frac{S''I \times IR}{S''I + IR} + \frac{\lambda^2}{16}} \quad (7.8)$$

where $\theta = (\vec{O_1x}, \vec{O_1O_2}) + (\vec{O_1x}, \vec{S''R})$;

4. calculation of the abscissa of I at the bank: if the angle $(\vec{O_1O_2}, \vec{O_1I})$ is nil, then $\bar{x}_l = O_1I$, otherwise $\bar{x}_l = -O_1I$;
5. calculation of ϵ , proportion of the intersection of the ellipsoid which coincides physically with the bank:

$$\epsilon = \begin{cases} 0 & \text{si } \bar{x}_l \leq -e \\ \min\left(\frac{l_T}{2e}, \frac{\bar{x}_l+e}{2e}\right) - \max\left(0, \frac{\bar{x}_l-e}{2e}\right) & \text{si } -e < \bar{x}_l < l_T + e \\ 0 & \text{si } l_T + e \leq \bar{x}_l \end{cases} \quad (7.9)$$

where $l_T = O_1O_2$;

6. the following is deduced

$$A_{talus} = -1.5\epsilon(2 - G_{talus}) \quad (7.10)$$

where G_{talus} is the ground factor of the bank (*Cf.* Section 7.3.2).

7.4 - Diffraction

The diffraction generally has to be studied at the tip of each obstacle in the propagation path. If the path passes ‘high enough’ over the diffraction edge, $A_{dif}=0$ can be set and a direct view calculated, in particular by evaluating A_{sol} (*Cf.* Section 7.3).

In practice, for *each third-octave nominal median frequency* the path difference δ is compared with the quantity $-\lambda/20$. If the path difference δ is less than $-\lambda/20$, there is no need to calculate A_{dif} for the third-octave in question. In other words, $A_{dif}=0$ in this case. Otherwise, A_{dif} is calculated as described in the remainder of this section. This rule applies in both homogeneous and downward-refraction conditions, for both single and multiple diffraction.



Warning

When, for a given third-octave, a calculation is performed under the procedure described in this Chapter, A_{sol} is set as equal to 0 dB when calculating the total attenuation. The ground effect is taken into account directly in the general diffraction calculation formula.

The formulae proposed here are used to process the diffraction in thin screens, thick screens, buildings, natural and artificial mounds of earth and via the edges of embankment, cut and viaducts.

When several diffracting obstacles are encountered in a propagation path, they are treated as a single multiple diffraction by applying the procedure described in Section 7.4.3².

The procedures presented in this chapter can be used to calculate in both homogeneous and downward-refraction conditions. Ray bending is taken into account in the path difference calculation and to calculate ground effects before and after diffraction.

7.4.1 - General principles

Figure 7.4 illustrates the general methodology for calculation attenuation from diffraction. This method is based on breaking down the propagation path into two parts: the ‘source side’ path, between the source and the diffraction point, and the ‘receiver side’ path, between the diffraction point and the receiver.

The calculation is:

- a ground effect, source side $\Delta_{sol(S,O)}$;
- a ground effect, receiver side $\Delta_{sol(O,R)}$;
- and three diffractions:
 - between the source S and the receiver R : $\Delta_{dif(S,R)}$;
 - between the source S' and the receiver R : $\Delta_{dif(S',R)}$;
 - between the source S and the image receiver R' : $\Delta_{dif(S,R')}$;

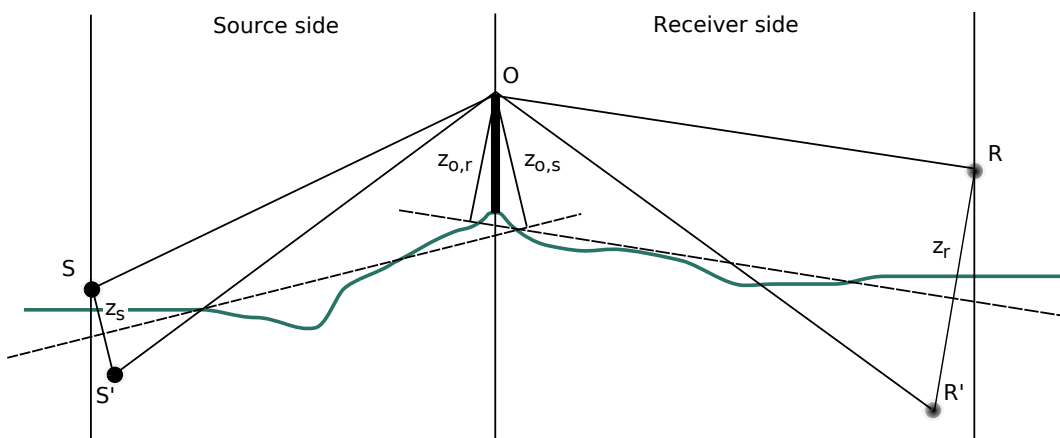


Figure 7.4: Geometry of calculating the attenuation from diffraction.

where

- S : source;
- R : receiver;

² Two successive diffraction calculations are only added together when the obstacles are really very far apart, but the reflections on the ground between the diffractions must then be considered.

- S' : image source compared with the mean ground plane source side;
- R' : image receiver compared with the mean ground plane receiver side;
- O : diffraction point;
- z_s : equivalent height of the source S compared with the mean ground plane source side;
- $z_{o,s}$: equivalent height of the diffraction point O compared with the mean ground plane source side;
- z_r : equivalent height of the receiver R compared with the mean ground plane receiver side;
- $z_{o,r}$: equivalent height of the diffraction point O compared with the mean ground plane receiver side.

The irregularity of the ground between the source and the diffraction point and between the diffraction point and the receiver is taken into account through equivalent heights calculated in relation to the mean ground planes, source side firstly and receiver side secondly (two mean ground planes), based on the method described in Section 7.3.1

7.4.2 - Pure diffraction

For pure diffraction, with no ground effect, the attenuation is given by

$$\Delta_{dif} = \begin{cases} 10C_h \log_{10}(3 + \frac{40}{\lambda} C'' \delta) & \text{si } \frac{40}{\lambda} C'' \delta \geq -2 \\ 0 & \text{sinon} \end{cases} \quad (7.11)$$

where

- when the diffraction edge is an element of natural land: $C_h = 1$, when the diffraction edge is a screen: $C_h = \min\left(\frac{f_m h_0}{250}, 1\right)$ where
 - f_m is the nominal median frequency of a third-octave band;
 - h_0 is the greatest of two heights of the diffraction edge compared with each of two mean ground planes source side and receiver side;
- λ is the wavelength at the nominal median frequency of the third-octave band in question;
- δ is the path difference between the diffracted and direct trajectories (Cf. Section 7.4.3);
- C'' is a coefficient used to consider multiple diffractions:
 - $C'' = 1$ for a single diffraction;
 - for a multiple diffraction, if e is the total distance between the diffraction closest to the source and the diffraction closest to the receiver (Cf. Figure 7.5 and Figure 7.7), this coefficient is defined by:

$$C'' = \frac{1 + (5\lambda/e)^2}{1/3 + (5\lambda/e)^2} \quad (7.12)$$

The values of Δ_{dif} must be bound

- if $\Delta_{dif} < 0 : \Delta_{dif} = 0$ dB ;
- if $\Delta_{dif} > 25 : \Delta_{dif} = 25$ dB for a diffraction in a horizontal edge and only in the term Δ_{dif} which figures in the calculation of A_{dif} . This upper bound must not be applied in the terms Δ_{dif} which are found in the calculation of Δ_{sol} or Δ_{talus} nor for diffraction in a vertical edge (side diffraction).

7.4.3 - Path difference calculation

The path difference δ is calculated in a vertical plane containing the source and the receiver. This is an approximation compared with the Fermat principle (*Cf.* Section E.1). The approximation remains applicable here (source lines). The path difference δ is calculated as in Figure 7.5 and Figure 7.6 based on the situations encountered:

7.4.3.1 - Homogeneous conditions

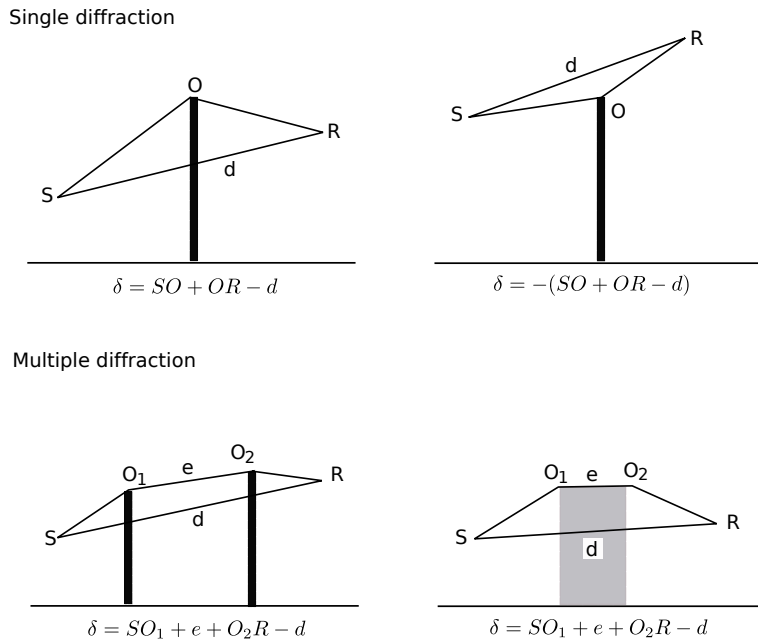


Figure 7.5: Path difference calculation in homogeneous conditions. O , O_1 and O_2 are diffraction points. The expression of δ is given for each configuration.

7.4.3.2 - Downward conditions

In downward-refraction conditions (*Cf.* Appendix C), it is considered that the three sound ray curves SO , OR and SR have identical radius of curvature Γ defined by

$$\Gamma = \max(1000, 8d) \quad (7.13)$$

where d is the length of the straight segment SR .

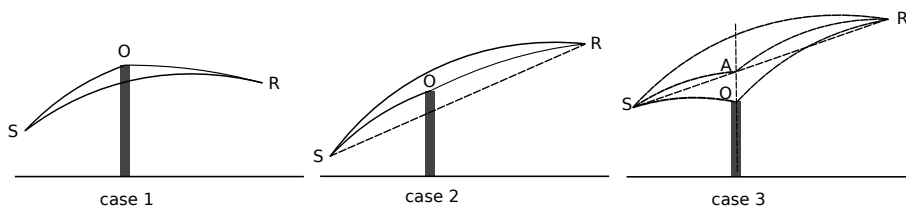


Figure 7.6: Path difference calculation in downward-refraction conditions (single diffraction).

The length of a sound ray curve MN is noted \widehat{MN} in downward-refraction conditions. This length is equal to:

$$\widehat{MN} = 2\Gamma \arcsin \left(\frac{MN}{2\Gamma} \right) \quad (7.14)$$

Theoretically three scenarios should be considered in calculating the path difference in downward-refraction conditions δ_F (*Cf.* Figure 7.6). In practice, two formulae are sufficient:

- if the straight sound ray SR is masked by the obstacle (1st and 2nd scenario in Figure 7.6): $\delta_F = \widehat{SO} + \widehat{OR} - \widehat{SR}$;
- if the straight sound ray SR is not masked by the obstacle (3rd scenario in Figure 7.6): $\delta_F = 2\widehat{SA} + 2\widehat{AR} - \widehat{SO} - \widehat{OR} - \widehat{SR}$

where A is the intersection of the straight sound ray SR and the extension of the diffracting obstacles.

For the multiple diffractions in downward-refraction conditions:

- determine the convex enveloped defined by the various potential diffraction edges;
- eliminate the diffraction edges which are not on the boundary of the convex envelope;
- calculate δ_F on the basis of lengths of sound ray curves, by breaking down the diffracted path into as many curve segments as necessary (*Cf.* Figure 7.7):

$$\delta_F = \widehat{SO}_1 + \sum_{i=1}^{i=n-1} \widehat{O_i O_{i+1}} + \widehat{O_n R} - \widehat{SR} \quad (7.15)$$

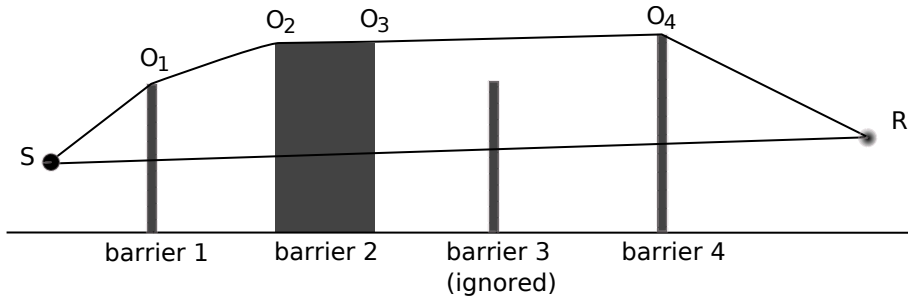


Figure 7.7: Sample calculation of the path difference in downward-refraction conditions for multiple diffractions.

In the scenario presented in Figure 7.7, the path difference is:

$$\delta_F = \widehat{SO} + \widehat{O_1 O_2} + \widehat{O_2 O_3} + \widehat{O_3 O_4} + \widehat{O_4 R} - \widehat{SR} \quad (7.16)$$

7.4.4 - Calculating the attenuation A_{dif}

The attenuation from the diffraction, taking the ground effects source side and receiver side into account, is calculated according to the following general formula:

$$A_{dif} = \Delta_{dif(S,R)} + \Delta_{sol(S,O)} + \Delta_{talus(S,O)} + \Delta_{sol(O,R)} \quad (7.17)$$

where:

- $\Delta_{dif(S,R)}$ is the attenuation from the diffraction between the source S and the receiver R;

- $\Delta_{sol(S,O)}$ is the attenuation from the ground effect source side, weighted by the diffraction source side (*Cf.* Section 7.4.4.1);
- $\Delta_{talus(S,O)}$ is the attenuation from a possible bank source side;
- $\Delta_{sol(O,R)}$ is the attenuation from the ground effect receiver side, weighted by the diffraction receiver side (*Cf.* Section 7.4.4.3).

7.4.4.1 - Calculating the term $\Delta_{sol(S,O)}$

$$\Delta_{sol(S,O)} = -20 \log_{10} \left(1 + (10^{-A_{sol(S,O)}/20} - 1) 10^{-(\Delta_{dif(S',R)} - \Delta_{dif(S,R)})/20} \right) \quad (7.18)$$

where:

- $A_{sol(S,O)}$ is the attenuation from the ground effect between the source S and the diffraction point O . This term is calculated as indicated in Section 7.3.3 in homogeneous conditions and in Section 7.3.4 in downward-refraction conditions, with the following assumptions:
 - $z_r = z_{o,s}$;
 - In homogeneous conditions, G_{trajet} is replaced by G'_{trajet} in the equation 7.6;
- $\Delta_{dif(S',R)}$ is the attenuation from the diffraction between the image source S' and R , calculated as in Section 7.4.2;
- $\Delta_{dif(S,R)}$ is the attenuation from the diffraction between S and R , calculated as in Section 7.4.2.

7.4.4.2 - Calculating the term $\Delta_{talus(S,O)}$

$$\Delta_{talus(S,O)} = -20 \log_{10} \left(1 + (10^{-A_{talus(S,O)}/20} - 1) 10^{-(\Delta_{dif(S'',R)} - \Delta_{dif(S,R)})/20} \right) \quad (7.19)$$

where

- $A_{talus}(S,O)$ is the attenuation from a possible bank on the edge of the platform between the source S and the diffraction point O . This term is calculated as indicated in Section 7.3.5;
- $\Delta_{dif(S'',R)}$ is the attenuation from the diffraction between the image source S'' relative to the bank plane and R , calculated as in Section 7.4.2;
- $\Delta_{dif(S,R)}$ is the attenuation from the diffraction between S and R , calculated as in Section 7.4.2,

7.4.4.3 - Calculating the term $\Delta_{sol(O,R)}$

$$\Delta_{sol(O,R)} = -20\log_{10} \left(1 + (10^{-A_{sol}(O,R)/20} - 1)10^{-(\Delta_{dif}(S,R') - \Delta_{dif}(S,R))/20} \right) \quad (7.20)$$

where:

- $A_{sol(O,R)}$ is the attenuation from the ground effect between the diffraction point O and the receiver R . This term is calculated as indicated in Section 7.3.3 in homogeneous conditions and in Section 7.3.4 in downward-refraction conditions, with the following assumptions:

- $z_s = z_{o,r}$;
- G_{trajet} is used in the equation 7.6 ;



Warning

There is no call here to take into account the correction G'_{trajet} as the source considered is no longer the road itself but the diffraction point. It is therefore clearly G_{trajet} which must be used in calculating the ground effects, including for the lower bound term of the formula which becomes $-3(1-G_{trajet})$.

- $\Delta_{dif}(S,R')$ is the attenuation from the diffraction between S and the image receiver R' , calculated as in Section 7.4.2;
- $\Delta_{dif}(S,R)$ is the attenuation from diffraction between S and R , calculated as in Section 7.4.2.

7.5 - Vertical edges

The equation 7.11 can be used to calculate the diffractions in vertical edges (side diffractions). In this case, $A_{dif} = \Delta_{dif}(S,R)$ and the term A_{sol} is kept in the equations 3.4 and 3.2. In addition, A_{atm} and A_{sol} will be calculated from the *total* length of the propagation path. A_{div} is still calculated from the direct distance d .

7.6 - Reflections in the vertical obstacles

The reflections in vertical obstacles are dealt with by image sources (*Cf.* Figure 7.8). Reflections in building facades and noise barriers are thus treated in this way.

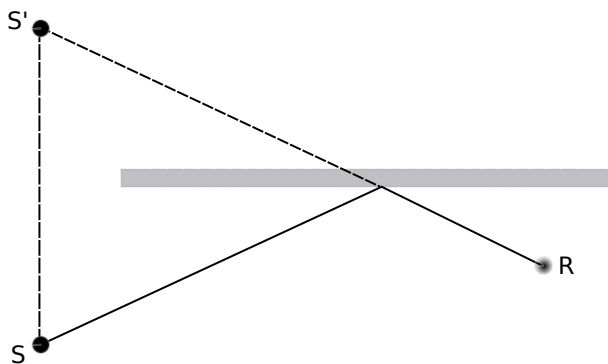


Figure 7.8: Specular reflection in an obstacle dealt with by the image source method (S : source, S' : image source, R : receiver).

An obstacle is taken to be vertical if it is less than 15° off vertical.

The method therefore has to be applied in 3D when dealing with reflections in highly sloping obstacles.

The obstacles with at least one dimension of less than 0.5 m must be ignored in the reflection calculation, except for special configurations³.

Remember that the reflections on the ground are not dealt with here. They are taken into account in the calculations of attenuation from the boundary (ground, diffraction, bank).

If L_w is the power level of the source S and α_r the coefficient of absorption of the surface of the obstacle, the power level of the image source S' is equal to:

$$L_{w'} = L_w + 10 \log_{10}(1 - \alpha_r) \quad (7.21)$$

with $0 \leq \alpha_r < 1$.

The propagation attenuations described earlier (*Cf.* Section 7.1 to Section 7.4) are then applied to this path (image source, receiver), as for a direct path.

7.7-Special elements

Trenches, tunnels and partial coverings are dealt with by equivalent sources as described in Appendix F (*Cf.* [GdB1980]).

³ A network of small obstacles in a plane at regular intervals is one example of a special configuration

8-Bibliography

8.1 - Articles

- [Bru1996] Y. Brunet, J.P. Lagouarde, and V. Zouboff, "Estimating long-term microclimatic conditions for long-range sound propagation studies".
7th Long Range Sound Propagation Symp., Lyon, France, 1996.
- [Def1999] Jérôme Defrance and Yannick Gabillet, "A new analytical method for the calculation of outdoor noise propagation", 57, 109-127.
Applied Acoustics, Copyright © 1999 Elsevier.
- [Emb1997] T.F.W. Embleton, "Tutorial on sound propagation outdoors", 100, 31-48.
Journal of the Acoustical Society of America, Copyright © 1996 ASA.
- [Kel1962] J.B. Keller, "Geometrical Theory of Diffraction", 52, 116-130.
Journal of the Optical Society of America, Copyright © 1962 OSA.

8.2 - Standards

- [EN1793p3] *EN 1793-3 Road traffic noise reducing devices - Test method for determining the acoustic performance - Part 3: normalised traffic noise spectrum*, Copyright © 1997 CEN.
- [ISO9613p1] *ISO 9613-1 Acoustics - Attenuation of sound during propagation outdoors - Part 1: Calculation of the absorption of sound by the atmosphere*, Copyright © 1993 ISO.
- [ISO9613p2] *ISO 9613-2 Acoustics - Attenuation of sound during propagation outdoors - Part 2: General method of calculation*, Copyright © 1996 ISO.
- [NFS31085] *NF S31-085, Acoustique - Caractérisation et mesurage du bruit dû au trafic routier -- Spécifications générales de mesurage*, Copyright © 2002 AFNOR (in french).
- [NFS31133] *NF S31-133 Acoustique - Bruit des infrastructures de transports terrestres -- Calcul de l'atténuation du son lors de sa propagation en milieu extérieur, incluant les effets météorologiques*, Copyright © 2007 AFNOR (in french).
- [prNFS31110] *NF S31-110 Acoustique - Caractérisation et mesurage des bruits de l'environnement -- Grandeurs fondamentales et méthodes générales d'évaluation*, revision in progress, AFNOR S30M/S30J (in french).

8.3 - Notes

- [SETRA04] Francis Besnard, *Evolution de la NMPB-Roads-96 - Calcul de la différence de marche en downward-refraction conditions : proposition de nouvelle formule*, Copyright © 2004 SETRA (in french).
- [SETRA07] Francis Besnard, *Liste des modifications actées pour l'évolution de la NMPB*, Copyright © 2007 SETRA (in french).
- [Zou1998] V. Zouboff, J.C. Laporte, and Y. Brunet, "Effets des conditions météorologiques sur la propagation du bruit", Prise en compte pratique, 51.
Collection Techniques et Méthodes des Laboratoires des Ponts et Chaussées, Copyright © 1998 LCPC (in french).

8.4 - Books

- [Abaques 2008] *Prévision du bruit routier*, 1 - Calcul des émissions sonores dues au trafic routier, juin 2009, SETRA, 124p, 978-2-11-095825-9 (in french).
- [Gau2009] B. Gauvreau, D. Ecotière, H. Lefèvre, and B. Bonhomme, "Propagation acoustique en milieu extérieur complexe - Caractérisation expérimentale *in situ* des conditions micrométéorologiques - Eléments méthodologiques et météorologiques", EG21, 68p.
Collection Etudes et Recherches des Laboratoires des Ponts et Chaussées, Copyright © 2009 LCPC (in french).
- [GdB1980] *Guide du bruit des transports terrestres - Prévision des niveaux sonores*, Copyright © 1980 CERTU (in french), 317p, 2-11-083290-8.
- [Guyot1999] Gérard Guyot, *Climatologie de l'environnement*, Copyright © 1999 Dunod (in french), 548p, 978-2-10-004441-2.
- [NMPB96] *Bruit des infrastructures routières*, Copyright © 1997 CERTU,CSTB,LCPC,SETRA (in french), Méthode de calcul incluant les effets météorologiques - version expérimentale - NMPB Routes 96, 98p, 2-11-089201-3 (in french).
- [Oke1987] Timothy R. Oke, *Boundary layer climates*, Copyright © 1987 Routledge, 464p, 978-0415043199.
- [Prj2001] *Bruit et études routières - Manuel du chef de projet* , Copyright © 2001 SETRA,CERTU, 236p, 2-11-090879-3 (in french).
- [Stu1988] Roland B. Stull, *An introduction to boundary layer meteorology*, Copyright © 1988 Springer, 680p, 978-9027727695.

8.5 - Reports

- [CSTB2002] Jérôme Defrance, *Evolution de la méthode de prévision du bruit routier "NMPB-Routes-96" - Rapport final*, Copyright © 2002 CSTB (in french).
- [CSTB2007] François Aballéa, Marine Baulac, and Jérôme Defrance, *Evolution de la méthode de prévision du bruit routier NMPB-Roads-96 - Rapport final*, Copyright © 2007 CSTB (in french).
- [HRM2005] Paul de Vos, Margreet Beuving, and Edwin Verheijen, *Harmonised Accurate and Reliable Methods for the EU Directive on the Assessment and Management of Environmental Noise - Final Technical Report*, Copyright © 2005 Consortium Harmonoise.
- [IMA2006] Margreet Beuving and Brian Hemsworth, *IMAGINE - Improved Methods for the Assessment of Generic Impact of Noise in the Environment - Final Synthesis Report*, Copyright © 2006 Consortium Imagine.
- [LRA1995] D. Delaunay and V. Zouboff, *Nouvelle méthode de prévision du bruit routier*, Copyright © 1995 Laboratoire Régional des Ponts et Chaussées d'Angers (in french), Caractérisation météorologique d'un site.
- [LRS2001] Vincent Steimer, *Validation de la NMPB Routes 96 - Calculs NMPBLRS sur sites simplifiés*, Copyright © 2001 LRPC de Strasbourg (in french).
- [LRS2003a] Guillaume Dutilleux, *NMPBLRS2 - Une programmation simplifiée de la NMPB Routes 1996 en langage Scilab*, Copyright © 2003 LRPC de Strasbourg (in french).
- [LRS2003b] Guillaume Dutilleux, *Révision de la NMPB Routes 96 - Test de nouvelles formules avec NMPBLRS2*, Copyright © 2003 LRPC de Strasbourg (in french).
- [LRS2004] Guillaume Dutilleux, *Révision de la NMPB-Roads-96 - Complément à l'étude 02 76 056*, Copyright © 2004 LRPC de Strasbourg (in french).

- [LRS2005] Guillaume Dutilleux, *Révision de la NMPB-Roads-96 - Tests selon le cahier des charges du 16 août 2004 - Calculs de moyen terme*, Copyright © 2005 LRPC de Strasbourg (in french).
- [LRS2007] Guillaume Dutilleux, *Révision de la NMPB-Roads-96 - Formules définitives et calculs de moyen terme*, Copyright © 2007 LRPC de Strasbourg (in french).
- [LRS2008] David Ecotière, *Révision de la NMPB-Roads-96 - Calcul des occurrences météorologiques favorables à la propagation*, Copyright © 2008 LRPC de Strasbourg (in french).
- [MEDD2006] Fabrice Junker, Benoît Gauvreau, Cora Cremezi, and Philippe Blanc-Benon, *Classification de l'influence relative des paramètres physiques affectant les conditions de propagation à grande distance - Rapport final du projet MEDD/PREDIT (2004-2006)*, Copyright © 2006 MEDD (in french).

8.6 - PhD theses

- [Def1996] Jérôme Defrance, *Méthode analytique pour le calcul de propagation de bruit extérieur*, Thèse de doctorat en acoustique, Copyright © 1996 Université du Maine, France (in french), 196p.
- [Gaulin2000] David Gaulin, *Caractérisation physique des sources sonores en milieu urbain*, Thèse de doctorat en acoustique, Copyright © 2000 Université du Maine, France (in french), 203p.

Appendices

A-Calculation method flow chart

The general flow chart for the calculation method presented in this document for a set of roads and a receiver can be found in Figure A.1. The step in this flow chart to calculate the attenuation from the boundary formed by the ground and the obstacles is broken down in Figure A.2.

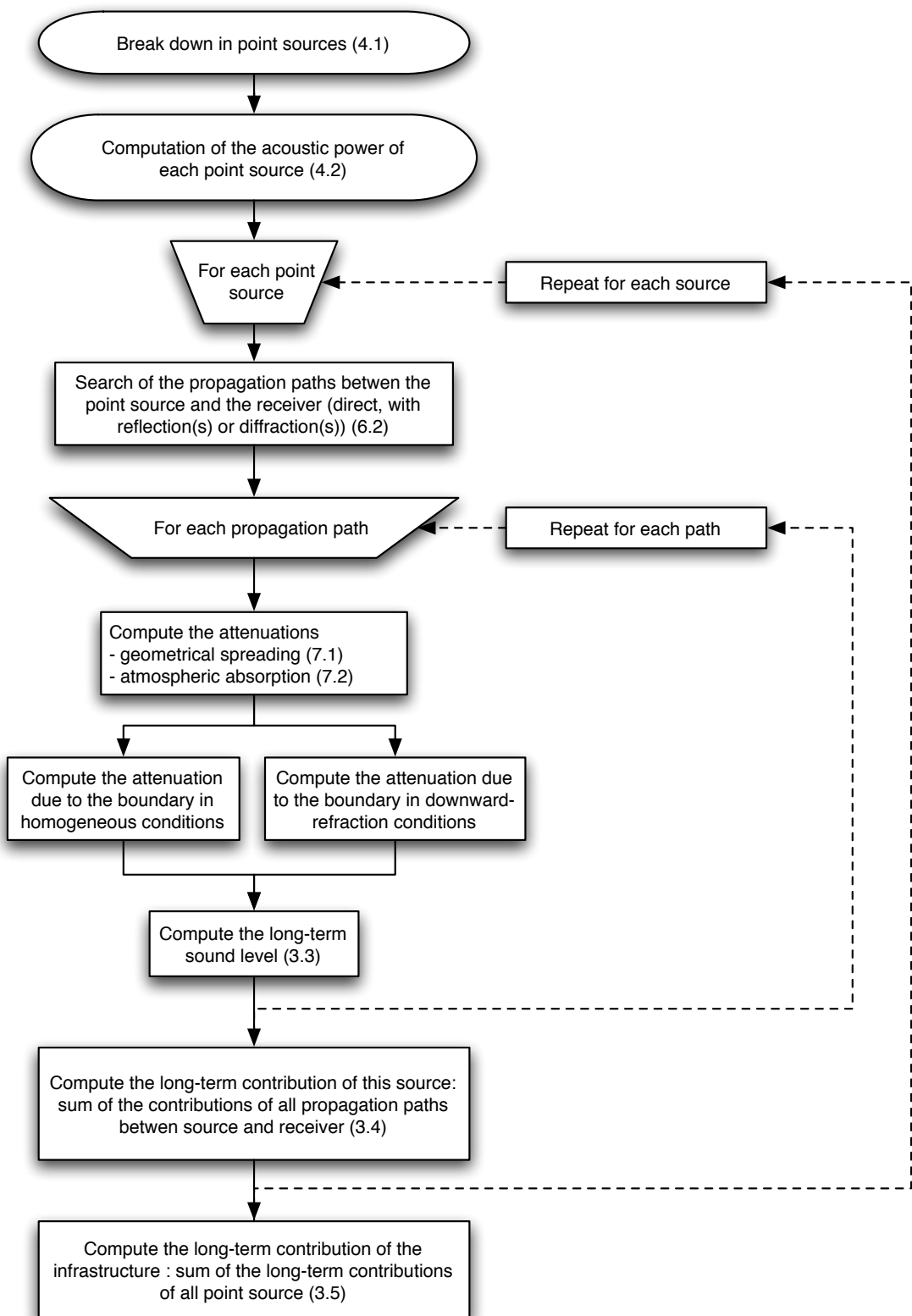


Figure A.1: General flow chart of the NMPB-Roads-2008 for a set of roads and a receiver.

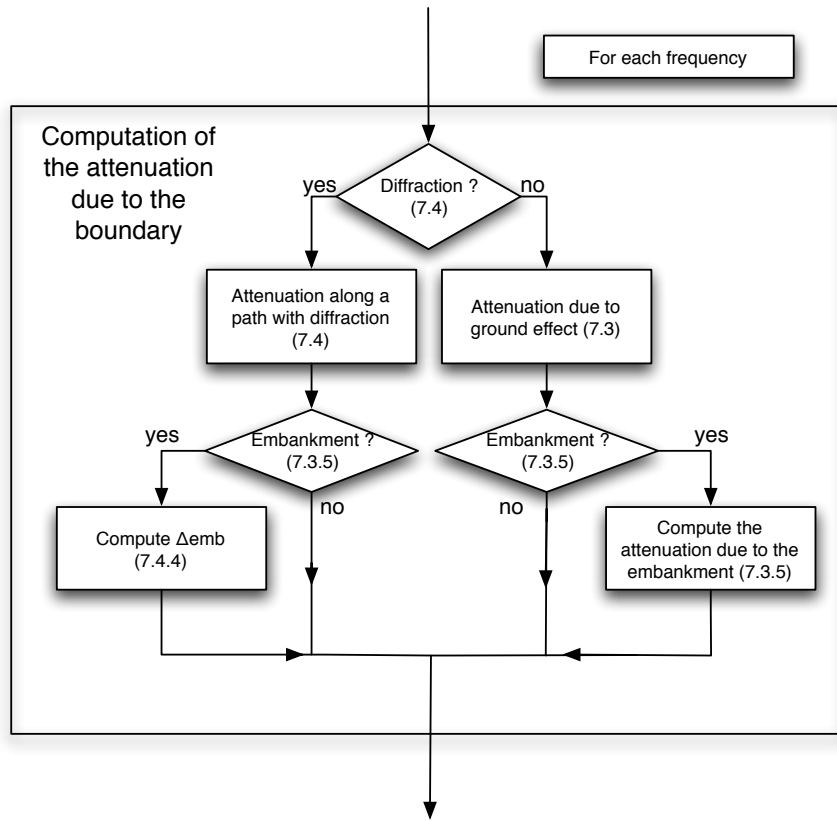


Figure A.2: Calculating the attenuation from the boundary of the fluid domain in the NMPB-Roads-2008.
Valid in homogeneous and downward-refraction conditions.

B-Occurrence values and maps of downward-refraction conditions for France

This appendix presents occurrences calculated for Metropolitan France in three forms:

- two series of tables defining, for each meteorological station, the probabilities of occurrence (percentages) of downward-refraction conditions by 20° sectors of receiver-source direction and for different periods (06.00-22.00, 22.00-06.00) and (06.00-18.00, 18.00-22.00 and 22.00-06.00);
- 41 polar diagrams (occurrence roses) which represent for each meteorological station the probabilities of occurrence of downward-refraction conditions as a function of the receiver-source direction for four legal periods, 06.00-18.00, 18.00-22.00, 06.00-18.00 and 22.00-06.00 (*Cf.* Section B.3) ;
- 4 maps, for two receiver-source directions (0° and 90°), the lines ‘of iso-occurrence’ of downward-refraction conditions for the periods 06.00-22.00 and 22.00-06.00. These maps have been obtained by interpolation between the closest stations. They are given for information to illustrate the spatial distribution of occurrences in the region (*Cf.* Section B.4).

The probabilities of occurrence of downward-refraction conditions provided in this appendix are expressed in percentages.

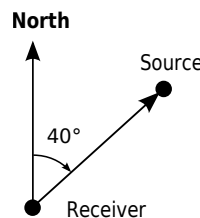


Figure B.1: Definition of the angle (\vec{N}, \vec{RS}) expressing the receiver-source direction, example for an angle of 40° .

The angle (\vec{N}, \vec{RS}) expressing the receiver-source direction is noted as for the wind roses: taking the receiver to be in the centre of the rose, it is the angle between the receiver-source vector and North, counted clockwise (*Cf.* Figure B.1). Examples:

- the source is in the North: direction 0°
- the source is in the East: direction 90°
- the source is in the South-West: direction 225°

To read the tables in this appendix correctly, the receiver-source direction interval associated with each of eighteen direction classes must be specified. The 20° column corresponds to a receiver-source orientation towards the North in the interval $]10^\circ, 30^\circ]$, the 40° column to the interval $]30^\circ, 50^\circ]$ and so on until the 360° column, which corresponds to a meeting of intervals $]0^\circ, 10^\circ]$ and $]350^\circ, 360^\circ]$.

Mathematically, a receiver-source direction ψ expressed in degrees becomes the associated class Ψ through the formula:

$$\Psi = \begin{cases} 360 & 0 < \psi \leq 10 \\ 20 h(\frac{\psi-10}{20}) & 10 < \psi \leq 360 \end{cases} \quad (\text{B.1})$$

with

$$h(x) = \begin{cases} \lfloor x \rfloor + 1 & x > \lfloor x \rfloor \\ \lfloor x \rfloor & x = \lfloor x \rfloor \end{cases} \quad (\text{B.2})$$

where $\lfloor \cdot \rfloor$ stands for the integer part.

The value of a probability of occurrence for a given direction thus corresponds to the percentage of time during which propagation takes place in downward-refraction conditions for a noise coming from this direction.

Note

The occurrences calculated for the 22.00-06.00 period can differ significantly from those established for the NMPB-Roads-96. This difference is due to the computer model used, which in particular allows the influence of the wind to be taken into account better during this period. These results agree with numerous experimental observations.

Altitudes over 500 metres are shown as a grey background on the map. *In these areas, the iso-value lines have no validity meteorologically. It is highly inadvisable to extrapolate values of probability of occurrence of downward-refraction conditions inside these areas from these maps.*

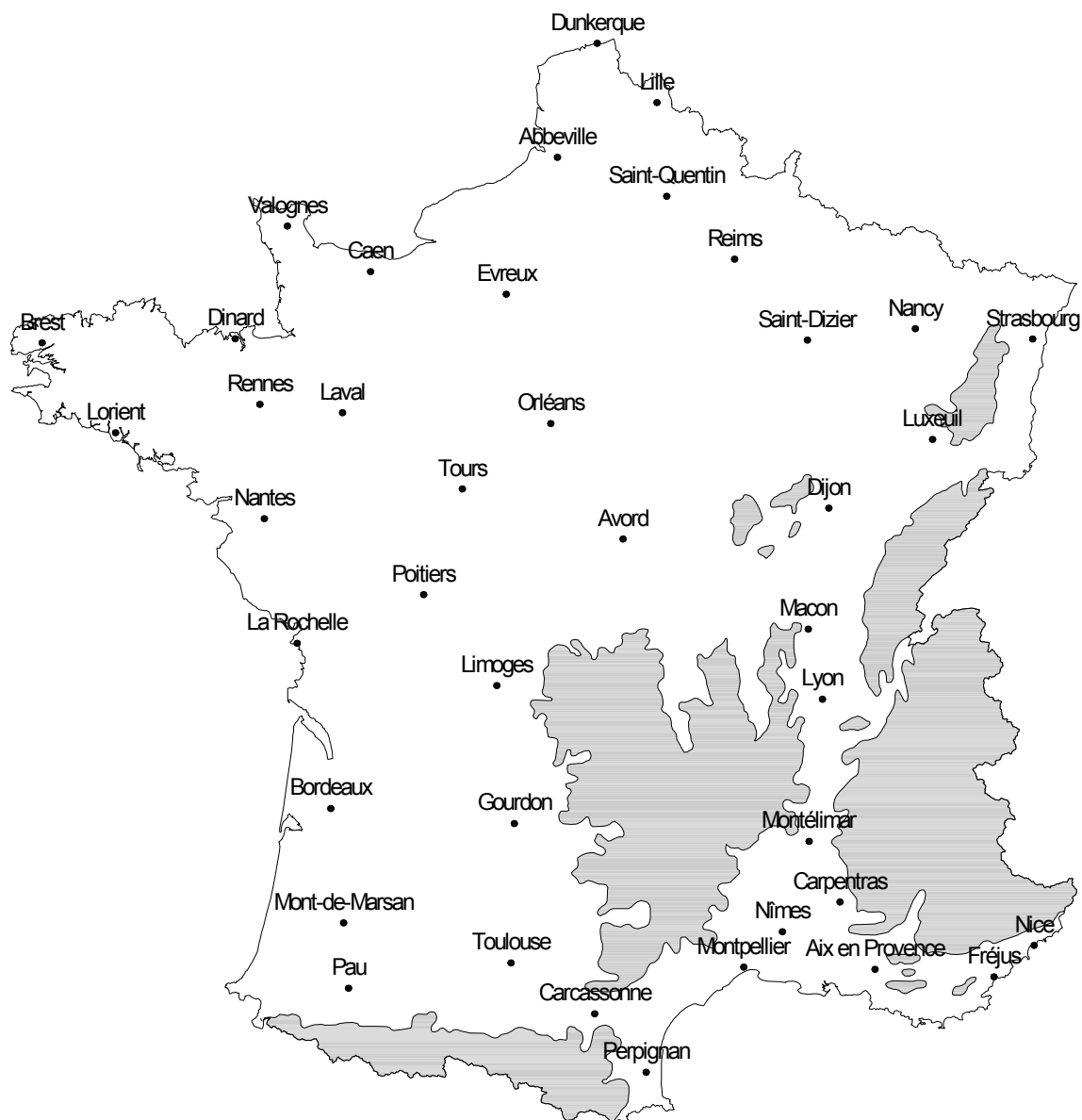


Figure B.2: Places with tabulated occurrences.

B.1 - Occurrences over two periods

Direction (°)	20	40	60	80	100	120	140	160	180	200	220	240	260	280	300	320	340	360
Abbeville	41	35	33	33	35	38	40	43	45	48	54	57	57	56	54	51	48	45
Aix-en-Provence	39	39	37	32	28	27	28	28	30	31	30	30	35	40	42	42	41	39
Avord	34	32	31	31	31	31	31	32	33	34	36	37	37	38	38	38	37	36
Bordeaux	41	38	38	38	38	37	36	36	39	43	47	48	47	47	48	49	48	45
Brest	43	40	36	34	34	34	36	40	43	47	50	53	55	55	53	50	48	46
Caen	39	34	34	34	34	34	36	40	44	50	55	56	56	56	55	54	50	45
Carcassonne	55	41	33	32	32	33	33	33	31	27	41	54	59	60	60	59	58	56
Carpentras	43	41	39	32	25	24	25	27	28	29	29	29	35	44	47	46	45	44
Dijon	43	42	40	38	35	33	34	37	39	41	42	43	45	47	47	44	43	43
Dinard	43	42	40	36	34	35	38	42	46	48	48	50	53	55	53	51	48	44
Dunkerque	38	36	34	34	35	38	41	46	49	51	54	56	56	54	50	47	44	41
Evreux	40	36	34	32	33	34	38	42	44	47	50	54	56	55	53	49	45	43
Fréjus	49	44	38	34	32	33	34	35	33	30	32	36	39	43	45	46	47	48
Gourdon	32	29	28	30	31	33	35	37	40	44	47	48	46	45	43	41	38	35
La Rochelle	47	45	41	38	37	38	36	33	32	34	38	42	46	48	47	48	49	49
Laval	38	38	37	36	35	34	35	39	43	45	47	48	49	50	51	49	46	41
Lille	37	33	31	31	32	36	41	43	47	53	57	59	59	58	55	49	46	42
Limoges	40	39	39	39	40	42	42	42	41	42	45	46	46	45	43	42	41	41
Lorient	44	41	39	38	37	36	35	35	36	42	48	51	52	53	53	51	48	
Luxeuil	29	29	31	33	34	35	38	43	47	49	49	48	46	45	45	42	36	31
Lyon	47	47	47	44	37	36	37	37	37	36	35	35	35	35	40	43	43	46
Mâcon	45	43	38	32	30	31	32	33	33	34	36	39	45	46	45	45	46	46
Mont-de-Marsan	36	35	34	34	34	33	34	36	38	40	41	42	43	44	45	44	41	38
Montélimar	66	67	67	66	64	55	31	21	21	21	22	21	21	22	27	44	60	65
Montpellier	53	49	44	41	39	36	32	30	31	32	35	38	39	41	44	50	53	54
Nancy	38	36	34	34	36	40	44	44	45	46	48	51	51	50	46	41	39	39
Nantes	40	37	35	36	37	38	39	39	39	43	48	50	50	49	48	46	44	43
Nice	50	53	53	46	32	30	32	33	33	28	24	24	33	45	48	48	47	47
Nîmes	57	57	56	52	46	38	32	28	26	25	25	25	27	32	39	47	52	55
Orléans	40	38	38	38	37	38	40	42	44	47	50	51	52	51	50	46	43	42
Pau	38	34	33	33	32	32	31	32	35	39	43	44	44	45	46	47	46	43
Perpignan	59	58	46	32	28	27	26	24	23	23	23	23	32	47	55	58	59	60
Poitiers	39	37	35	33	32	33	36	38	41	45	48	50	51	52	50	46	44	41
Reims	35	33	32	30	30	32	34	40	47	51	52	54	56	55	54	52	46	38
Rennes	37	36	36	35	35	35	37	42	45	47	48	49	50	50	50	48	43	39
Saint Dizier	33	35	36	36	37	39	43	48	52	52	51	51	52	51	49	44	38	33
Saint Quentin	38	36	35	36	37	38	39	41	45	49	52	53	53	52	51	48	46	42
Strasbourg	38	35	32	29	28	32	35	38	41	45	47	49	51	51	47	44	43	41
Toulouse	41	29	25	28	30	31	32	33	35	41	50	54	52	52	52	51	50	48
Tours	39	38	38	38	38	39	41	42	43	45	47	49	49	49	48	44	42	40
Valognes	43	40	37	35	34	33	34	36	38	40	44	48	51	52	53	51	48	45

Table B.1: 2 periods - Day (06.00-22.00).

Direction (°)	20	40	60	80	100	120	140	160	180	200	220	240	260	280	300	320	340	360
Abbeville	43	40	40	42	44	48	52	56	58	61	64	64	61	59	55	52	48	46
Aix-en-Provence	64	72	69	62	53	47	46	44	43	42	36	33	38	42	45	48	51	56
Avord	48	46	46	46	46	46	47	49	51	52	52	51	50	50	51	51	51	50
Bordeaux	49	45	44	44	43	42	42	43	48	55	59	61	60	60	62	63	61	55
Brest	49	45	43	42	42	43	46	49	51	54	56	59	60	60	59	57	55	52
Caen	39	33	33	33	34	37	42	49	55	63	69	71	70	68	66	60	54	47
Carcassonne	67	44	34	34	36	38	39	41	47	58	69	69	68	68	66	64	63	64
Carpentras	54	65	72	68	60	58	58	57	54	49	41	34	36	39	39	39	40	45
Dijon	60	58	56	52	44	36	32	35	37	39	41	44	50	60	70	70	65	62
Dinard	42	42	41	39	38	41	48	55	60	61	60	61	63	64	61	54	48	43
Dunkerque	39	39	39	40	44	49	55	60	63	63	63	62	59	53	48	42	40	
Evreux	49	45	42	40	40	41	46	49	51	54	58	62	64	65	63	59	55	53
Fréjus	94	89	74	56	36	22	17	15	14	15	30	52	72	84	87	88	90	92
Gourdon	36	38	46	53	56	58	61	64	67	72	75	72	60	52	47	43	40	38
La Rochelle	71	68	63	59	57	54	48	43	39	37	40	44	48	51	54	61	67	71
Laval	53	52	51	48	45	39	38	41	46	49	51	52	55	61	67	67	63	58
Lille	45	41	39	40	42	45	49	51	55	59	63	65	64	63	60	58	56	51
Limoges	64	60	58	58	58	57	55	53	48	45	47	48	48	48	50	54	60	64
Lorient	64	57	51	48	46	43	41	38	36	38	44	49	52	55	58	61	64	67
Luxeuil	51	56	59	61	61	61	63	66	65	58	50	44	40	39	40	39	40	45
Lyon	53	55	57	57	49	49	50	50	51	51	51	52	57	70	68	59	55	53
Mâcon	69	67	60	42	32	31	31	31	32	35	42	59	78	83	79	73	71	70
Mont-de-Marsan	48	46	44	42	41	41	42	46	50	52	50	51	52	53	54	53	51	49
Montélimar	79	79	79	80	83	79	54	31	24	22	22	22	23	27	44	71	80	80
Montpellier	82	77	69	61	54	47	35	26	23	27	36	45	52	59	69	79	84	84
Nancy	44	44	44	46	50	55	60	58	56	55	56	56	54	51	46	42	44	45
Nantes	55	51	48	47	47	49	49	49	47	49	52	55	56	56	56	59	60	59
Nice	92	92	90	79	31	18	15	13	13	11	12	18	54	82	86	88	89	90
Nîmes	87	88	87	84	73	52	35	27	23	20	21	25	38	56	73	80	83	86
Orléans	49	47	46	47	47	47	50	51	50	52	54	55	54	54	55	54	52	51
Pau	38	40	45	48	49	50	53	57	65	72	74	69	60	54	51	49	46	41
Perpignan	77	69	53	30	21	18	18	20	26	33	41	63	79	84	86	87	87	83
Poitiers	47	45	42	38	37	37	40	42	46	50	53	55	59	61	61	59	56	52
Reims	42	40	38	35	35	38	42	50	58	61	62	64	67	69	66	62	54	46
Rennes	48	45	43	42	40	40	43	47	51	54	56	57	59	61	62	60	55	51
Saint Dizier	42	49	51	51	53	58	64	70	73	70	61	55	53	51	48	43	37	36
Saint Quentin	49	48	48	48	48	48	47	48	51	53	55	55	54	54	53	55	55	52
Strasbourg	47	43	39	36	35	40	45	49	53	57	61	66	73	77	73	64	58	51
Toulouse	44	30	27	32	34	39	43	46	49	60	75	82	77	72	67	61	57	53
Tours	52	50	50	49	47	47	49	50	49	50	51	52	53	55	55	54	54	54
Valognes	58	52	47	43	40	38	39	42	44	47	51	55	59	63	66	65	63	61

Table B.2: 2 periods - Night (22.00-06.00).

B.2 - Occurrences over three periods

Direction (°)	20	40	60	80	100	120	140	160	180	200	220	240	260	280	300	320	340	360
Abbeville	34	30	28	30	33	36	39	43	45	48	52	55	54	53	51	47	42	39
Aix-en-Provence	32	33	31	28	26	26	26	26	25	22	22	22	26	31	33	34	33	32
Avord	25	25	25	26	26	26	27	28	29	30	31	32	32	32	31	30	28	27
Bordeaux	33	31	32	35	35	35	34	35	39	43	45	44	43	42	42	42	40	37
Brest	39	36	33	31	31	32	35	38	42	46	49	52	53	52	49	46	42	41
Caen	33	29	28	29	29	31	34	39	45	50	55	56	55	54	52	49	44	39
Carcassonne	47	34	30	30	31	31	31	30	27	21	36	51	57	58	58	57	55	52
Carpentras	36	34	32	26	22	22	22	23	23	23	23	22	26	34	38	39	38	37
Dijon	38	37	36	33	29	26	28	32	35	37	39	40	41	42	41	37	37	38
Dinard	37	36	34	31	30	32	35	41	46	49	49	51	53	53	51	47	42	38
Dunkerque	34	32	30	30	32	35	39	44	47	50	53	54	55	52	48	43	39	37
Evreux	34	31	29	28	29	31	35	39	42	45	49	52	53	52	50	44	40	37
Fréjus	47	41	34	28	25	25	27	27	25	21	23	28	33	39	43	45	46	46
Gourdon	23	20	20	23	26	29	32	35	38	41	42	42	39	37	35	32	30	26
La Rochelle	40	39	37	36	37	37	35	33	31	33	36	39	41	41	40	40	41	41
Laval	33	33	33	32	32	31	32	36	40	43	44	45	46	46	46	44	40	36
Lille	32	29	27	27	29	33	38	41	45	51	55	58	58	56	51	44	40	36
Limoges	34	34	35	36	37	39	40	40	40	40	42	42	41	39	36	34	33	34
Lorient	41	39	38	37	36	35	34	34	34	38	44	47	48	49	49	47	45	43
Luxeuil	23	22	24	26	28	29	33	39	43	44	44	42	41	40	39	36	30	25
Lyon	41	41	40	36	28	29	32	34	34	34	33	32	31	34	35	36	38	40
Mâcon	39	36	30	24	22	26	30	31	32	32	33	35	39	39	37	38	40	40
Mont-de-Marsan	27	28	29	30	31	31	31	33	35	36	36	37	38	39	39	37	33	29
Montélimar	64	65	64	63	60	48	25	17	17	18	19	18	17	16	18	34	54	62
Montpellier	52	47	43	40	37	32	26	24	24	25	27	30	31	33	37	45	50	53
Nancy	31	30	29	29	30	35	39	40	41	44	46	48	48	46	41	35	33	32
Nantes	35	34	33	33	35	37	37	37	37	40	44	46	46	44	42	40	37	37
Nice	48	50	50	40	25	24	25	26	25	22	18	17	26	42	45	46	46	46
Nîmes	54	55	53	49	42	32	26	22	20	19	18	17	19	23	31	40	47	52
Orléans	35	34	34	34	34	34	36	38	41	45	48	49	49	48	46	41	37	36
Pau	28	26	27	28	29	29	28	29	31	35	38	38	38	39	39	39	38	34
Perpignan	54	51	39	26	24	23	22	20	20	19	20	28	43	51	55	56	56	55
Poitiers	34	33	31	29	28	30	33	35	39	43	46	47	49	49	46	41	38	35
Reims	29	28	27	25	25	28	30	36	43	48	50	52	53	52	50	48	41	33
Rennes	32	31	31	30	30	31	35	39	43	45	47	48	48	48	46	42	38	34
Saint Dizier	26	29	30	31	32	35	39	44	49	49	48	48	48	47	44	38	31	26
Saint Quentin	32	31	31	32	33	35	36	39	44	48	50	50	50	49	47	44	41	36
Strasbourg	31	29	26	23	22	25	30	34	39	42	45	46	47	45	40	36	35	34
Toulouse	34	22	17	22	26	28	31	32	33	38	46	49	47	48	47	46	45	42
Tours	34	34	34	34	35	37	39	39	40	43	45	46	46	46	43	39	35	34
Valognes	37	35	33	32	30	30	31	33	35	38	41	45	48	49	49	46	42	39

Table B.3: 3 periods - Day (06.00-18.00).

Direction (°)	20	40	60	80	100	120	140	160	180	200	220	240	260	280	300	320	340	360
Abbeville	60	51	46	44	43	43	44	43	44	49	58	64	65	64	63	64	64	64
Aix-en-Provence	64	63	57	46	37	33	34	38	45	53	57	59	68	72	72	70	68	65
Avord	63	58	54	51	49	47	46	46	47	49	52	55	57	60	63	66	68	67
Bordeaux	65	60	54	49	46	43	39	37	40	46	53	58	60	62	66	71	72	70
Brest	57	52	47	44	42	41	42	43	45	49	53	57	61	64	66	65	65	63
Caen	58	51	50	49	47	44	42	41	44	50	56	57	58	62	64	68	68	64
Carcassonne	82	62	44	38	37	37	38	40	43	45	56	63	65	65	65	66	71	
Carpentras	67	67	64	54	36	33	36	40	44	47	50	53	66	77	77	73	70	68
Dijon	57	55	53	52	51	53	53	51	50	50	52	55	58	62	66	65	62	59
Dinard	61	60	58	52	46	44	44	45	46	45	46	48	53	59	62	63	64	62
Dunkerque	51	48	46	45	46	48	48	52	54	55	57	59	59	59	59	57	54	
Evreux	57	53	48	46	44	45	48	49	49	51	55	59	63	65	65	62	60	59
Fréjus	58	57	53	55	58	60	62	62	61	60	65	66	62	57	52	50	50	54
Gourdon	61	57	55	53	49	45	45	46	49	56	63	69	71	70	70	68	66	64
La Rochelle	69	62	53	43	39	38	37	35	34	37	43	51	63	68	69	71	73	74
Laval	54	53	50	47	44	44	44	48	52	53	54	56	60	63	66	66	63	57
Lille	52	47	45	45	44	45	48	49	51	58	61	63	64	66	66	63	63	60
Limoges	61	55	52	51	50	50	48	46	46	49	56	63	69	71	70	68	66	66
Lorient	53	45	41	39	37	36	36	38	41	53	62	65	67	67	68	69	68	64
Luxeuil	54	54	56	56	54	54	56	60	63	66	68	67	64	63	64	63	59	55
Lyon	65	66	68	69	64	58	51	46	44	43	43	44	47	60	66	64	63	64
Mâcon	68	68	67	62	57	49	43	40	39	40	45	55	65	72	73	70	69	69
Mont-de-Marsan	64	59	51	46	43	43	43	46	50	55	59	60	61	62	64	67	68	67
Montélimar	74	73	73	74	78	76	51	35	32	31	31	32	34	40	57	77	79	75
Montpellier	56	52	48	46	46	47	48	51	53	55	60	65	65	65	66	66	62	59
Nancy	59	56	53	51	52	56	59	59	56	54	57	60	62	63	62	60	60	61
Nantes	56	47	43	42	41	42	43	45	46	52	58	62	64	65	66	67	66	64
Nice	56	61	62	62	52	49	52	55	56	51	44	45	54	56	55	53	50	50
Nîmes	64	63	63	63	62	58	52	48	47	47	48	51	54	59	66	70	69	66
Orléans	55	51	49	48	48	49	52	53	52	53	56	57	59	61	62	61	60	59
Pau	71	62	54	48	45	43	43	45	48	54	60	64	65	66	68	71	74	74
Perpignan	76	77	70	51	43	40	39	37	35	33	33	46	60	65	67	69	71	74
Poitiers	54	50	47	46	45	45	45	45	49	52	54	57	59	61	62	64	64	61
Reims	51	49	47	46	46	44	46	50	56	59	60	61	64	66	66	66	61	55
Rennes	53	53	52	51	48	45	45	49	52	53	53	53	55	59	64	66	60	55
Saint Dizier	55	53	53	52	51	52	56	59	62	61	61	62	64	65	66	64	59	56
Saint Quentin	54	51	49	48	47	48	48	48	49	53	57	60	61	61	61	62	61	58
Strasbourg	58	54	51	49	50	53	52	48	49	52	56	60	65	70	71	70	67	63
Toulouse	63	52	48	49	43	39	38	38	40	49	61	69	68	67	67	68	67	67
Tours	56	52	50	48	46	47	49	50	51	53	55	58	60	61	62	62	62	59
Valognes	61	54	49	45	44	43	44	45	46	48	53	58	61	64	65	65	65	64

Table B.4: 3 periods - Evening (18.00-22.00).

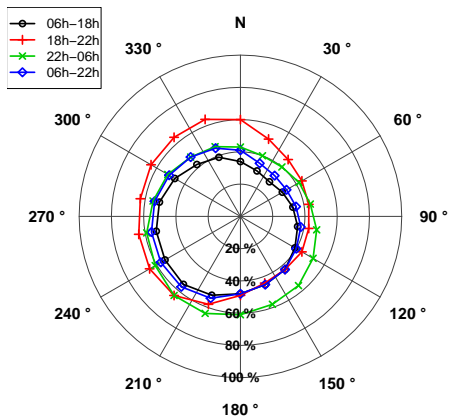
Direction (°)	20	40	60	80	100	120	140	160	180	200	220	240	260	280	300	320	340	360
Abbeville	43	40	40	42	44	48	52	56	58	61	64	64	61	59	55	52	48	46
Aix-en-Provence	64	72	69	62	53	47	46	44	43	42	36	33	38	42	45	48	51	56
Avord	48	46	46	46	46	46	47	49	51	52	52	51	50	50	51	51	51	50
Bordeaux	49	45	44	44	43	42	42	43	48	55	59	61	60	60	62	63	61	55
Brest	49	45	43	42	42	43	46	49	51	54	56	59	60	60	59	57	55	52
Caen	39	33	33	33	34	37	42	49	55	63	69	71	70	68	66	60	54	47
Carcassonne	67	44	34	34	36	38	39	41	47	58	69	69	68	68	66	64	63	64
Carpentras	54	65	72	68	60	58	58	57	54	49	41	34	36	39	39	39	40	45
Dijon	60	58	56	52	44	36	32	35	37	39	41	44	50	60	70	70	65	62
Dinard	42	42	41	39	38	41	48	55	60	61	60	61	63	64	61	54	48	43
Dunkerque	39	39	39	40	44	49	55	60	63	63	63	63	62	59	53	48	42	40
Evreux	49	45	42	40	40	41	46	49	51	54	58	62	64	65	63	59	55	53
Fréjus	94	89	74	56	36	22	17	15	14	15	30	52	72	84	87	88	90	92
Gourdon	36	38	46	53	56	58	61	64	67	72	75	72	60	52	47	43	40	38
La Rochelle	71	68	63	59	57	54	48	43	39	37	40	44	48	51	54	61	67	71
Laval	53	52	51	48	45	39	38	41	46	49	51	52	55	61	67	67	63	58
Lille	45	41	39	40	42	45	49	51	55	59	63	65	64	63	60	58	56	51
Limoges	64	60	58	58	58	57	55	53	48	45	47	48	48	48	50	54	60	64
Lorient	64	57	51	48	46	43	41	38	36	38	44	49	52	55	58	61	64	67
Luxeuil	51	56	59	61	61	61	63	66	65	58	50	44	40	39	40	39	40	45
Lyon	53	55	57	57	49	49	50	50	51	51	51	52	57	70	68	59	55	53
Mâcon	69	67	60	42	32	31	31	31	32	35	42	59	78	83	79	73	71	70
Mont-de-Marsan	48	46	44	42	41	41	42	46	50	52	50	51	52	53	54	53	51	49
Montélimar	79	79	79	80	83	79	54	31	24	22	22	22	23	27	44	71	80	80
Montpellier	82	77	69	61	54	47	35	26	23	27	36	45	52	59	69	79	84	84
Nancy	44	44	44	46	50	55	60	58	56	55	56	56	54	51	46	42	44	45
Nantes	55	51	48	47	47	49	49	49	47	49	52	55	56	56	59	60	59	59
Nice	92	92	90	79	31	18	15	13	13	11	12	18	54	82	86	88	89	90
Nîmes	87	88	87	84	73	52	35	27	23	20	21	25	38	56	73	80	83	86
Orléans	49	47	46	47	47	47	50	51	50	52	54	55	54	54	55	54	52	51
Pau	38	40	45	48	49	50	53	57	65	72	74	69	60	54	51	49	46	41
Perpignan	77	69	53	30	21	18	18	20	26	33	41	63	79	84	86	87	87	83
Poitiers	47	45	42	38	37	37	40	42	46	50	53	55	59	61	61	59	56	52
Reims	42	40	38	35	35	38	42	50	58	61	62	64	67	69	66	62	54	46
Rennes	48	45	43	42	40	40	43	47	51	54	56	57	59	61	62	60	55	51
Saint Dizier	42	49	51	51	53	58	64	70	73	70	61	55	53	51	48	43	37	36
Saint Quentin	49	48	48	48	48	48	47	48	51	53	55	55	54	54	53	55	55	52
Strasbourg	47	43	39	36	35	40	45	49	53	57	61	66	73	77	73	64	58	51
Toulouse	44	30	27	32	34	39	43	46	49	60	75	82	77	72	67	61	57	53
Tours	52	50	50	49	47	47	49	50	49	50	51	52	53	55	55	54	54	54
Valognes	58	52	47	43	40	38	39	42	44	47	51	55	59	63	66	65	63	61

Table B.5: 3 periods - Night (22.00-06.00)¹

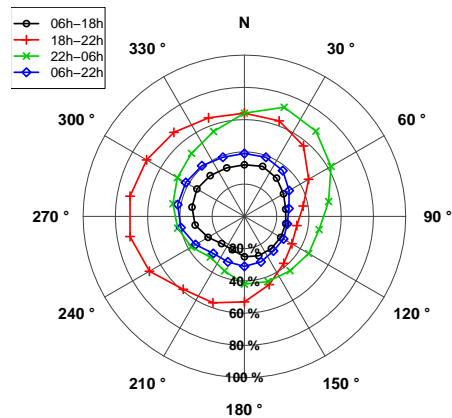
¹ Table B.5 is strictly identical to Table B.2. It is reproduced here for convenience of reading.

B.3 - Occurrence roses

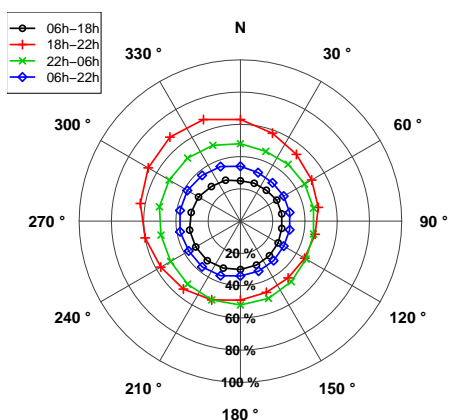
ABBEVILLE



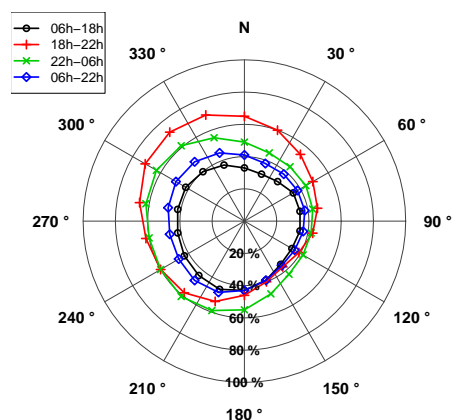
AIX EN PROVENCE

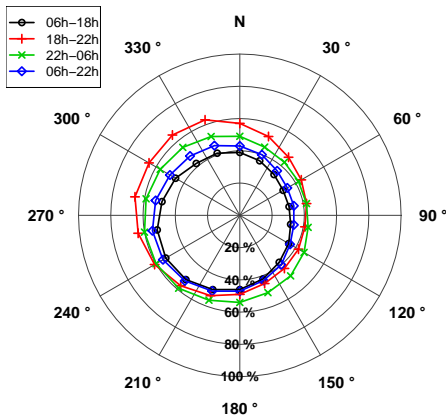
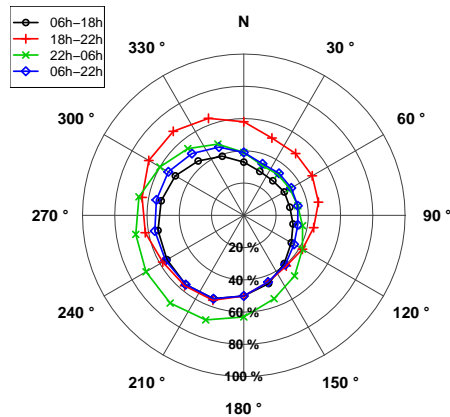
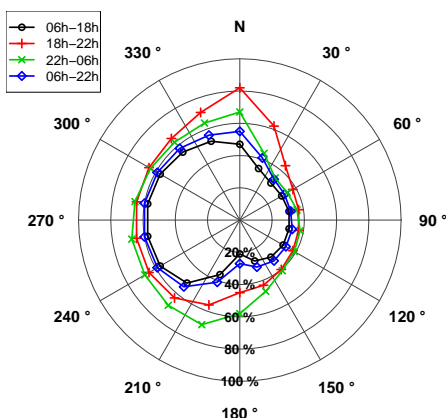
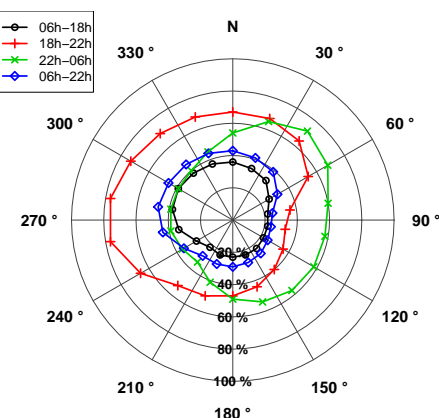
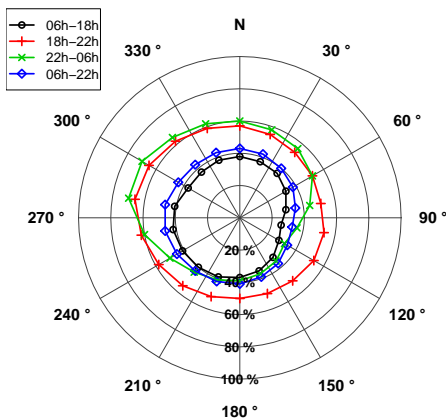
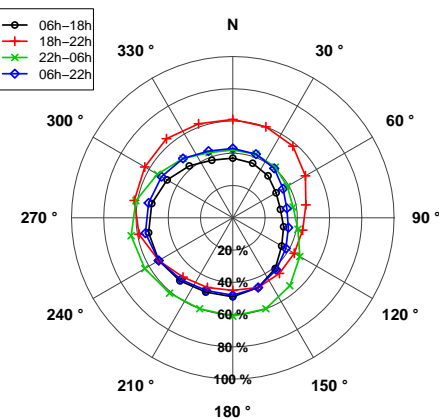


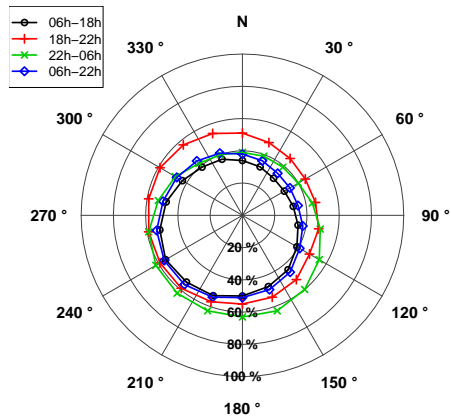
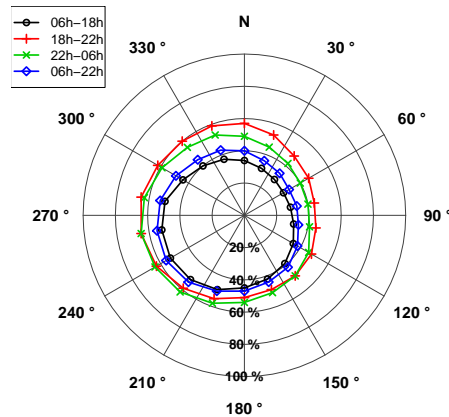
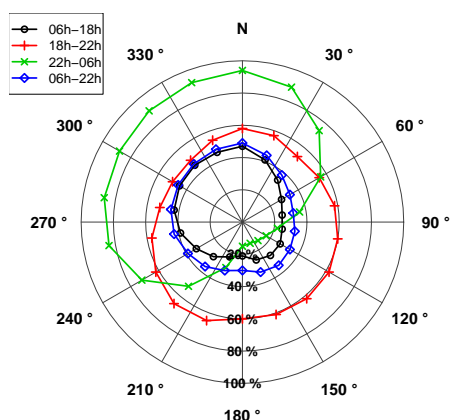
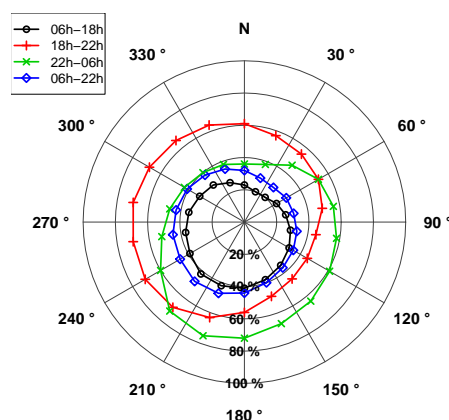
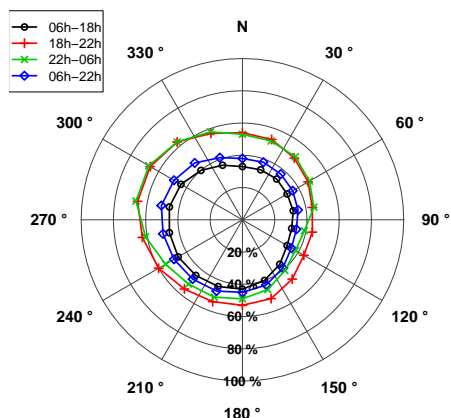
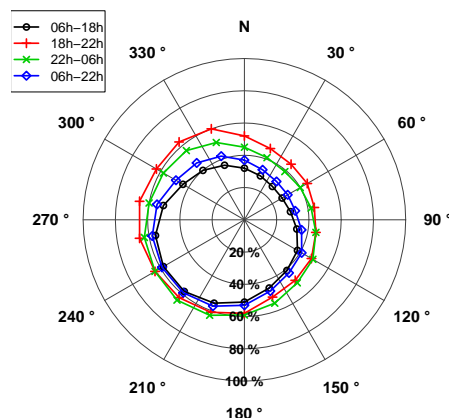
AVORD

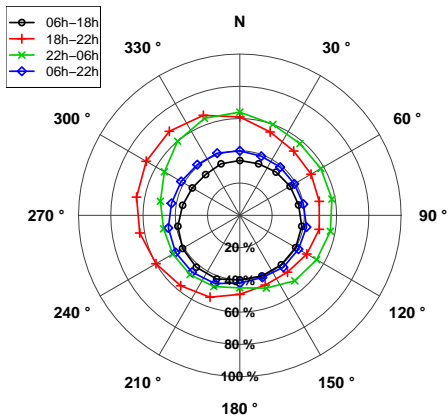
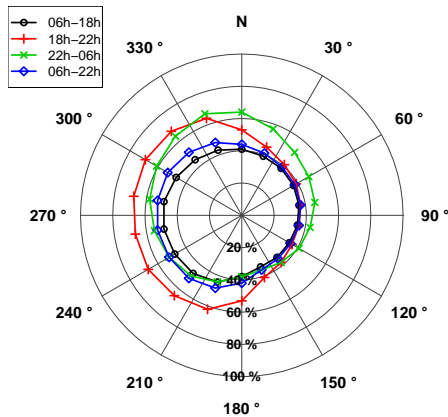
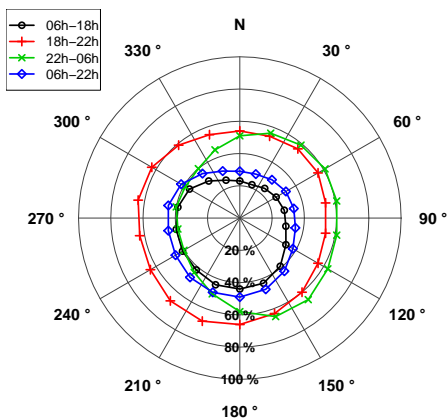
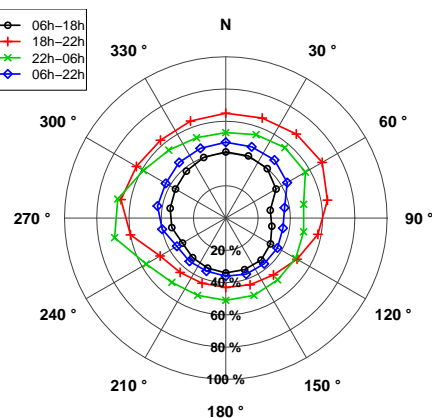
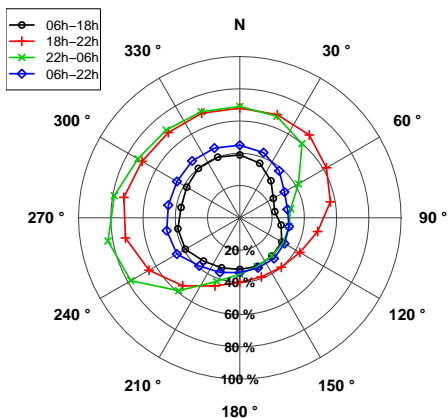
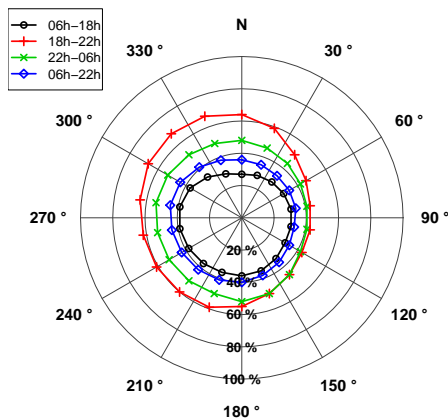


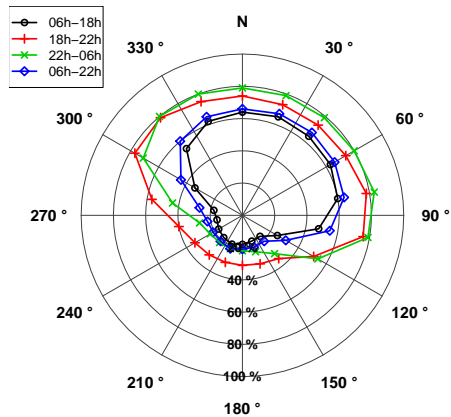
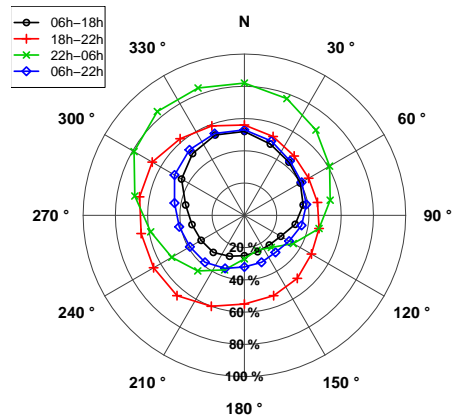
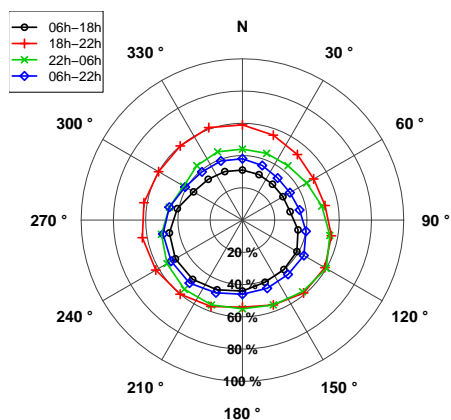
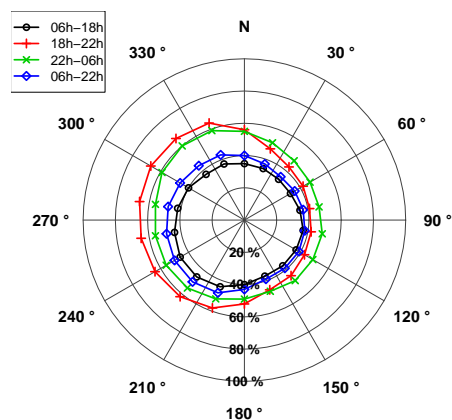
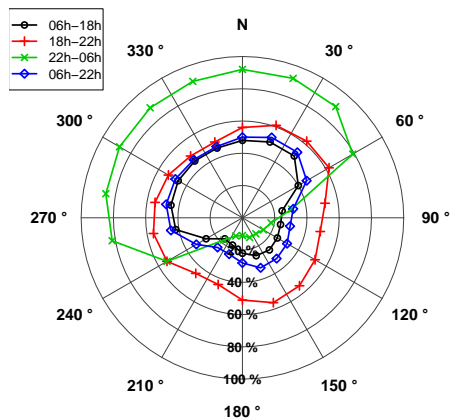
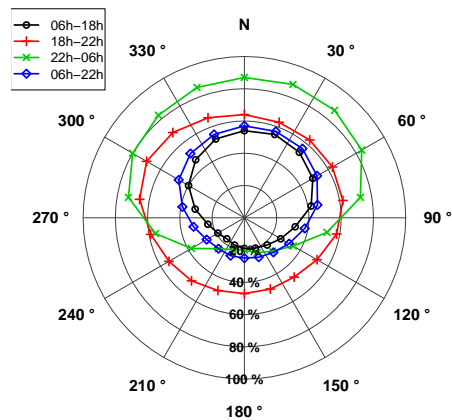
BORDEAUX

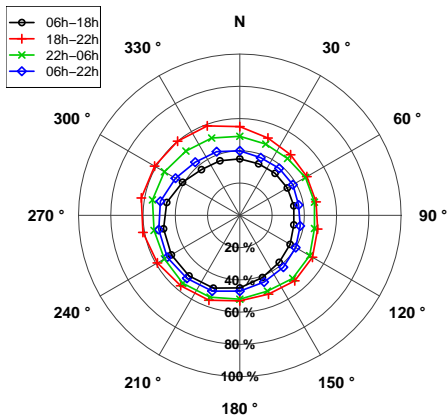
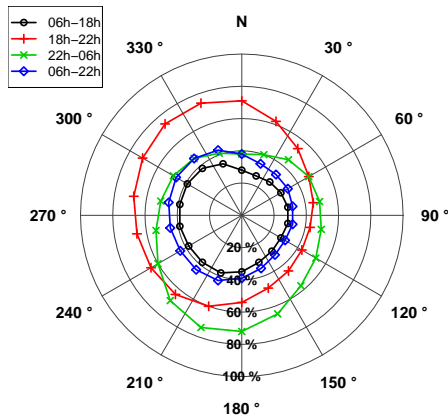
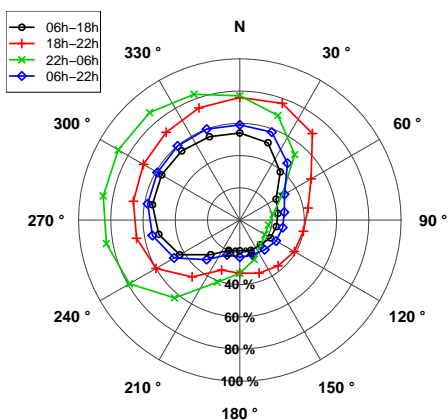
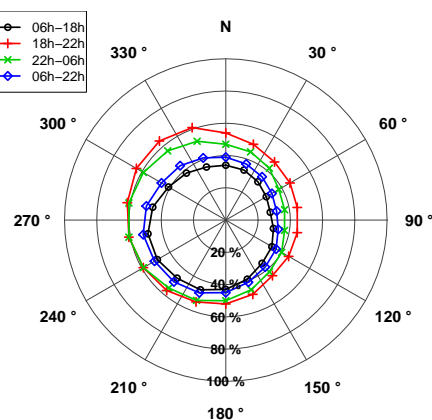
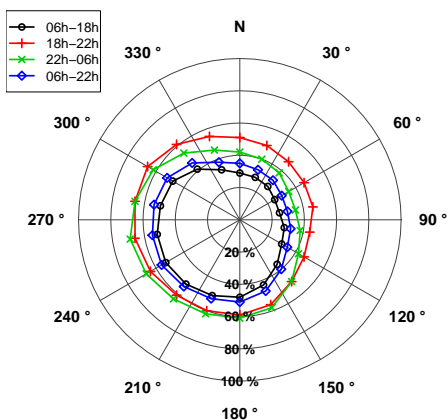
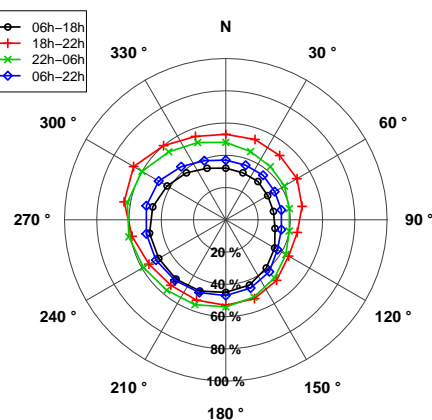


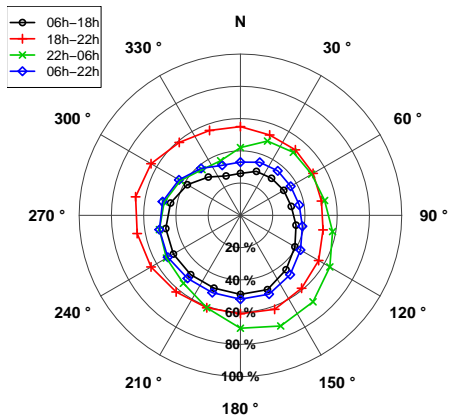
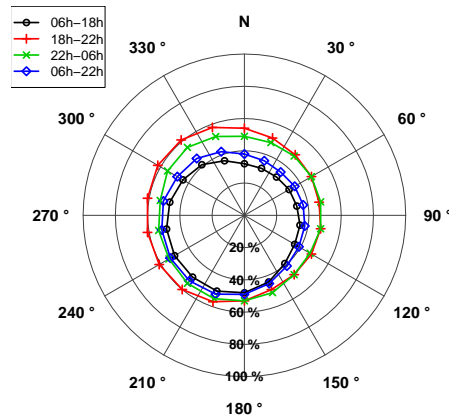
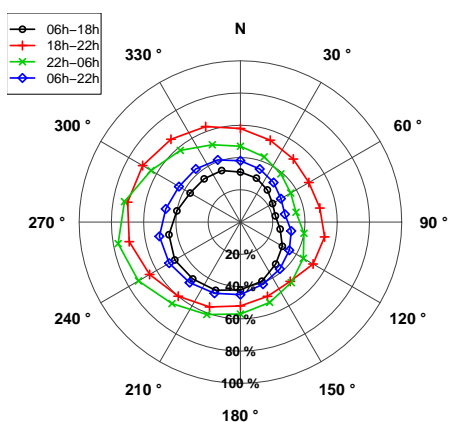
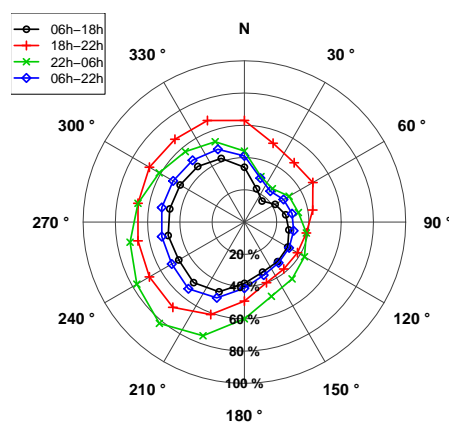
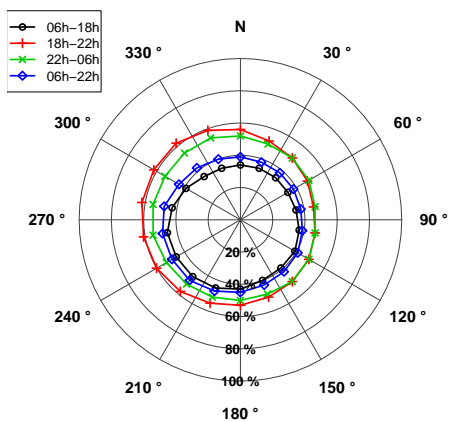
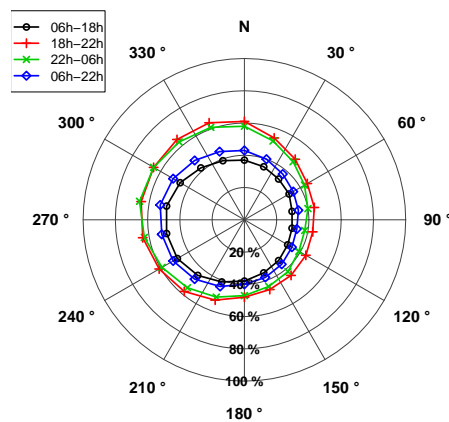
BREST**CAEN****CARCASSONNE****CARPENTRAS****DIJON****DINARD**

DUNKERQUE**EVREUX****FREJUS****GOURDON****LAVAL****LILLE**

LIMOGES**LORIENT****LUXEUIL****LYON****MACON****MONT-DE-MARSAN**

MONTELIMAR**MONTPELLIER****NANCY****NANTES****NICE****NIMES**

ORLEANS**PAU****PERPIGNAN****POITIERS****REIMS****RENNES**

ST-DIZIER**ST QUENTIN****STRASBOURG****TOULOUSE****TOURS****VALOGNES**

B.4 - Maps

The maps in this section have been obtained by kriging assuming a linear variogram model.

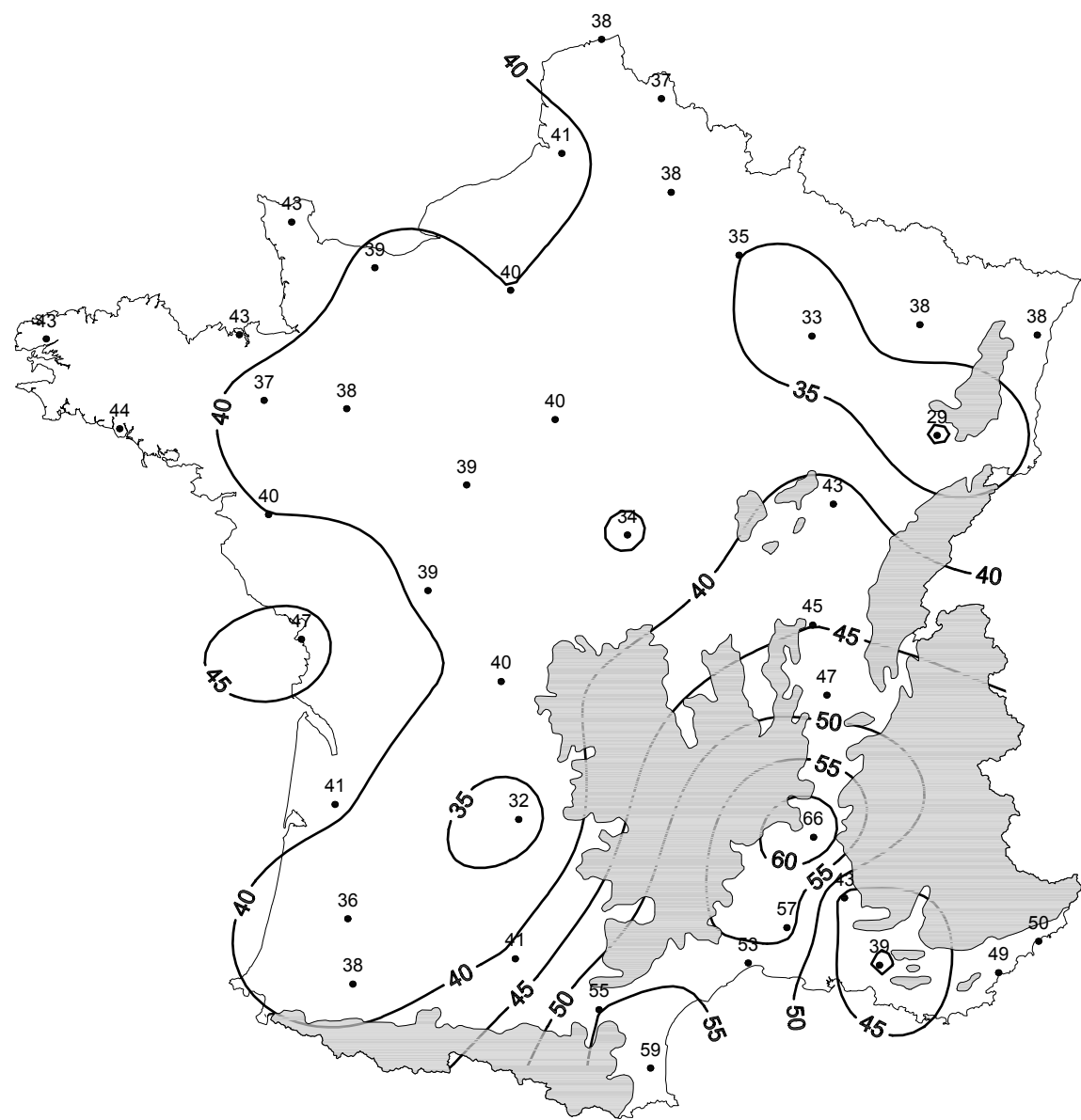


Figure B.3: Occurrences for the 06.00-22.00 period in the direction 0°.

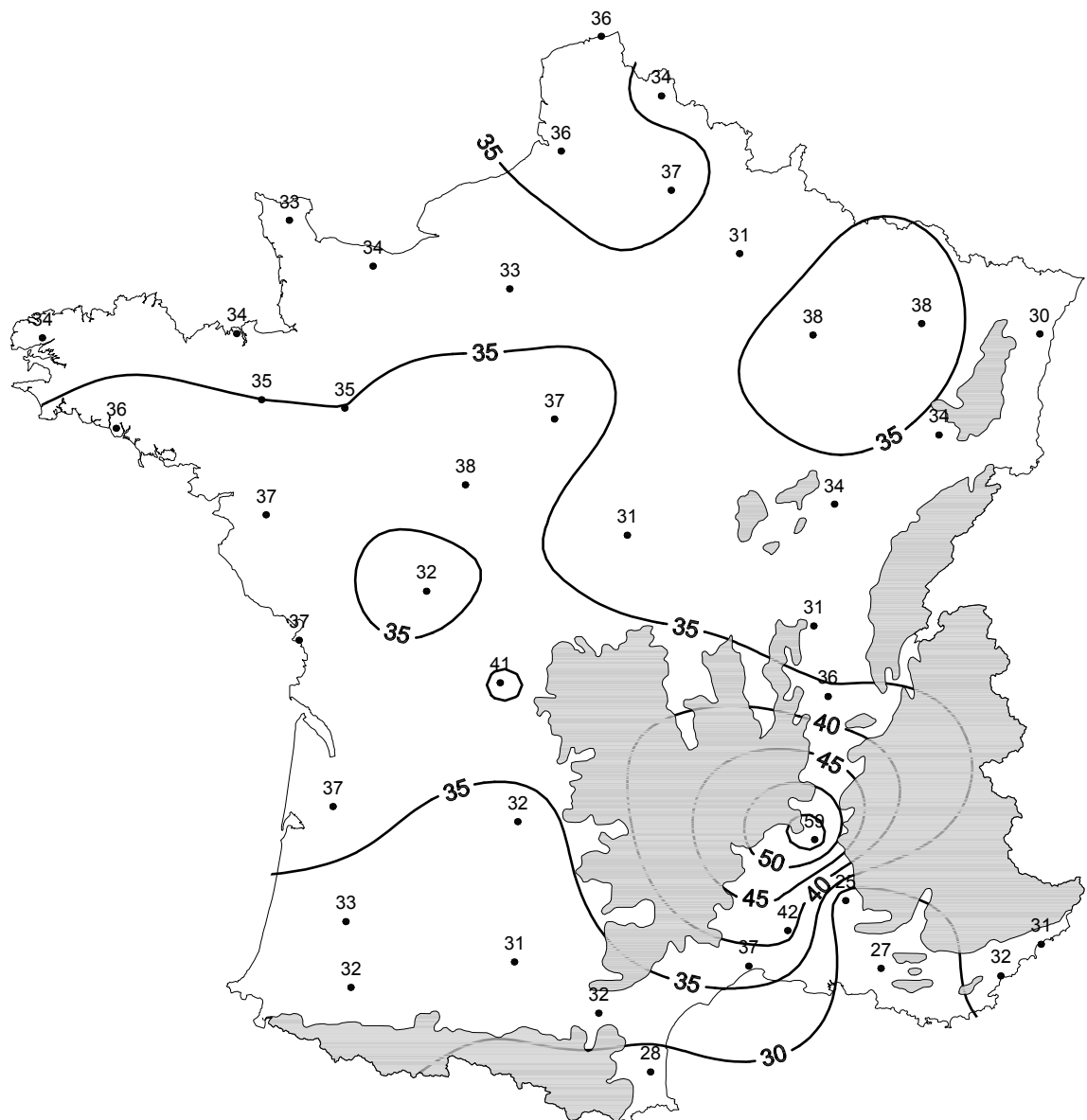


Figure B.4: Occurrences for the 06.00-22.00 period in the direction 90°.

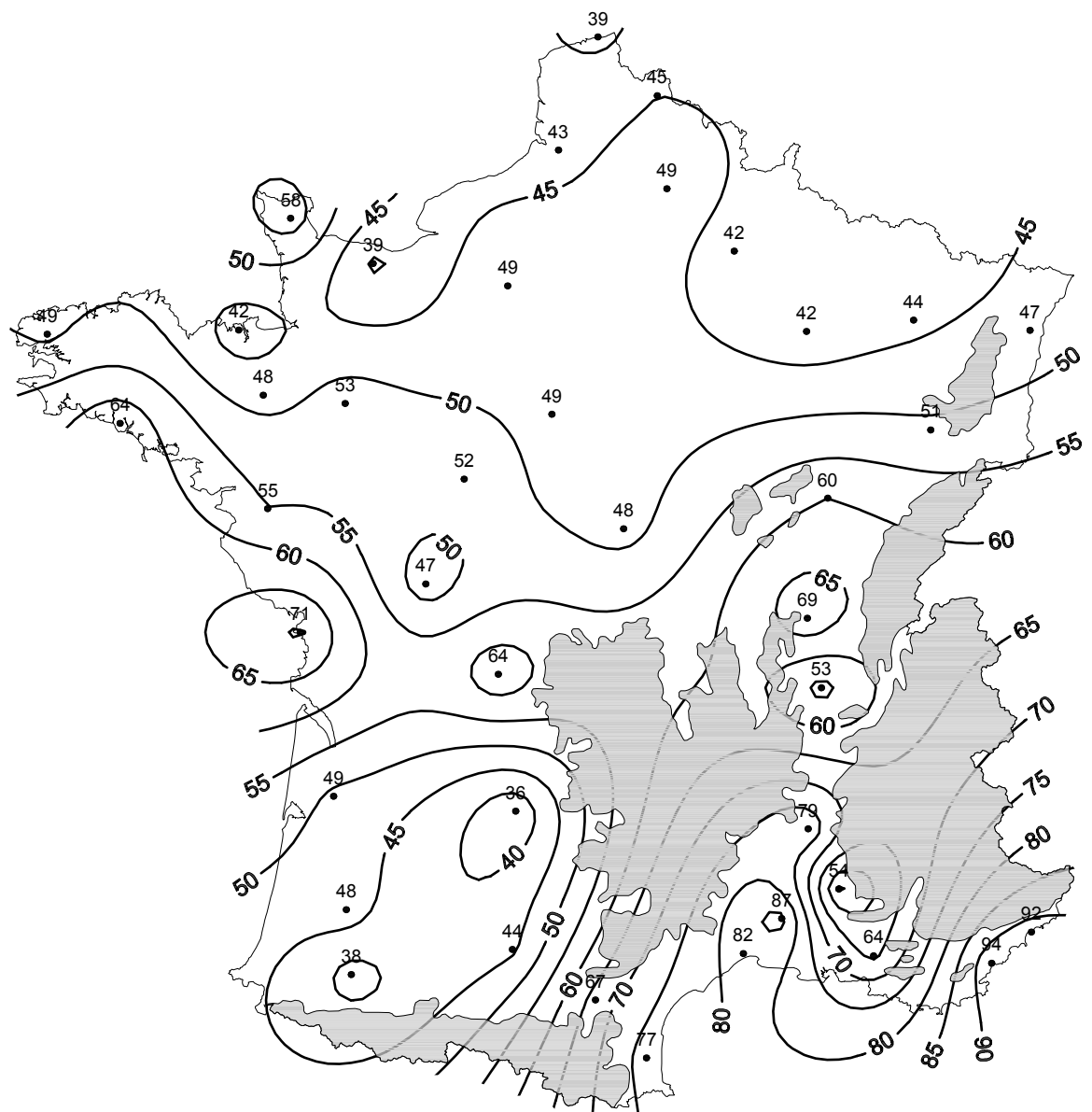


Figure B.5: Occurrences for the 22.00-06.00 period in the direction 0°.

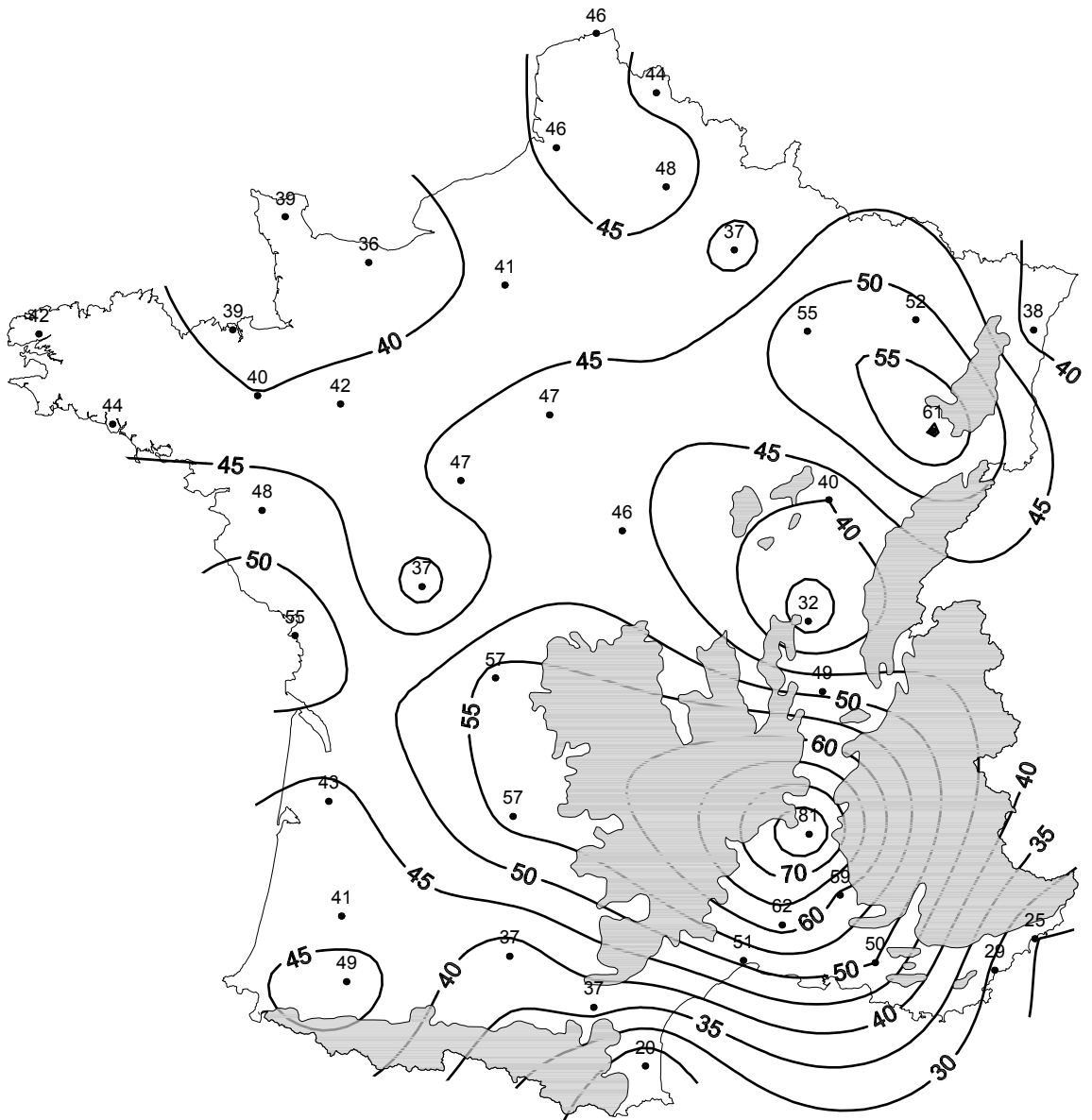


Figure B.6: Occurrences for the 22.00-06.00 period in the direction 90°.

C - Meteorology and sound propagation

The purpose of this appendix is to present briefly the micrometeorological effects on acoustic propagation in an outdoor heterogeneous medium. The reader will find this explained in more detail in [MEDD2006].

C.1 - Atmospheric absorption

The attenuation of sound waves can result from miscellaneous processes linked to the characteristics of fluids in which they propagate. These dissipating processes appear most frequently in complex, heterogeneous or polyphasic fluids as well as in simple fluids, particularly gases. Their significance has been definitively established in many real situations. For 'simple' fluids which do not host special phenomena like cavitation, the acoustic energy is basically dissipated by three processes relating to viscosity, thermal conduction and molecular relaxation respectively. The molecular relaxation phenomenon dominates in atmospheric propagation. This involves delaying establishing a balance due to external stress (physical, thermal, chemical, etc.) and which does not appear instantly. This phenomenon can be significant in the air during propagation from far away or in certain circumstances. The delays are affected greatly by the polyatomic molecule concentrations, especially water vapour molecules, or in laymen's terms by the relative humidity. This effect is directly proportional to the atmospheric pressure and the hygrometry. Standard ISO 9613-1 gives a calculation method to quantify these effects. The attenuation provoked by the atmospheric absorption is a function of two relaxation frequencies f_{rO} and f_{rN} , respectively oxygen and nitrogen. The values of f_{rO} and f_{rN} (in Hz) depend on the atmospheric pressure, temperature and ambient hygrometry; they produce a value for the coefficient of attenuation α , expressed in dB/m for each frequency [ISO9613p1].

Some authors have shown that beyond about 500 Hz, the conversion of a fraction of the sound energy into internal vibration and rotation modes (molecular absorption) was basically determined by the relaxation of *oxygen* molecules in the damp air. Quantitatively, they put this effect at less than 2 dB loss per kilometre, increasing very rapidly with the frequency. It can, therefore, be a not insignificant factor during outdoor sound propagation. Below 500 Hz, the dominant mechanism of molecular absorption is the relaxation of *nitrogen* molecules in the damp air. The energy absorption is far less than generated by the relaxation of oxygen molecules.

Atmospheric absorption must therefore be taken into account during the propagation of sound waves. However, this can be implicit by considering the *relative* sound pressure levels in the free field, or *excess attenuation*.

C.2 - Effects of wind and temperature

The propagation of an acoustic wave is also considerably affected by the characteristics of the environment: the atmospheric conditions (wind, temperature, hygrometry). Considering the spatial-temporal scales brought into play in environmental acoustics (*i.e.* outdoors), these physical phenomena need to be understood through micrometeorological theories rather than through meteorology on a regional scale. Thermal (heat transfer) and aerodynamic (wind profiles) laws, as described at very low altitude (less than 100 m), are therefore used as the framework. The phenomena found at this altitude therefore interact very strongly with the ground (topography, surface and sub-surface temperature, hygrometry, crops, forests, obstacles, buildings, *etc.*). They also change rapidly in time and space, which makes their analytical description and numerical modelling complex.

The thermal and aerodynamic factors with an influence on propagation are as follows:

- **Thermal factors:** the thermal exchanges between the ground and the lower atmospheric layer vary the air temperature based on the height above the ground and vary the sound speed.
- **Aerodynamic factors:** given the state of roughness of the surface of the ground, the wind speed is always faster at a height than at ground level. In a given situation, the sound speed when windy corresponds to the algebraic sum of the sound speed with no wind and the projection of the wind vector on the propagation direction in question. This speed varies therefore depending on the height above the ground.

Through analogy with optical laws, the effect of atmospheric conditions on acoustic propagation can be described through the expression of the acoustic index n of the propagation medium. In a vertical section, it is assumed that this index varies with the altitude z and with the source-receiver distance r , such that:

$$n(r, z) = \frac{c(r, z)}{c_0} = \langle n(r, z) \rangle + \mu(r, z) \quad (\text{C.1})$$

where c is the effective sound speed of the source wave in the medium crossed and c_0 the reference sound speed, typically 340 m/s.

Distinction can thus be made between two phenomena influencing the acoustic propagation: (i) refraction and (ii) atmospheric turbulence. These phenomena are linked respectively to the (i) deterministic $\langle n \rangle$ and (ii) the stochastic μ parts of the index in the propagation medium. In practice, these refraction and turbulence phenomena described in succession below exist side by side and interact, which produces complex propagation conditions and very wide *dispersion* of sound levels encountered *in situ*, with all parameters identical elsewhere (topography, nature of ground, source-receiver geometry, etc.).

C.2.1 - Refraction

The *average* part $\langle n \rangle$ of the index of the medium accounts for the *refraction* of sound waves induced by the *horizontal stratification* of the atmosphere. The average sound speed profiles are calculated from the average values of micrometeorological variables. The timescales involved are in the order of one minute, even one hour. These data are acquired *in situ* via masts fitted with sensors at several heights, or by using instrumentation specific to a single height which requires suitable processing of data based on the Monin-Obukhov theory of similitude. These methods are described in [Gau2009].

A typical calculation is the average of values of sound speed profiles in temporal samples of the order of ten minutes, during which the average wind and temperature profiles are assumed constant or ‘stationary’. However, this assumption of stationary state is rarely verified. The values of micrometeorological parameters, particular the wind - speed and direction - fluctuate considerably during this period due to large-scale circulation phenomena in the troposphere. This so-called ‘intermittency’ phenomenon can produce ‘aerodynamic events’ (e.g. wind flurries) which are not representative of the average of the sample considered and follow on from significant modifications to sound levels during these intermittent events. In terms of the time and space scales involved, this ‘intermittency’ (or ‘turbulence’ for a meteorologist) must not be confused with ‘atmospheric turbulence’ as understood by an acoustician; the effects of this are described in Section C.2.2.

‘Average’ conditions (wind, temperature, hygrometry) therefore relate to each ‘stratum’. This produces so many respective values for the effective average sound speed (its expression $c(z)$) is given below when considering flat, clear land) that its evolution with the distance (dependence in r) is ignored:

$$\langle c(z) \rangle = \sqrt{\gamma RT(z)} + \langle u(z) \rangle \cos \theta = c_0 \sqrt{\frac{\langle T(z) \rangle}{T_0}} + \langle u(z) \rangle \cos \theta \quad (\text{C.2})$$

where $\gamma = \frac{C_p}{C_v} \simeq 1.4$ is the dimensionless ratio of specific heats, R is the specific constant of the dry air ($R=287 \text{ J/(kg K)}$, $c_0 = \sqrt{\gamma RT_0}$ the sound speed reference value in these same conditions with no wind. T_0 is the average air temperature for the time sample considered (Kelvin). The magnitudes $\langle T(z) \rangle$ and $\langle u(z) \rangle$ are the average temperature (K) and the average wind at altitude z respectively and $\cos \theta$ is the projection of the wind direction in the acoustic propagation direction.

The average vertical gradient of the effective sound speed $Grad_c$ is thus expressed by:

$$Grad_c = \frac{\partial \langle c(z) \rangle}{\partial z} = \frac{K}{\sqrt{T(z)}} \frac{\partial \langle T(z) \rangle}{\partial z} + \frac{\partial \langle u(z) \rangle}{\partial z} \cos \theta \quad (\text{C.3})$$

where the constant K can be expressed by:

$$K = \frac{1}{2} \frac{c_0}{\sqrt{T_0}} = \frac{1}{2} \sqrt{\gamma R} \simeq 10 \text{ m.s}^{-1}.K^{-1/2} \quad (\text{C.4})$$

The expression of $\langle c(z) \rangle$ can be linearised by a development limited to the first order, which is therefore written:

$$\langle c(z) \rangle \simeq c_0 + \frac{1}{2} \frac{\gamma R}{c_0} (T(z) - T_0) + \langle u(z) \rangle \cos \theta \quad (\text{C.5})$$

The simpler expression is thus obtained:

$$Grad_c = \frac{\partial \langle c(z) \rangle}{\partial z} \simeq \frac{1}{2} \frac{\gamma R}{c_0} \frac{\partial \langle T(z) \rangle}{\partial z} + \frac{\partial \langle u(z) \rangle}{\partial z} \cos \theta \quad (\text{C.6})$$

The average sound speed profile thus depends on average wind and temperature profiles. This speed profile can be described analytically depending on whether it follows a linear ('lin'), logarithmic ('log'), hybrid ('log-lin') or other law. Figure C.1 shows the potential differences between such sound speed profiles.

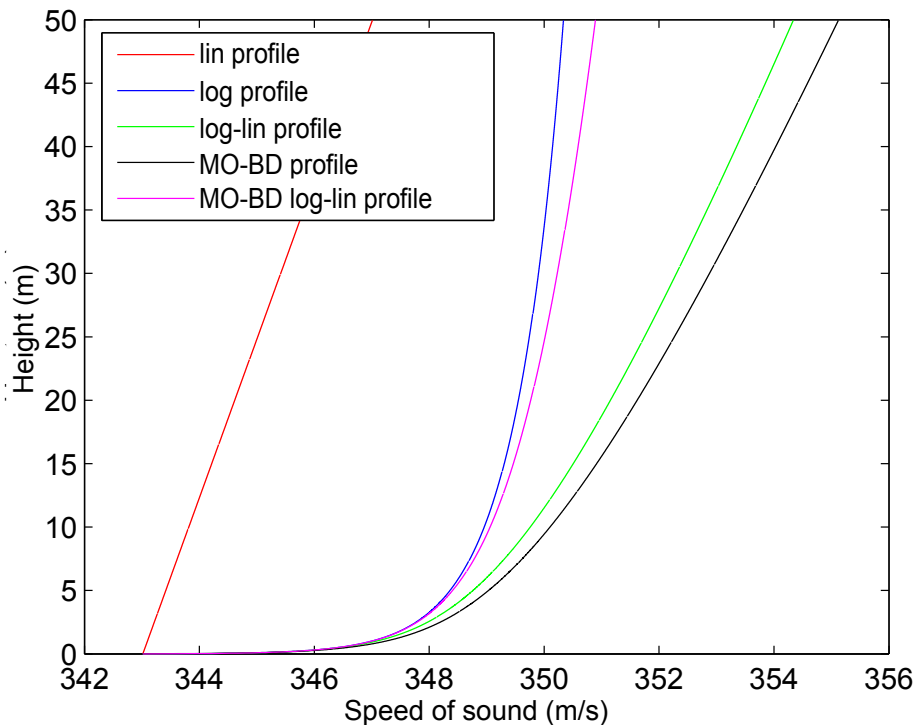


Figure C.1: comparison of 'log', 'lin', 'log-lin', Monin-Obukhov (Businger-Dyer) and Monin-Obukhov 'log-lin' (Businger-Dyer) sound speed profiles [Stu1988] in very downward refraction conditions U4T5, *i.e.* average tail wind and stable atmosphere (*Cf.* Section D.3.2.1).

The 'log' profiles thus have the advantage of conveying the very strong vertical gradient of the sound speed very close to the ground but fail to account for the more modest changes with the altitude above a certain height. Conversely, the 'lin' profiles minimise the effects of being near the ground and do not therefore represent reality at very low altitude.

A good compromise is therefore to use 'log-lin' hybrid profiles, expressed through the parameters a_{log} et b_{lin} which appear in the analytical expression of the vertical profile of the effective sound speed:

$$\langle c(z) \rangle = c_0 + a_{log} \ln \left(1 + \frac{z}{z_0} \right) + b_{lin} z \quad (\text{C.7})$$

where z_0 is the roughness parameter. The value of this parameter is in the order of the 10th of the average height of roughness elements. The typical values of z_0 extend to 0.01 m for closely-mown grass several metres away in an urban environment (*Cf.* Table C.1).

Type of ground	z_0 (m)
Free water	0.002-0.006
Bare earth	0.005-0.02
Closely-mown lawn	0.001
Thick lawn	0.02
Corn (1 m high)	0.1-0.16
Sparse habitat (farms, villages, trees, hedges)	0.2-0.6
Not very dense urban periphery (residential areas, gardens)	0.4-1.2
Dense urban periphery	0.8-1.8
Dense urban area	1.5 - 10

Table C.1: Typical values for the roughness parameter z_0 (according to [Guyot1999] and [Oke1987]).

The vertical gradient is therefore expressed as a derivative of the variable z :

$$\frac{\partial \langle c(z) \rangle}{\partial z} = \frac{a_{log}}{z} + b_{lin} \quad (\text{C.8})$$

The actual profiles are in reality more complex and a more detailed description calls for models with more sophisticated wind and temperature profiles (*Cf.* Figure C.1, Monin-Obukhov profile) [Stu1988].

The main effect of propagation in a variable-sound speed medium is to curve the sound rays downwards or upwards depending on whether the vertical sound speed gradient is respectively positive (*downward refraction conditions*) or negative (*upward refraction conditions*). The transient - and frequently very short - state between these two states represents the *homogeneous propagation conditions*.

Schematically, three main types of propagation can be considered depending on the form of the vertical sound speed profile. These three types are detailed in the following paragraphs.

C.2.1.1 - Propagation of sound in the presence of a negative vertical sound speed gradient

Thermal origin: in this case, the temperature drops with the height above the ground. This phenomenon is produced during the day: the sun heats the ground which transfers its heat to the lower atmospheric layers. The result is that the air temperature near the ground is higher than at a height. The sound speed decreases with the height in relation to the ground.

Aerodynamic origin: when the wind blows in the opposite direction from the sound propagation direction, the wind speed is subtracted from the sound speed in an immobile atmosphere. The sound speed, in the direction of propagation, therefore drops with the height above the ground.

The acoustic effect of these thermal or aerodynamic conditions can be represented in Figure C.2.

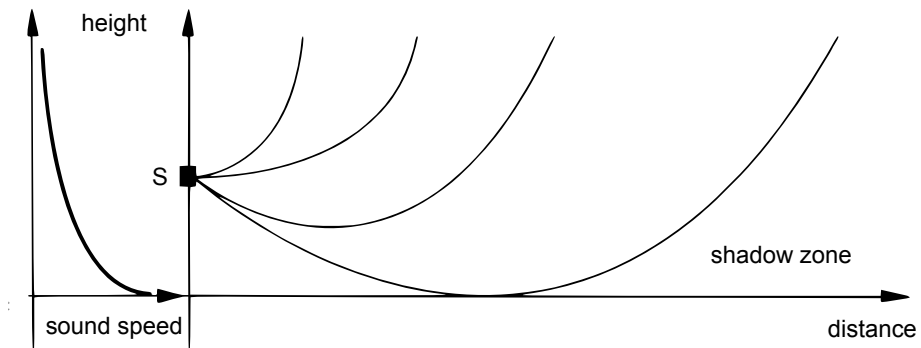


Figure C.2: Acoustic propagation in upward refraction conditions.

The acoustic rays travel upwards. In these conditions, the far field sound level is weaker than without meteorological effects. In theory, there is even a ‘shadow zone’ where no direct acoustic ray can penetrate and where the very weak sound level in actual fact comes from scattering and turbulence phenomena. This type of conditions does not therefore favour sound propagation. In this document they are called ‘upward refraction’ conditions.

C.2.1.2 - Propagation of sound in the presence of a positive vertical sound gradient

Thermal origin: at night, when the sky is clear, the ground radiates and cools more easily than the air. The low atmospheric layers become colder than the upper layers and the air temperature rises with the height above the ground. This situation is called ‘temperature inversion’. It corresponds to a situation of positive vertical sound speed gradient.

Aerodynamic origin: if the wind direction corresponds to the direction of the acoustic wave propagation, the algebraic sum of the sound speed in homogeneous atmosphere and of the wind speed will provide a sound speed profile which increases with the height.

The acoustic effect of these conditions is represented in Figure C.3.

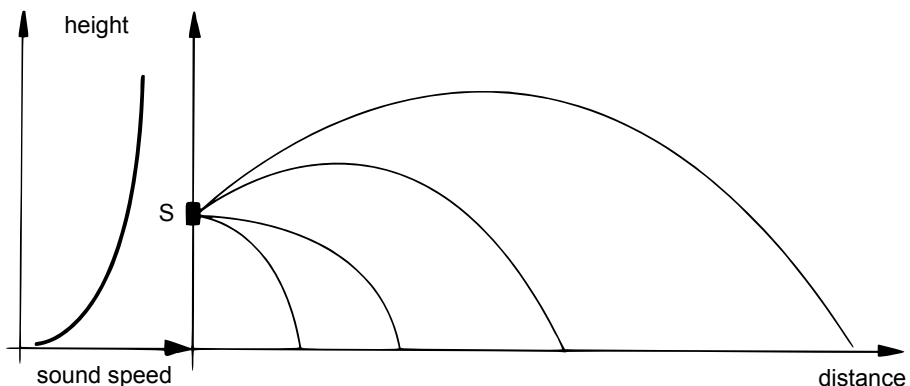


Figure C.3: Acoustic propagation in downward-refraction conditions.

The acoustic rays travel downwards. In these conditions, the far field sound level is stronger than without meteorological effects. This meteorological situation therefore favours sound propagation. In this document this is referred to as ‘downward refraction’ conditions.

For example, during the day, downward refraction conditions are obtained for tail winds from the source to the receiver at more than 1.5 m/s in dull weather and more than 3 m/s when the sun is out. At night, these conditions are obtained when there is no wind or with a tail wind. Temperature inversion is considered to be systematic.

C.2.1.3 - Propagation of sound in the presence of a nil vertical sound gradient

The likelihood of given thermal and aerodynamic situations occurring jointly on a site varies tremendously. In particular, micrometeorological situations inducing a lack of these effects are relatively rare. In acoustic terms, this means a lack of vertical sound speed gradient. This phenomenon can occur in two types of circumstance:

- When the wind speed is totally nil AND the air temperature is constant according to the height above the ground. This normally occurs fleetingly close to sunrise and sunset or under total, thick cloud cover.
- When the thermal and aerodynamic effects tend to offset each other. One example of this is a wind blowing in the opposite direction from the propagation at night, when the sky is clear, or during a very sunny day with an average or light tail wind. However, this compensation is only possible for very accurate values of these phenomena and does not necessarily occur for all heights.

These two phenomena are therefore fairly rare and the propagation of the sound with no vertical sound speed gradient should be considered more as a boundary between the two previous propagation conditions than as a propagation method in its own right. In this document, this situation is qualified as ‘homogeneous’, by implying that it involves propagation conditions in a homogeneous medium. These conditions lead to sound propagation in straight rays (*Cf.* Figure C.4).

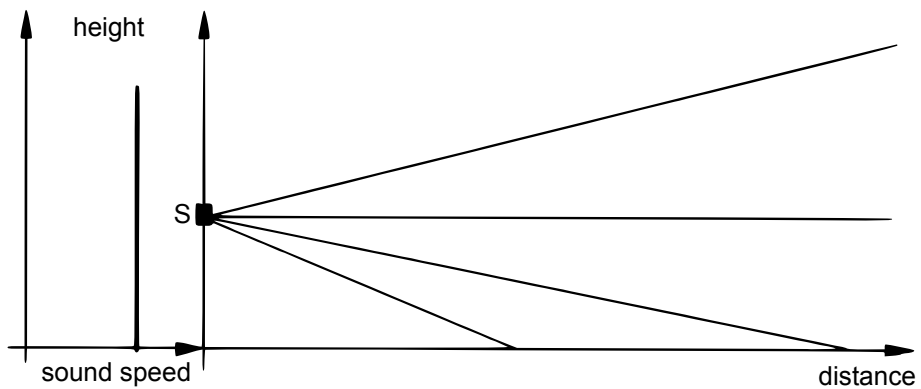


Figure C.4: Acoustic propagation in homogeneous conditions.

The effects of refraction are illustrated in Table C.2 on sound level maps for propagation above firstly, a totally-reflecting ground (up to 10 m from the source) and secondly, a ground which absorbs the sound waves partially. This figure thus shows the changes in spatial distribution (curve) of sound energy concentration areas (lobes). The ground effects (attenuation of the acoustic energy by absorption - read above) are boosted more (downward-refraction conditions) or less (upward refraction conditions). Without turbulence, the ‘shadow zone’ due to the ground effects can thus be boosted considerably in upward refraction conditions compared with propagation in homogeneous conditions ($a_{log}=0$ m/s - *Cf.* Table C.3 - scenario 1). Note that these refraction effects do not depend on the frequency considered.

It must be emphasised that the differences in sound levels observed in ‘downward’ and ‘upward’ areas (compared with homogeneous) are not equal in absolute value. In practice, there are far more sound level reductions than increases. In addition, sound level dispersion is far weaker when propagating in a ‘downward refraction’ situation than an ‘upward refraction’ one. Figure C.5 illustrates this phenomenon, following the sign of the vertical sound speed gradient, by providing the value of attenuations noted in flat land as a function of the point source-receiver distance, for a source 6 m high and a receiver 1.5 m high.

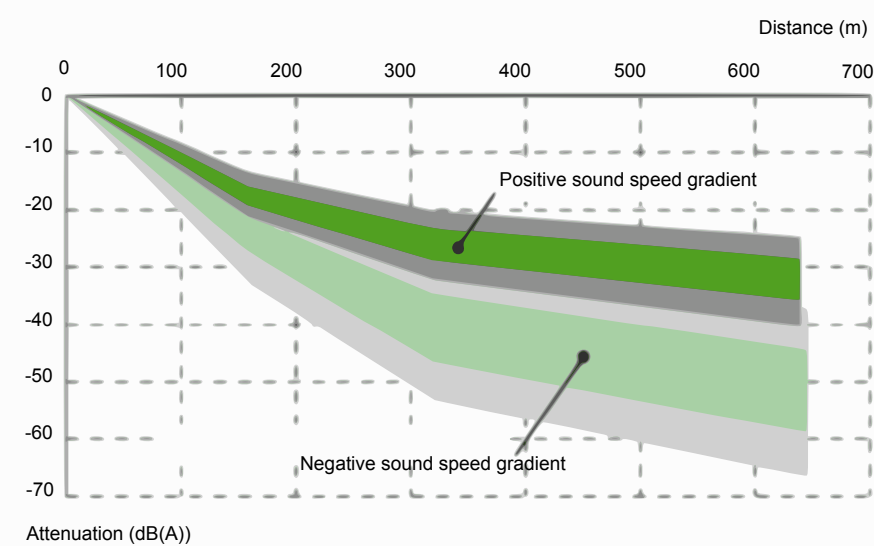


Figure C.5: Attenuation and dispersion of sound levels based on the distance from the source for downward (positive gradient) and upward (negative gradient) refraction conditions [Zou1998].

C.2.2 - Atmospheric turbulence

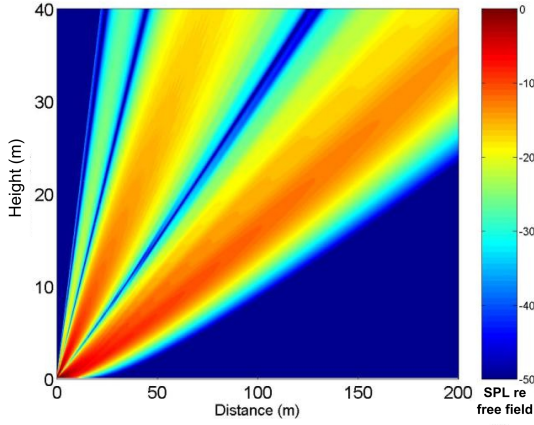
The fluctuating (or stochastic) part μ of the index of the medium conveys the effect of atmospheric turbulence on acoustic propagation caused by random fluctuations of micrometeorological magnitudes. The timescale considered here is less than one second (0.02 to 0.1 s). It is the scale of temporal variation where the effects are most significant in acoustic propagation at a tremendous distance. The problem then lies in characterising this turbulence experimentally, where the characteristic parameters can be evaluated using equipment with high frequency acquisition equipment like a three-dimensional ultrasonic anemometer or a hot wire anemometer. In theory, this atmospheric turbulence is basically described by its scale(s) and by the variance in the refraction index $\langle \mu^2 \rangle$. This variance is frequently incorrectly called ‘turbulence intensity’. As a first approach, the fluctuating part is linked to the fluctuations in micrometeorological variables by the following approximation:

$$\mu(r, z) = -\frac{T'(r, z)}{2T_0} - \frac{u'(r, z)}{c_0} \quad (\text{C.9})$$

where T' and u' represent respectively the stochastic parts of the temperature T and the longitudinal component of the wind u , aligned with the propagation direction. T_0 and c_0 are (constant) reference values for the temperature and the sound speed (typically $T_0=288$ K and $c_0=340$ m/s).

Assuming ‘frozen turbulence’, the turbulence characteristics can be therefore considered as invariant for the time taken by the sound wave to cross. An additional assumption of isotropy and homogeneity allows us to model its effects numerically in the acoustic propagation. These effects depend significantly on the frequency and are presented in Table C.3 (monochromatic calculation at 4 kHz). The atmospheric turbulence homogenises the sound levels in space. Thus, the destructive interference figures (‘lines’ of lesser sound energy) which appear with a deterministic calculation, *i.e.* turbulence free, are ‘smoothed over’ when there is turbulence. Similarly, the sound energy at the limit of the shadow zone which appears in the deterministic scenario (ground effect + any upward refraction conditions) is diffused in this area with turbulence present, where the calculated sound levels thus have realistic values once more.

**Scenario 1: upward refraction conditions
with $a_{log}=-2$ m/s**



**Scenario 2: downward refraction conditions
with $a_{log}=+2$ m/s**

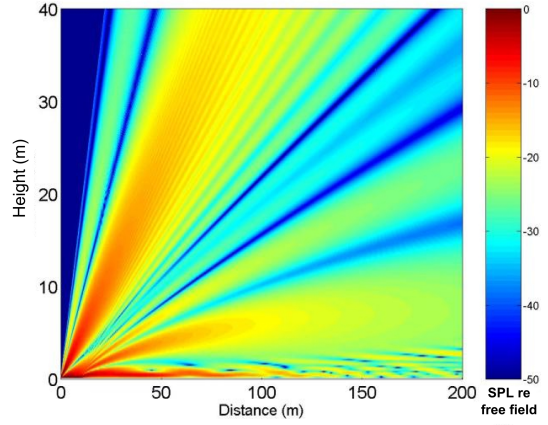
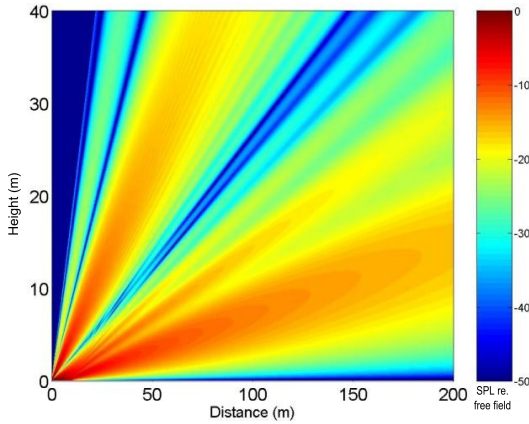


Table C.2: Illustration of the effect of the horizontal stratification of the atmosphere on the acoustic propagation (refraction); $f=4$ kHz, $h_s=0.1$ m, $\sigma_1=100000$ kNsm $^{-4}$, $\sigma_2=1000$ kNsm $^{-4}$, $D_{impedance-discontinuity}=10$ m, ‘log’ profile [MEDD2006]. σ is the air flow resistivity.

**Scenario 1: homogeneous atmosphere
(deterministic calculation)**



**Scenario 2: turbulent atmosphere
($\langle \mu^2 \rangle = 8 \cdot 10^{-6}$)**

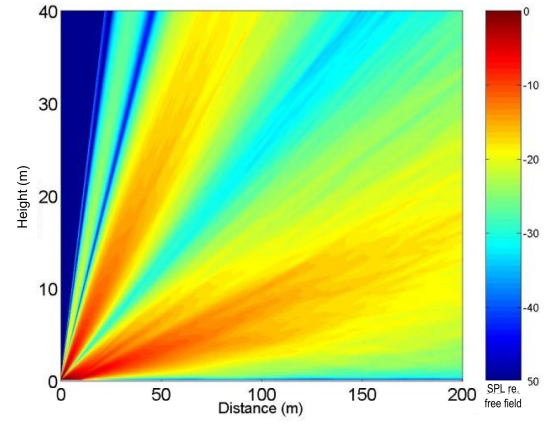


Table C.3: Illustration of the effect of stochastic variations of the index of the medium (atmospheric turbulence) $f=4$ kHz, $h_s=0.1$ m, $\sigma_1=100000$ kNsm $^{-4}$, $\sigma_2=1000$ kNsm $^{-4}$, $D_{impedance-discontinuity}=10$ m, ‘log’ profile [MEDD2006].

D - Meteorological analysis of an acoustic situation

D.1 - Opening remarks

The influence of micrometeorological effects on acoustic propagation is a major phenomenon relatively far and very far from a random sound source (road, railway or industrial noise, *etc.*). Understanding these physical phenomena, one cause of acoustic fluctuations, is therefore important to analyse the results from measured or calculated sound levels correctly. Depending on the anticipated configuration (geometry, topography, ground characteristics, *etc.*), these effects can even be significant from a few dozen metres away from the source. In strictly French legal terms, these effects only have to be taken into account from 250 m, as stipulated in the order of 5 May 1995 on noise from road infrastructures. From a normative viewpoint, the distance limit is set at 100 m for road noise [NFS31085]. Similarly, these official documents only consider ‘average’ meteorological effects on acoustic propagation, *i.e.* the *deterministic* effects relating to timescales in the order of one minute or one hour - even one day - which convey the phenomenon of *average refraction* of the sound field (downward or upward refraction conditions). Other physical phenomena, however, no longer deterministic but *stochastic*, such as *intermittency* or *atmospheric turbulence* can also have a major influence on the sound levels in some circumstances, in particular at the highest frequencies and greatest distances for the turbulence.

These micrometeorological effects on the acoustic propagation are presented briefly in Appendix C to this document. In the NMPB-Roads-2008, refraction and turbulence are considered from the first metres of propagation.

This section (including Appendix C) has been slightly expanded compared with the NMPB-Roads-96 [NMPB96] so as to introduce a few results from recent work on the topic [MEDD2006]. These results are presented in summary and, we hope, instructive fashion with the intention of harmonising the notations, criteria, magnitudes, limit values and practices encountered in the European acoustician community, be it in the scientific or technical field (technicians, design engineers, scientists, developers, *etc.*) or in a legal and normative context (client function, project management, *etc.*).

This section attempts more specifically to describe the meteorological analysis method for an acoustic situation, *i.e.* characterising *in situ* propagation conditions in the sense of average refraction. Analysing an acoustic situation meteorologically must account for *propagation conditions representative* of those existing between source(s) and receiver(s) for one or more fixed periods as fully and as accurately as possible. This therefore involves a strict assessment of the *characteristics averaged out in space and time*.

This section therefore sets out firstly to specify these terms in our study framework (*Cf.* Section D.2) before describing the methods for analysing an acoustic situation meteorologically, to be in a position to determine the propagation conditions in the short, mid and long term (*Cf.* Section D.3).

D.2 - Spatio-temporal averages and scales

D.2.1 - Spatial representativeness

In many cases, it is assumed, to make things simple, that the atmosphere is horizontally homogeneous, *i.e.* that the wind speed and temperature values only depend on the height of the point considered in relation to the ground and that they are independent from horizontal coordinates (*Cf.* Appendix C).

In practice, these conditions are only found, as a first approximation, in a so-say ‘ideal’ site, corresponding to the following characteristics:

- flat, horizontal site;
- obstacle-free site;
- homogeneous ground and vegetation;
- no large water masses nearby (lakes, rivers);

- site clear and homogeneous well beyond the area concerned by the sound propagation.

In these conditions, the vertical wind speed and temperature profiles can be considered, in a first approximation, as independent from horizontal coordinates (distance from the source). Thus, under certain conditions, the vertical profiles can be modelled from regional meteorological information, for example from official Météo-France regional stations, or reconstituted theoretically from information on wind and temperature (*Cf. Section D.3.2*).

However, these ideal conditions are very rarely met: in reality, the vertical temperature and wind speed profiles dependent on a number of local factors linked to the topography, type of ground, plant cover, *etc..* The ideal site hypotheses are not always valid given these factors, which frequently means, therefore, that systematic correlation between the regional meteorological data and the micrometeorological characteristics of a precise site (local scale) can no longer be considered, despite the site being very near an official meteorological station ('site effect'). In addition, the vertical profiles depend frequently on the distance (from the source and/or an obstacle) and do not, therefore, follow the same theoretical laws.

It can prove very complex to determine the micrometeorological conditions characteristic of a site, especially given the potential spatial heterogeneities between the source and the receiver. It can even occasionally be necessary to use advanced (geo)statistical tools to estimate them. These considerations are valid for a point source and all the more for a linear (road noise) or surface (industrial noise) source, and all the more again in a dense urban environment. It is therefore up to the chief designer to estimate the *average vertical profiles he deems representative of the spatial configuration studied* (type of ground, topography, buildings, vegetation, miscellaneous obstacles, *etc.*), to be able to return to the *spatially homogeneous vertical profiles according to the vertical section(s) between source(s) and receiver(s)*.

D.2.2 - Temporal representativeness

The vertical wind speed and temperature profiles vary significantly over time due to fluctuations in meteorological conditions. These random fluctuations can occur in very different timescales, from a few fractions of a second to several hours, even longer periods based on daily, seasonal or annual cycles or even more 'long-term' trends (*Cf. Section C.2.2*). The result is that, like any random variable, characterising the atmospheric medium crossed by the acoustic wave is, with everything else equal, basically linked to its observation time.

Thus, the far field sound level is formed by overlapping very short-lived fluctuations and cyclic phenomena of random amplitude relating to the hourly, daily and seasonal cycles.

Given the phenomena brought into play and the purpose of acoustic results, consideration should be given to taking meteorological effects into account in long range sound propagation in three different timescales:

- 'short-term' scale
- 'mid-term' scale
- 'long-term' scale

D.2.2.1 - Short-term scale

This scale relates to a period during which the statistical characteristics of meteorological conditions can be considered as stationary. This type of information can be acquired experimentally by meteorological and acoustic measurements in *synchronised periods in the order of ten minutes to two hours* and by calculating the average of meteorological variables measured over this period or 'basic interval' in normative terms.[\[NFS31085\]](#) In this interval, the meteorological conditions can be considered as locally stationary, *i.e.* their statistical characteristics are relatively constant in the interval in question. This approximation comes down to ignoring the intermittency and turbulence phenomena and their effects (*Cf. Appendix C*) during the period in question.

The acoustic phenomena observed in this timescale can normally be modelled correctly by current propagation models, provided a representative sound speed profile is available as input data for the model.

D.2.2.2 - Mid-term scale

This is a fundamental timescale, as it corresponds to the durations of *legal reference periods* (or ‘reference interval’ in normative terms [NFS31085]) and therefore to the *minimum measuring periods* (or ‘measuring interval’ in normative terms [NFS31085]):

- Nationally (road and railway noise)
 - Day: 06.00-22.00
 - Night: 22.00-06.00
- Under European Directive 2002/49/EC in France
 - Day: 06.00-18.00
 - Evening: 18.00-22.00
 - Night: 22.00-06.00

During measurements, this timescale characterises the acoustic and micrometeorological fluctuations between several short-term samples. A measurement taken in a given reference period can thus be interpreted at a later date. It is always possible to know the meteorological conditions during particular measurements provided certain customary precautions are taken. Used in calculations, this timescale can either use meteorological information at a later date to compare calculation results with a measurement taken in special conditions or use theoretically values making up the hypotheses to calculate a sound level in given atmospheric states. In both cases, the sound levels can be calculated by a composition of ‘short-term’ situations weighted by a distribution of propagation conditions observed or defined by hypothesis.

D.2.2.3 - Long-term scale

Where a calculated *value representative of an average over a long period* is sought, the meteorological conditions must be defined by analysing them in a ‘long-term’ scale. This approach differs considerably from the previous ones, as it calls for statistical knowledge of the phenomenon. It corresponds to the statistical distribution of ‘short-term’ data over a sufficiently representative period to give this statistical estimation meaning and provide robust results.

Meteorologists consider that observation times should be about thirty years to be representative of long-term conditions. This period covers virtually all meteorological situations on a site. Averages over shorter periods become too sensitive to exceptional years. Calculations relating to ‘seasonal normals’ well-known in meteorology are performed especially in this timescale.

The ‘long-term’ calculation results must therefore furnish information which, to be representative, must incorporate meteorological data corresponding to the order of magnitude of this timescale to minimise the inaccuracy provided by the meteorological fluctuations. Theoretically, the ‘long-term’ sound level should therefore be presented statistically, for example by providing the distribution function of the L_{Aeq} over a period of about thirty years. It is clear that this statistical characteristic cannot be measured directly and therefore remains inaccessible at first glance.

Nevertheless, the need for such representation becomes quite clear as soon as the following basic questions are asked:

- how is a calculation result compared with a measurement?
- how accurate should a measurement be when it has to be compared with a legal value?
- is it acceptable for a measurement to exceed a calculated sound level occasionally? If yes, what is the percentage of overshoot risk?

It is difficult to respond to these questions given that the far field sound levels are caused by complex physical and not always independent phenomena (*Cf.* Appendix C). In addition, these levels are often considered to be deterministic variables whereas in reality they are fairly stochastic. A method for estimating the sound level representative of ‘long-term’ meteorological conditions must therefore be used (*Cf.* Section 5.1).

D.3 - Meteorological analysis of an acoustic situation

D.3.1 - Classifying propagation conditions

The timescales considered here have been discussed in Section D.2.2: assuming that the atmosphere is ‘frozen’ as the sound wave passes through it, it can be considered - as a first approximation, *i.e.* by ignoring intermittency and atmospheric turbulence phenomena (*Cf.* Appendix C) - that the short-term scale can characterise a state representative of the propagation medium correctly, *i.e.* a period when the average wind and temperature fields can be considered ‘stationary’.

In practice, the acoustic propagation conditions are characterised over a total measuring period where the temporal scale is in the order of the ‘mid-term’ (*Cf.* Section D.2.2), frequently called ‘measuring interval’ in the normative domain. This period is therefore discretised temporally by the short-term samples mentioned above (or ‘basic intervals’ in normative terms). The operator fixes the sampling, which typically ranges from *ten minutes to two hours* depending on the stability conditions of the atmosphere.

Propagation conditions can also be associated with each acoustic measurement sample during each basic interval.

National class	‘European class’	Propagation conditions:	Grad_c	Effects on the sound levels
--	M0	Very upward refraction	$\text{Grad}_c \ll 0$	Extremely high attenuation and dispersion
-	M1	Upward refraction	$\text{Grad}_c < 0$	High attenuation and dispersion
Z	M2	Homogeneous	$\text{Grad}_c = 0$	‘Normal’ propagation and dispersion
+	M3	Downward refraction	$\text{Grad}_c > 0$	Major increase and moderate dispersion
++	M4	Very downward refraction	$\text{Grad}_c \gg 0$	Extremely high increase and very moderate dispersion

Table D.1: *Qualitative* definition of average acoustic propagation classes - French and ‘European’ notation conventions.

For this, the characteristic magnitude for the refraction phenomenon is considered *i.e.* the average¹ for the vertical gradient of the effective sound gradient Grad_c , expressed as a function of the vertical temperature gradient Grad_T and the vertical wind speed gradient projected on the propagation axis Grad_{VV} (*Cf.* Appendix C):

$$\text{Grad}_c = \frac{\partial c_{eff}}{\partial z} = \frac{K}{\sqrt{T}} \text{Grad}_T + \text{Grad}_{VV} \cdot \cos \theta \simeq \frac{1}{2} \frac{\gamma R}{c_0} \text{Grad}_T + \text{Grad}_{VV} \quad (\text{D.1})$$

where θ is the angle between the propagation direction and the wind direction, $\gamma = \frac{C_p}{C_v} \simeq 1.4$ is the dimensionless ratio of specific heats, R is the specific constant of the dry air ($R=287 \text{ J}/(\text{kg K})$), $c_0 = \sqrt{\gamma R T_0}$ the sound speed reference value in these same conditions with no wind and T_0 is the average air temperature for the time sample considered (Kelvin).

Thus, five average¹ propagation classes are defined for each noise/weather synchronised sample (*Cf.* Table D.1).

The following comments apply to this table:

- in reality, perfectly homogenous conditions are relatively rare and fleeting. In addition, these conditions are extremely tricky to characterise experimentally for methodological (intermittency) and metrological

¹ temporal and spatial ‘average’ value, if appropriate, *i.e.* average over each basic interval and in several points of space if necessary (*Cf.* Section D.2.2).

(accuracy) reasons. The propagation class M2 must therefore be understood as a transient state for moving from classes M1 to M3 or M3 to M1;

- to limit the dispersion of sound levels during the measurement, independently of experimental uncertainties, normative reference documents stipulate acoustic measurements over a ‘sufficiently long’ period in terms of changes in propagation conditions and that only samples in classes M3 or M4 should be adopted (*Cf.* Appendix C). This also over-estimates the sound level, thereby providing greater protection for local residents;
- this classification applies to ‘short-term’ temporal samples, when the propagation conditions are assumed to be fairly stationary, and in all circumstances averaged over time (typically ten minutes to two hours), which comes down to ignoring the intermittency phenomena (*Cf.* Section D.2 and Appendix C);
- to characterise a ‘long-term’ situation, the legal reference periods (*Cf.* Section D.2.2.2) of the closest or most representative Météo-France station of the studied site must be averaged out over several decades. These aspects are detailed in Section 5.2;
- the number of propagation classes depends on the distance from the noise source. Thus, a short distance away, *i.e.* up to a few dozen metres, the micrometeorological effects on the acoustic propagation, and thus this classification, can be ignored. Conversely, far away from the source, *i.e.* more than 500 m or even 1 km, it can sometimes be useful for the analysis to fine tune this grid by adding other intermediate classes, especially for the downward refraction conditions between M2 and M3. This classification is therefore a compromise, justifiable nevertheless in a large number of propagation situations;
- this classification is only valid for a point source. For a lineic source, *e.g.* a road, certain ‘sections’ (*Cf.* Section 4.1.1) can be in one class and others in another.

D.3.2 - Meteorological situation analysis methods

The trick is therefore to determine to which propagation class each short-term acoustic sample (basic interval) belongs. These propagation conditions can be determined either *qualitatively* (*i.e.* approached by more or less local observations) or *quantitatively* (*i.e.* measured directly on site), or a combination of the two. The qualitative approach, the most simple but also the least accurate, is used for the most common studies. The quantitative approach can be necessary for more complex or tricky studies: ‘expertise’ (even counter-expertise) in the normative sense.

D.3.2.1 - Qualitative methods and UiTi grid

The ‘qualitative’ methods are based on collecting information, either directly on site (local scale) or supplied by regional meteorological stations, like the official Météo-France meteorological stations, or special networks (for example, the INRA network (French National Agronomic Research Institute).

These stations work to very precise specifications and are normally located in flat, clear land (*Cf.* Section D.2.1). They do not furnish information on vertical wind and temperature profiles but on aerodynamic (wind speed and direction 10 m above the ground) and thermal (temperature, insulation period, cloud cover and sometimes sunshine expressed in W/m²) data.

There are fundamentally two methods of analysing a meteorological situation qualitatively. The first is based on the UiTi grid (standardised French method [NFS31085]) and the second on the WiSi grid, a product of research work under the Harmonoise and Imagine European projects [HRM2005][IMA2006]. Note that both these methods have similar approaches and converging results. Work is currently in progress nationally to enrich and homogenise the related normative documents [prNFS3110].

For information, the analysis principle currently used nationally is re-stated below: as the effects of thermal and aerodynamic refraction co-exist in practice, Table D.2 shows a double-entry grid which can be used to understand the qualitative variation in the far field sound level obtained, based on ‘observable’ meteorological features. Columns U1 to U5 relate to the atmosphere’s aerodynamic characteristics and lines T1 to T5 to its thermal characteristics.

This UiTi grid uses the same notations as Table D.1. The comments made for Table D.1 therefore also apply here. The empty boxes correspond to impossible meteorological scenarii.

	U1	U2	U3	U4	U5
T1		M0	M1		
T2	M0		M1	M2	M3
T3		M1	M2		M3
T4	M1	M2		M3	M4
T5		M3		M4	

Table D.2: UiTi grid for the qualitative meteorological analysis of an acoustic situation (local weather observations and/or regional data).

Aerodynamic (U_i) and thermal (T_i) conditions can be determined from local observations (or simple measurements) directly on the site or from information obtained at the closest meteorological station. If this regional station is a long way away (more than 10 km), it is advisable to supplement this information with purely visual local observations or with the help of simple measuring equipment.

Strictly speaking, this type of method (*Cf.* Section D.2.1) should only be used on flat, homogeneous and clear land to ensure good correlation between the regional information and the local values (on site) of vertical wind and temperature gradients. In practice, this method is sometimes used even if the land does not comply totally with the ‘ideal’ site conditions. Its relevance and validity must be justified by the expert in charge of the study. This type of method therefore has the advantage of not requiring complex measuring equipment (unlike the methods described in Section), except when far away from an official meteorological station and the site is very different from the ‘ideal’ site.

The input criteria for the UiTi grid (regional information) are indicated in Table D.3. They correspond to average values of meteorological conditions observed over a ‘short-term’ period (*Cf.* Section D.2.2). In this table, the aerodynamic (U_i , $i=1$ to 5) and thermal (T_i , $i=1$ to 5) classes are defined in terms of observations and vertical gradients.

As a rough guide, the orders of magnitude of vertical wind and temperature gradients associated with each criterion are also indicated in this table (*Cf.* Section D.3.1).

Class		Regional observations/data	Vertical gradients
U	U1	Strong head wind	$Grad_{VV} < -0.13 \text{ s}^{-1}$
	U2	[Light head wind] OR [Only very light head wind]	$-0.13 \text{ s}^{-1} \leq Grad_{VV} < -0.05 \text{ s}^{-1}$
	U3	[No wind] OR [Cross wind]	$-0.05 \text{ s}^{-1} \leq Grad_{VV} < 0.05 \text{ s}^{-1}$
	U4	[Light tail wind] OR [Only very light tail wind]	$0.05 \text{ s}^{-1} \leq Grad_{VV} < 0.13 \text{ s}^{-1}$
	U5	Strong tail wind	$Grad_{VV} \geq 0.13 \text{ s}^{-1}$
T	T1	Day AND strong radiation AND dry surface AND no or little wind	$Grad_T < -0.04 \text{ K.m}^{-1}$
	T2	Day AND [average radiation OR damp surface OR strong wind]	$-0.04 \text{ K.m}^{-1} \leq Grad_T < -0.02 \text{ K.m}^{-1}$
	T3	[Hourly duration including sunrise or sunset] OR [dull weather and light wind and non-dry surface]	$-0.02 \text{ K.m}^{-1} \leq Grad_T < 0.01 \text{ K.m}^{-1}$
	T4	Night AND [cloudy or no wind]	$0.01 \text{ K.m}^{-1} \leq Grad_T < 0.15 \text{ K.m}^{-1}$
	T5	Night AND clear sky AND little or no wind	$Grad_T \geq 0.15 \text{ K.m}^{-1}$

Table D.3: UiTi grid input criteria and associated values for the vertical wind and temperature gradients defined 6 m high, assuming a ‘logarithmic’ profile of the sound speed. If all conditions are met in T2, T3 then applies.

The terms ‘Day’ and ‘Night’ which appear in Table D.3 must be understood as their common meaning, *e.g.* Day means between sunrise and sunset.

In Table D.3, the extreme aerodynamic conditions which could interfere with the sound level measurements

are discarded. The following therefore apply:

- ‘strong wind’ means wind with an average value measured at 6 m high for a basic sample (short-term sample - *Cf.* Section D.2.2) extending to 3 to 5 m/s;
- ‘light wind’ means wind with an average value measured at 6 m high for a basic sample (short-term scale - *Cf.* Section D.2.2) extending to 1 to 3 m/s.

If the wind speed (V_{zm}) is known at altitude z , it is then possible to ‘return’ to its approximate value at 10 m (V_{10m}) by assuming a logarithmic aerodynamic profile with a roughness parameter z_0 (*Cf.* Appendix C). This then gives the following transitory relationship:

$$V_{10m} = V_{zm} \frac{\ln(1 + 10/z_0)}{\ln(1 + z/z_0)} \quad (\text{D.2})$$

The *wind direction* is characterised from definitions supplied in Figure D.1. For a road, it is customary for the direction of the source to correspond to the perpendicular of the road via the receiver. This discretisation of different wind directions in ‘angular sectors’ has been validated [[Zou1998](#)].

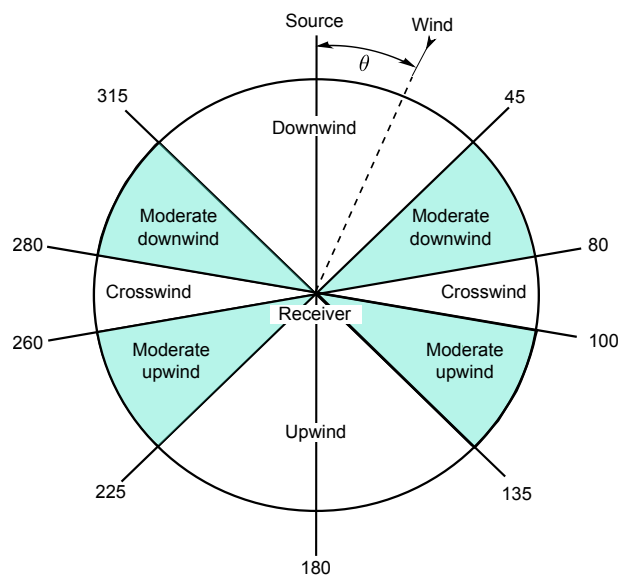


Figure D.1: Defining angular sectors of wind between source and receiver.

For the regional *temperature* data, a few details must be given on the cloud cover and radiation:

- the cloud cover represents the percentage of the surface of the sky occupied by the cloud layer. The meteorological stations furnish this information in octas: 0/8 octa corresponds to a totally clear sky and 8/8 octas to a totally covered sky. In these conditions, the definitions taken to characterise the state of the cloud cover are as follows:
 - dull weather: 8/8 octas;
 - cloudy weather: more than 4/8 octas;
 - clear sky: less than or equal to 4/8 octas.
- the radiation quantifies the solar energy reaching the ground and is expressed in W/m^2 . The following conventional values are accepted:
 - *strong radiation*: radiation higher than 400 W/m^2 ;
 - *average radiation*: radiation in the interval $[40 \text{ W/m}^2, 400 \text{ W/m}^2]$.



Warning

The state of knowledge at the time of writing this method is insufficient to produce a complete UiTi grid. For example, it is impossible to associate an acoustic propagation class with the Night and Clear sky and Strong head wind or tail wind conditions.

D.3.2.2 - Quantitative and hybrid methods

The propagation classes presented in Section D.3.1 can also be determined from adapted micrometeorological measurements performed *in situ* according to specific experimental protocols and special measuring equipment: tower fitted with conventional sensors, three-dimensional ultrasonic anemometer, *etc.*

Hybrid methods are talked about when values of influential observable factors (vertical wind direction and temperature gradients, u^* , T^* , L_{MO} for example [Stu1988]) are determined approximately through local observations, without real measurements in the strict meaning of the term as mentioned in Section D.3.2.1.

The reader can consult [Gau2009], [MEDD2006] or [IMA2006] for further detail on these methods.

E-Geometric aspects

E.1-Fermat's principle

Fermat's principle is that a ray always takes the fastest path between the source and the receiver. Applying this principle reveals that the rays propagate in a straight line in a medium of constant refraction index. It also explains the curve of acoustic rays in the variable-index media. Keller has suggested an extension of the Fermat principle known as the 'generalised Fermat's Principle' which reveals all the possible rays in a given geometry, especially the diffracted rays [Kel1962]. It is thus shown that in a constant-index medium the angle between the diffracted ray and the edge is identical to the angle of the incident ray. Fermat's principle can thus be reformulated for the diffracted rays as follows: *in a constant-index medium, a diffracted acoustic ray follows the shortest path between the source and the receiver, passing through each edge considered.*

Take, for example, a double diffraction in the vertical side edges. In the vertical plane view, the ray follows the straight line (SR). The angle between the vertical diffracting edges and the ray is clearly constant, with the notations illustrated in Figure E.1:

$$\mathbf{u}_1^- \cdot \mathbf{u} = \mathbf{u}_1^+ \cdot \mathbf{u} = \mathbf{u}_2^- \cdot \mathbf{u} = \mathbf{u}_2^+ \cdot \mathbf{u} \quad (\text{E.1})$$

with

$$\left\{ \begin{array}{l} \mathbf{u}_1^- = \frac{1}{\|SM_1\|} S \vec{M}_1 \\ \mathbf{u}_1^+ = \frac{1}{\|M_1 M_2\|} M_1 \vec{M}_2 = \mathbf{u}_2^- \\ \mathbf{u}_2^+ = \frac{1}{\|M_2 R\|} M_2 \vec{R} \end{array} \right. \quad (\text{E.2})$$

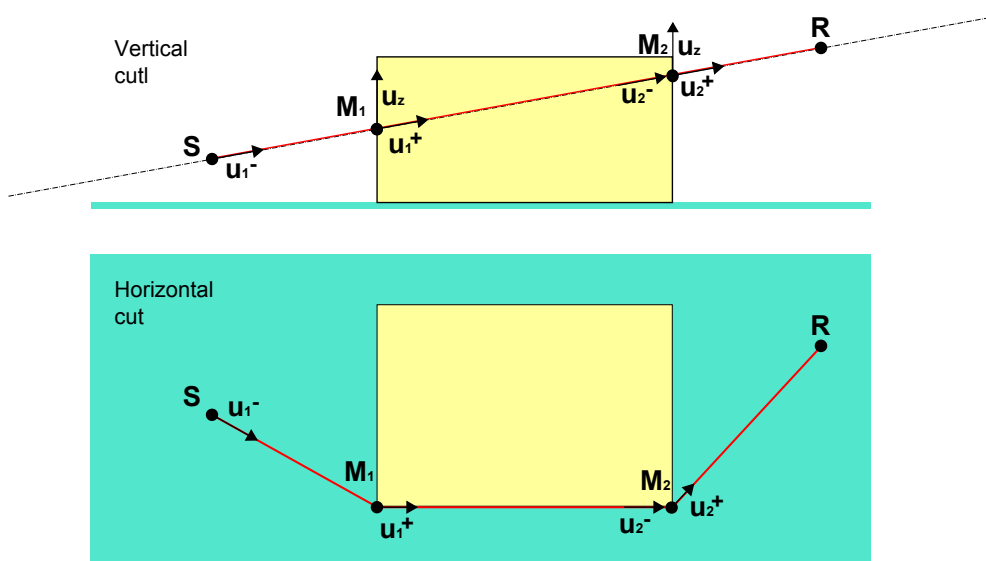


Figure E.1: Double diffraction application example of Fermat's principle.

E.2 - Ellipsoid and weighting by Fresnel zone

The Fresnel weighting extends to the principle of locality¹ of the optical acoustics to take into account the dimension of obstacles in relation to the wave length. As in geometric acoustics, the propagation of the sound is assimilated with particular geometric trajectories: the sound rays. Nevertheless, each ray is considered as bearer of an extended wave front. The extent of this wave front is characterised by the Fresnel criterion (*Cf.* Figure E.2):

$$SX + XR \leq SR + \frac{\lambda}{n} \quad (\text{E.3})$$

where n is a whole.

This comes down to associating a volume with each ray: the Fresnel ellipsoid. It is therefore accepted that a sound ray can interact not just with the obstacles encountered but also with obstacles intersected by its associated ellipsoid.

In 3D, calculating an intersection between the ellipsoid and obstacles, like the search for rays, is a complex procedure.

The 2D1/2 approach involves firstly seeking propagation paths in the horizontal plane, then constructing sound rays in the corresponding cut plane. The Fresnel weighting can therefore be applied separately to the 2D descriptions of the propagation path in the horizontal plane and in the cut plane. The basic problem is therefore reduced to calculating the intersection between an ellipse and a straight segment (*Cf.* Figure E.2).

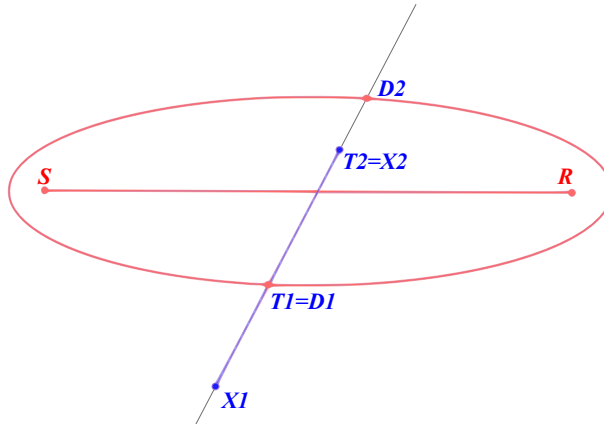


Figure E.2: Fresnel ellipse.

The stages for the geometric construction of the Fresnel ellipse are:

1. segment (X_1, X_2)
2. source S , receiver R
3. ellipse E
4. straight line D bearing the segment (X_1, X_2)
5. intersection points $\{D_1, D_2\}$ of D with the ellipse E
6. intersection of the segment (X_1, X_2) with the segment (D_1, D_2) gives the segment (T_1, T_2) .

¹ The principle of locality assumes the concentrated wave front in an infinitely small area around the sound (or light) ray. The behaviour of the ray, and especially the calculation of the amplitude of the associated wave, is therefore determined solely by the obstacles encountered. In other words, it is the criterion of visibility, in the sense of light rays, which determines whether a reflection should be taken into account. With this principle, a simple guard rail is enough to create a reflection.

The Fresnel weighting coefficient is then defined as the relationship:

$$F = \frac{T_1 T_2}{D_1 D_2} \quad (\text{E.4})$$

E.2.1 - Applications

- Reflection in a vertical obstacle like a wall or facade - finite length correction:
 - R : receiver position in the plane;
 - S : image source position in the plane;
 - X_1, X_2 : extremities of reflective obstacle in the plane.
- Reflection in a vertical obstacle like a wall or facade - finite height correction:
 - R : receiver position in the unfolded section;
 - S : source position in the unfolded section;
 - X_1, X_2 : image of the top of the obstacle in relation to the local ground, *i.e.* at the foot of the obstacle;
 - This principle can be extended to sloping obstacles.
- Side diffraction by a vertical edge:
 - R : receiver position in the unfolded section;
 - S_1 : source position in the unfolded section;
 - X_1 : top of the vertical edge;
 - X_2 : image of the top of the edge in relation to the ground.
- Diffraction above an obstacle of finite length: this is more complicated. The continuity of the solution must be maintained with side-diffracted paths.

F-Dealing with special elements

This appendix supplements Chapter 7 in terms of special elements like trenches, tunnels and partial covers. It reproduces the pages of the [GdB1980] covering these points, with the kind consent of the CERTU.

5.3 Couvertures complètes des chaussées

5.3.1. Couverture infiniment longue

Lorsqu'un bâtiment est protégé du bruit par une couverture complète des chaussées, le niveau sonore en façade peut être estimé égal au niveau sonore sans couverture diminué de l'efficacité de la couverture. Autrement dit, l'efficacité de la couverture peut être définie comme la différence entre le niveau sonore avant et le niveau sonore après sa mise en place.

Dans ce cas, le niveau sonore en présence d'une couverture infiniment longue est la somme de deux termes :

- . énergie sonore rayonnée par la couverture, (**terme positif**)
- . perte par atténuation due à la propagation du son depuis la couverture jusqu'au point récepteur considéré (**terme négatif**).

a) Energie sonore rayonnée par la couverture

a.o. énergie émise.

Pour une circulation de Q véhicules par heure sur une voie, à la vitesse V , la puissance acoustique à l'émission par mètre de voie est égale à :

$$(L_w)_m = L_w + 10 \log \frac{Q}{1000 V}$$

avec : L_w = puissance acoustique d'un véhicule moyen, v étant exprimé en Km/h

L'énergie, émise par un mètre de voie, va être répartie dans la couverture et y constituer un champ acoustique diffus. Les ondes seront soumises à deux causes d'affaiblissement principales, entre la source et le récepteur :

- . une perte d'énergie sous la couverture par absorption,
- . une perte d'énergie dans la couverture lors de sa transmission.

a.1- Perte d'énergie sous la couverture

. Absorption par les parois

Supposons que la couverture soit constituée de matériaux dont on connaît le facteur d'absorption α_{sabine} (voir à ce sujet le fascicule « Recommandations techniques pour les ouvrages de protection contre le bruit » du *Guide du bruit*, paragraphe 3.3.4 page 35).

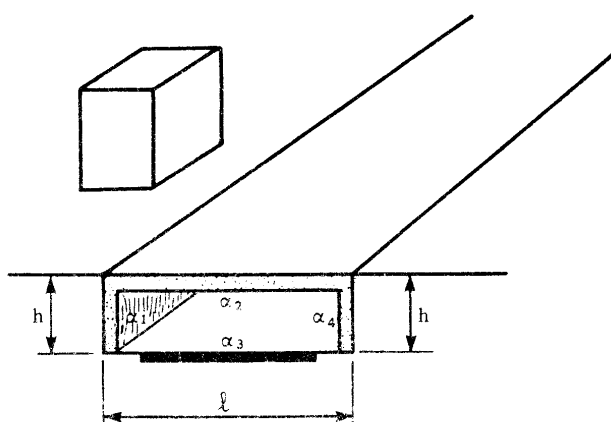


Schéma 4.111 : Chaque élément de paroi dans la couverture peut être affecté d'un facteur d'absorption α_{sabine} . Ici, les parois verticales ont une absorption α_1 et α_3 , la surface de la couverture un facteur α_2 et la voie un facteur α_4 .

Partie IV : Méthode détaillée routes

On peut calculer la surface d'absorption équivalente à l'intérieur de la couverture.

Pour une couverture homogène dans toute sa longueur, nous aurons par mètre de longueur de tunnel :

$$A (\text{parois}) = \sum_i (\ell_i \cdot \alpha_i) = (h \cdot \alpha_1) + (h \cdot \alpha_2) + (\ell \cdot \alpha_3) + (\ell \cdot \alpha_4) \quad (38)$$

Dans le champ diffus qui règne sous une couverture, chaque rayon sonore est réfléchi sur les parois en grand nombre de fois. A chaque réflexion, il perd une part d'énergie acoustique. L'énergie absorbée est proportionnelle à A, ce terme « A » est donc directement utilisé dans les équations du champ diffus.

Remarque : Le facteur d'absorption α s'est mesuré, pour l'ensemble des matériaux, par octave ou par tiers d'octave, selon la norme NFS 31 003.

Une liste des facteurs d'absorption des matériaux usuels peut être obtenue aisément dans les publications spécialisées, et notamment dans les cahiers du Centre Scientifique et Technique du Bâtiment.

Il est à noter que le facteur d'absorption α s'utilisé ici, doit être mesuré à partir d'un spectre de bruit routier.

De plus, la valeur octave par octave peut être utilisée dans un calcul par programme informatique. Cependant, pour l'utilisation d'une méthode de calcul manuelle, même détaillée, cette indication est trop fine pour être exploitable.

Il conviendra donc d'utiliser un α sabine globalisé pour toutes les bandes de fréquence. Ce facteur d'absorption global peut être défini comme suit :

On peut écrire que l'énergie incidente globale s'exprime de la façon suivante en fonction de l'énergie par bande de fréquence, pour un bruit routier et une mesure en dB (A) :

$$W_{\text{incidente}} = \sum_i \left[10^{\frac{L(f)_i \text{ pondéré A}}{10}} \right]$$

avec : $L(f)_i$ = niveau de puissance dans chaque bande de fréquence (i).

De la même façon, il est possible d'écrire que l'énergie absorbée globale s'exprime en fonction de l'énergie absorbée dans chaque bande de fréquence (i) :

$$W_{\text{absorbée}} = \sum_i \left[\alpha(i) \cdot 10^{\frac{L(f)_i \text{ pondéré A}}{10}} \right]$$

avec : $\alpha(i)$ = facteur d'absorption de chaque bande de fréquence. $= \frac{W_{\text{absorbée}}}{W_{\text{incidente}}}$

Il vient l'expression du facteur d'absorption global d'un matériau, pour un spectre de bruit routier normalisé, mesuré en dB (A) :

$$\alpha_{\text{global, bruit route}} = \frac{\sum_i \left[\alpha(i) \cdot 10^{\frac{L(f)_i \text{ pondéré A}}{10}} \right]}{\sum_i \left[10^{\frac{L(f)_i \text{ pondéré A}}{10}} \right]} \quad (39)$$

Absorption par les véhicules

Les véhicules routiers en circulation sous un tunnel apportent une absorption acoustique. La valeur de cette absorption est proportionnelle à la concentration des véhicules sur la voie.

Pour les prévisions des niveaux sonores, on pourra considérer que la surface absorbante apportée par la présence des véhicules, est égale à la densité des véhicules multipliée par 1 m^2 (il s'agit ici d'une valeur moyenne approchée, utilisable en cas de trafic de véhicules légers ou des véhicules lourds, quelle que soit leur proposition), pour 1m de longueur de tunnel.

$$A (\text{véhicules}) = \frac{Q}{1000 V} \cdot 1 \text{ m}^2 \quad (40)$$

Absorption par l'air

Dans un tunnel, loin des extrémités, on peut admettre que le champ acoustique est un champ diffus.

Un rayon sonore est soumis dans un tel champ à un grand nombre de réflexions sur les parois

La théorie de EYRING nous enseigne que, dans une salle de volume V , le parcours moyen d'un rayon sonore à une longueur égale à $\frac{4V}{S}$ avec S , section de la salle dans le plan considéré.

Plus le trajet du rayon sonore est grand, plus l'air absorbe une part importante d'énergie sous la couverture.

Pour l'ensemble des rayons sonores contenus dans une tranche de couverture de 1 mètre de longueur, on démontre que la surface d'absorbant parfait équivalente à l'absorption par l'air est égale à approximativement $5S \cdot 10^{-3} \text{ m}^2$, avec $S = h^2$ (selon le schéma 4.1.1).

On peut donc définir un terme représentant l'absorption par l'air et qui est fonction des dimensions du tunnel. Il est sensiblement égal à :

$$A(\text{air}) \equiv 5S \cdot 10^{-3} \text{ en m}^2 \quad S = \text{surface de la coupe de la tranchée} \quad (41)$$

Surface absorbante équivalente du tunnel

Cette surface est égale à la somme des trois termes précédents :

$$\Delta \equiv \Delta(\text{parois}) + \Delta(\text{véhicules}) + \Delta(\text{air})$$

$$A = \sum (\ell_i \cdot \alpha_i) + \left[\frac{Q}{1000 \cdot V} \times 1 \text{ m}^2 \right] + [5 S \cdot 10^{-3} \text{ m}^2] \quad (42)$$

« A » représente la surface d'absorption équivalente du tunnel exprimée en m^2 , pour 1m de longueur de tunnel.

a) Perte d'énergie par transmission dans la couverture

Le matériau utilisé pour réaliser la couverture des chaussées sera caractérisé par son indice d'affaissement en transmission « R » (voir le fascicule « Recommandations techniques pour les ouvrages de protection contre le bruit » du *Guide du bruit des Transports Terrestres*, paragraphe 3.3.1, page 31). Il est mesuré selon les indications de la norme NFS 31 002 et sera défini, pour ce qui nous concerne, à partir d'un spectre de bruit routier normalisé, mesuré en dB (A) et cumulé sur toutes les bandes de fréquences, pour aboutir à l'expression d'un chiffre « R » global.

C'est cet indicateur qui représente la perte d'énergie par transmission dans la couverture.

Si la couverture est composée de matériaux différents (ex : une couverture en béton comportant des parties translucides en plastique), il convient d'affecter chaque matériau de surface S_i par un indice d'affaiblissement en transmission R.

Partie IV : Méthode détaillée routes

On peut alors définir la « transparence » du matériau comme :

$$\tau_i = \frac{R_i}{10}$$

Pour une tranche de tunnel de 1 mètre de longueur, on pourra alors faire la somme des transparences en fonction de la longueur des différents éléments de couverture :

$$\bar{\tau} = \sum_i \tau_i \cdot l_i$$

a.3 - Calcul de l'efficacité propre de la couverture

L'efficacité propre de la couverture est égale à la différence entre le niveau de puissance acoustique émis par la circulation et celui rayonné par la couverture.

Cette efficacité est également égale à la somme de l'efficacité en transmission pure et de la perte d'énergie par absorption sous la couverture.

Pour une tranche de tunnel de 1 mètre de longueur, on peut écrire :

$$\Delta L = R + 10 \log \frac{A}{l} \quad (43)$$

avec : ΔL = efficacité propre de la couverture,

A = surface d'absorption équivalente dans une unité de longueur du tunnel en m^2

l = largeur de la couverture en mètres.

Pour une couverture infiniment longue, l'efficacité propre de l'ensemble de la couverture peut être considérée comme égale à l'efficacité précédemment calculée pour 1 m de tunnel. Ce résultat approché est en effet valable si l'on admet que l'efficacité de la couverture est indépendante de l'angle d'incidence des rayons sonores.

Il est à noter que pour des couvertures lourdes (dalles supportant des véhicules), on pourra admettre, en première approximation, que R est très grand et que $\bar{\tau}$ est voisin de 1. Dans ce cas, l'efficacité de la couverture est très grande.

Les calculs ci-dessus ne s'appliquent en fait qu'à des couvertures légères (rôle uniquement acoustique) ou des ensembles possédant des joints entre dalles, où qui présentent un indice « R » sur l'ensemble de leur surface voisin de 35 dB (A).

a.4 - Energie rayonnée par la couverture

L'énergie rayonnée par la couverture est égale à la différence entre l'énergie émise par la circulation et l'efficacité propre de la couverture.

Le niveau d'énergie rayonné par la couverture sera donc le suivant, par unité de longueur de couverture :

$$(L'_{Wm}) = (L_{Wm}) \left[R + 10 \log \frac{A}{l_c} \right] \text{ avec } l_c = \text{longueur de la couverture}$$

Il est également possible de calculer le niveau sonore sous la couverture, par application des équations du champ diffus dans une salle : on aura pour 1 mètre de longueur de tunnel :

$$L_p (\text{sous la couverture}) = \left[L_w + 10 \log \frac{A}{1000v} \right] - 10 \log A + 6 \quad (44)$$

b) Niveau sonore en façade d'un bâtiment protégé par une couverture

Pour une couverture infiniment longue, l'énergie rayonnée par l'ensemble de la couverture est approximativement égale à celle rayonnée par 1 m de longueur de tunnel.

Le niveau sonore en façade d'un bâtiment protégé par une couverture est égal au niveau rayonné par la couverture diminué par l'atténuation due à la propagation du son depuis la couverture jusqu'au point récepteur.

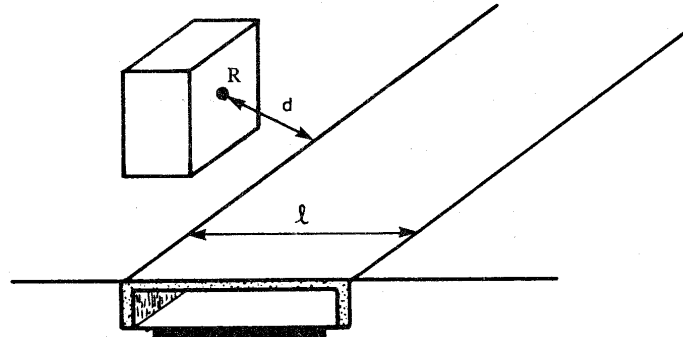


Schéma 4.112 : Récepteur en façade d'un bâtiment protégé par une couverture

On a vu qu'une circulation de Q véhicules par heure à une vitesse V , émet un niveau de puissance (L_W) m par mètre de longueur de voie qui s'exprime de la façon suivante par rapport au niveau de puissance d'un véhicule moyen L_W :

$$(L_W) \text{ m} = L_W + 10 \log \frac{Q}{1000 V}$$

En présence de la couverture, les ondes sonores sont atténuées par absorption sous la couverture et par transmission dans la couverture. L'efficacité propre de la couverture a été définie pour 1 m de longueur de tunnel comme :

$$\Delta L = R + 10 \log \frac{A}{\ell} \quad \text{avec } \ell = \text{longueur de la couverture}$$

La couverture peut être assimilée à une voie circulée fictive, qui émettrait un niveau de puissance par unité de longueur de voie égale au niveau de puissance rayonné par la couverture.

Ainsi, le calcul du niveau sonore en façade sera effectué à l'aide des méthodes classiques exposées aux paragraphes 4.2 et 4.3 ci-dessus, pour une voie fictive au niveau du sol.

Pour la couverture infiniment longue, le niveau sonore en façade du bâtiment sera :

$$L_p = L_W + 10 \log \frac{Q}{1000 V} - 12 \log \left(d + \frac{\ell c}{3} \right) - \left[R + 10 \log \frac{A}{\ell} \right] + 3 \quad (45)$$

$$\text{ou } L_p = (L'_W) \text{ m} - \left[R + 10 \log \frac{A}{\ell} \right] - 12 \log \left(d + \frac{\ell c}{3} \right) + 3 \quad (46)$$

$$\text{ou } L_p = (L'_W) \text{ m} - 12 \log \left(d + \frac{\ell c}{3} \right) + 3 \quad (47)$$

avec : $(L'_W) \text{ m} = \text{puissance acoustique rayonnée par 1 m de longueur de couverture.}$

L_W = puissance acoustique d'un véhicule moyen.

$(L_W) \text{ m} = \text{puissance acoustique par unité de longueur de voie.}$

Partie IV : Méthode détaillée routes

Il est également possible d'exprimer le niveau de pression en façade à partir du niveau de pression qui règne sous la couverture :

$$L_p = L_p (\text{sous la couverture}) - 12 \log(d + \frac{l_c}{3}) - R + 10 \log \frac{l}{3} - 3 \quad (48)$$

avec : L_p (*sous couverture*) = $L_W - 10 \log A + 6$,
 ΔL = efficacité propre de la couverture,
 d = distance entre le récepteur et la couverture,
 l_c = largeur de la chaussée (assimilée ici à la largeur de la couverture).

5.3.2. Couverture de longueur limitée

Un récepteur situé en façade d'un bâtiment protégé par une couverture de longueur limitée percevra une énergie sonore qui sera la somme de trois termes :

- . l'énergie rayonnée par la couverture,
- . l'énergie en vue directe issue des parties non protégées de la source, de part et d'autre de la couverture,
- . l'énergie d'une source fictive représentant l'effet de sortie du tunnel.

a) La couverture est étudiée dans un plan particulier

En toute rigueur, il conviendrait de raisonner en angles solides sous lesquels on voit la couverture et les parties non protégées de la source de part et d'autre de la couverture, depuis le récepteur.

Cette rigueur n'est pas nécessaire pour les calculs de prévision et présente l'inconvénient de compliquer sensiblement les calculs.

De façon approchée, il est possible de mener l'ensemble du raisonnement qui conduit au calcul d'efficacité d'une couverture dans un plan particulier, sans altérer les résultats de façon excessive.

Ce plan particulier peut être défini comme celui qui passe par le point récepteur R où l'on cherche à connaître le niveau sonore et la ligne émettrice. Il est donc défini à priori en l'absence de la couverture.

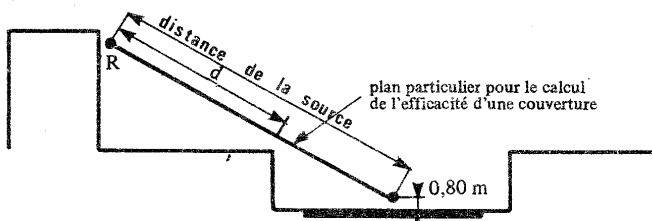


Schéma 4.113

Schéma 4.113 : Le plan est défini comme passant par le point récepteur R et la ligne émettrice, centrée sur l'axe de la voie et située à 0,80 m au-dessus du niveau de la chaussée.

Dans ce plan, il est possible de définir plusieurs zones caractéristiques de la façon dont le bruit va se propager jusqu'au récepteur R.

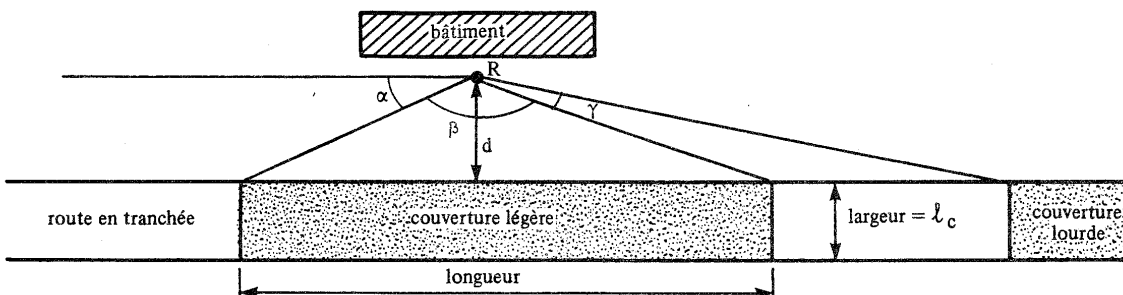


Schéma 4.114 : Vue en plan (dans le plan particulier défini ci-dessus).

Dans l'exemple ci-dessus :

- . la couverture est vue sous l'angle β
- . l'énergie directe parviendra, de part et d'autre de la couverture, sous les angles α et γ

b) Energie rayonnée par la couverture

Dans le paragraphe 5.3.1 ci-dessus, le niveau de puissance rayonné par 1 m de longueur de couverture a été indiqué comme égal à :

$$(L'_W)_{\bar{m}} = (L_W)_{\bar{m}} \left[R + 10 \log \frac{A}{\ell} \right]$$

De plus, l'efficacité de l'ensemble d'une couverture infiniment longue a été admise comme égale à l'efficacité de 1 m de longueur de couverture. Il en est de même pour l'énergie rayonnée.

L'énergie rayonnée par la couverture va se propager jusqu'à R comme l'aurait fait le bruit d'une route fictive située à l'emplacement de la couverture, émettant une énergie égale à l'énergie rayonnée par la couverture et ayant une longueur égale à celle de la couverture.

Tout se passe donc comme si nous avions à calculer le niveau sonore d'une route située à la distance d du point récepteur R et vue sous l'angle β . Soit pour un point récepteur R en façade d'un bâtiment :

$$L_p(\beta) = (L'_W)_{\bar{m}} - 12 \log \left(d + \frac{\ell_c}{3} \right) + 10 \log \frac{\beta}{180^\circ} + 3 \quad (49)$$

$$\text{ou } L_p(\beta) = (L_W)_{\bar{m}} \left[R + 10 \log \frac{A}{\ell} \right] - 12 \log \left(d + \frac{\ell_c}{3} \right) + 10 \log \frac{\beta}{180^\circ} + 3 \quad (50)$$

Pour un calcul en champs libre, il conviendrait de retrancher 3 dB (A) aux valeurs issues de l'utilisation des formules (49) et (50).

avec : L_W = puissance acoustique d'un véhicule moyen,

$(L_W)_{\bar{m}}$ = puissance acoustique par unité de longueur de voie,

R = indice d'affaiblissement en transmission de la couverture,

A = surface absorbante équivalente sous la couverture,

S_c = surface de la couverture,

L_p = niveau de pression en façade du bâtiment,

L_p' = niveau de pression sous la couverture.

$(L'_W)_{\bar{m}}$ = puissance acoustique rayonnée par la couverture infiniment longue

Partie IV : Méthode détaillée routes

c) Energie directe parvenant des segments source non protégés par la couverture

Sous les angles α et γ du schéma 4.114 ci-dessus, l'énergie parvient au récepteur sans être affectée par la couverture.

On applique à cette énergie les équations d'extension fine, comme pour tout autre écran acoustique, telles que définies au paragraphe 5.2.4 ci-dessus.

En façade du bâtiment, on percevra donc un niveau sonore L tel que :

$$L (\alpha + \gamma) = L_W + 10 \log \frac{Q}{1000 V} - 12 \log (d + \frac{l_c}{3}) + 10 \log \frac{\alpha + \gamma}{180^\circ} + 3 \quad (51)$$

avec : d = distance de récepteur à la voie.
 l_c = largeur de la chaussée.

Eventuellement, dans le cas d'une route en tranchée, on pourra retrancher un affaiblissement en diffraction (à calculer selon les indications du paragraphe 5.2 ci-dessus) si le plan particulier dans lequel on raisonne coupe le bord de tranchée.

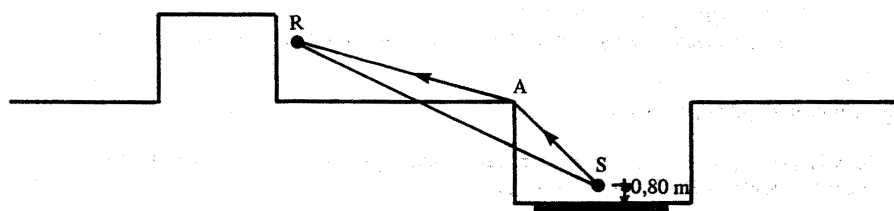
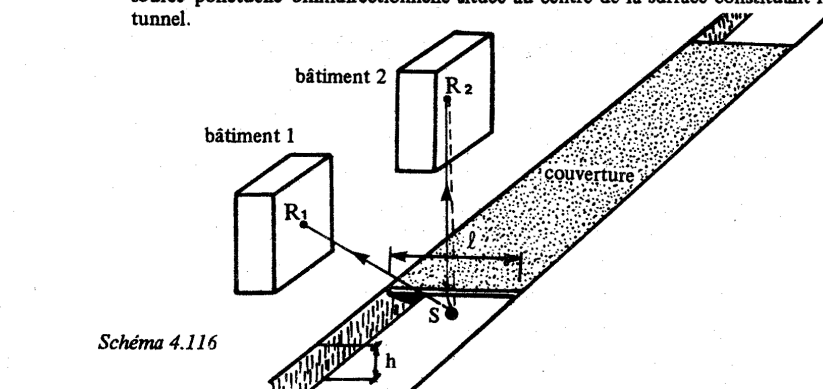


Schéma 4.115 : Si le plan SR coupe le bord de tranchée, il y a lieu de tenir compte d'un affaiblissement en diffraction pour le calcul de l'énergie parvenant par les côtés de la couverture.

d) Energie d'une source fictive représentant l'effet de sortie du tunnel

L'espace compris entre l'extrémité du tunnel et une distance d'environ 1 fois à 3 fois sa largeur, à l'intérieur du tunnel, constitue un espace intermédiaire où le champ acoustique n'est ni un champ direct (champ régnant à l'extérieur du tunnel), ni un champ diffus (champ régnant à l'intérieur, loin de l'extrémité). Dans cet espace intermédiaire le champ acoustique peut être assimilé à un champ diffus progressif.

Ce champ diffus progressif sera assimilé (par extension du théorème de HUYGENS [*]), à une source ponctuelle omnidirectionnelle située au centre de la surface constituant l'extrémité du tunnel.



(*) En toute rigueur, le théorème de HUYGENS s'applique entre deux champs diffus. Il permet de remplacer un des champs acoustiques par une courbe continue de sources ponctuelles omnidirectionnelles, monopolaires et indépendants, situées à la frontière des deux champs acoustiques.

Le niveau de puissance de cette source ponctuelle devrait correspondre, de façon théorique, à celui du champ acoustique qu'elle remplace, pour les calculs.

De façon approchée, on peut admettre pour les calculs de prévision des niveaux sonores que cette source possède un niveau de puissance égal à :

$$(L_W) \text{ source ponctuelle} = (L_W) m - 10 \log \frac{A}{S} \quad (52)$$

avec : (L_W) source ponctuelle = niveau de puissance de cette source,
 $(L_W) m$ = niveau de puissance émise par la circulation, par 1m de voie.
 A = surface absorbante équivalente du tunnel, par unité de longueur de voie A,
 S = surface de la coupe du tunnel.

Le niveau de pression s'obtient ensuite par un calcul classique de propagation pour une source ponctuelle : propagation directe dans le cas du bâtiment 1 du schéma 4.116 (affaiblissement en $1/d^2$ en fonction de la distance d du récepteur à la source) et propagation comportant une diffraction sur l'arête de la couverture dans le cas du bâtiment 2 du schéma 4.116 (utilisation de l'abaque de MAEKAWA indiquée au 5.2.1 ci-dessus).

e) Niveau sonore en façade d'un bâtiment protégé par une couverture de longueur limitée de longueur limitée

Le niveau sonore résultant en façade du bâtiment protégé par une façade de longueur limitée est égal au cumul (selon les indications de l'annexe 2 ci-après) des trois contributions :

$$L_R = L_p (\beta) \oplus L_p (\alpha + \gamma) \oplus L_p (\text{sortie tunnel})$$

5.4 Couvertures partielles des chaussées

Le calcul de l'efficacité d'une couverture partielle, ou bien celui du niveau sonore en façade d'un bâtiment protégé par ce type d'écran acoustique, est basé sur des lois de nature comparable à celles utilisées pour le calcul d'efficacité des couvertures complètes des chaussées.

On peut cependant noter quelques différences importantes entre ces deux types d'écrans acoustiques :

- pour le calcul des couvertures partielles, on négligera la part d'énergie rayonnée par la couverture elle-même, et l'on ne prendra en compte que l'énergie acoustique qui se propage à travers les parties laissées ouvertes. En effet, alors que pour une couverture complète l'énergie rayonnée est l'une des deux sources importantes demeurant après réalisation de la protection (avec les segments non protégés, de part et d'autre de la couverture), pour une couverture partielle cette énergie rayonnée par la couverture elle-même est souvent faible devant l'énergie qui se propage à travers l'ouverture laissée libre ;
- La puissance acoustique émise par la voie sera décomposée en deux termes lors du calcul d'efficacité d'une couverture partielle :
 - . l'énergie directe qui se propage sans réflexions
 - . l'énergie diffuse qui se propage par la surface demeurée ouverte, après de multiples réflexions acoustiques.

5.4.1. Couverture partielle

On appelle couverture partielle d'une chaussée, par opposition à la couverture complète qui clôture l'espace autour de la ligne émettrice, une couverture qui offre une surface ouverte importante (supérieure à 1 m x 1m) [*].

Une couverture partielle sera décrite en coupe par sa section couverte S et son ouverture Ω

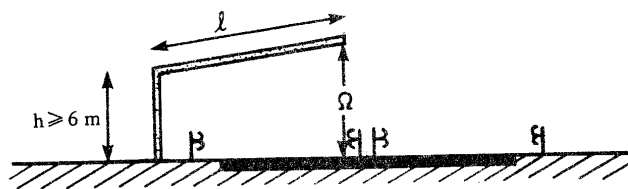


Schéma 4.117 : Couverture d'une demi-chaussée. Ici, $S = h + \ell$ et l'ouverture Ω aura la dimension figurée sur le schéma, pour un mètre de longueur de voie.

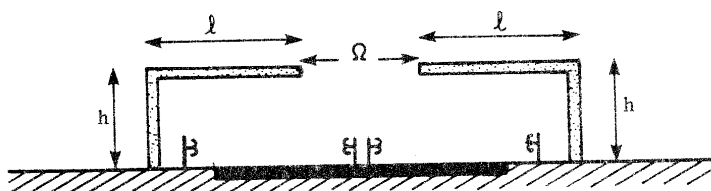


Schéma 4.118 : Deux couvertures partielles face à face. Ici, $S = 2(h + \ell)$ et l'ouverture Ω est figurée sur le schéma, pour un mètre de longueur de voie.

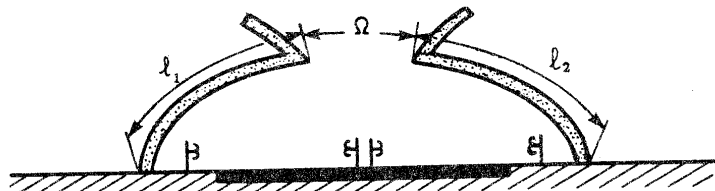


Schéma 4.119 : Couverture partielle. Ici, $S = \ell_1 + \ell_2$ et l'ouverture Ω est figurée sur le schéma.

(*) La présente méthode de calcul n'est pas applicable aux systèmes à conduits, aux systèmes à ouvertures dissipatives du type « damier phonique », ou aux couvertures comportant des ouvertures de petites dimensions traitées en matériaux absorbants.

5.4.2. Calcul de rayonnement direct à travers l'ouverture

a) Convention : angle de rayonnement direct

On appelle angle de rayonnement direct d'une ligne de sources S , l'angle θ dont le sommet coïncide avec la source, et qui passe par les extrémités de l'ouverture Ω

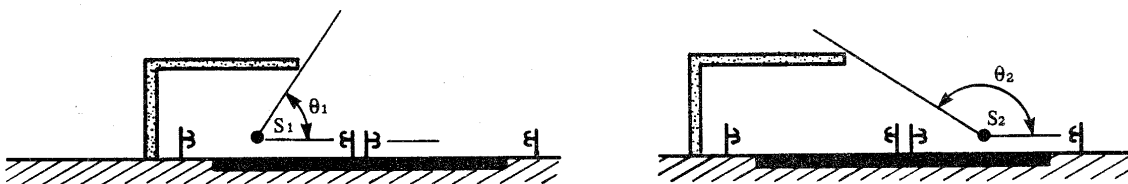


Schéma 4.120 : La route est ici décomposée en deux lignes de sources parallèles S_1 et S_2 . Les angles de rayonnement direct pour une couverture couvrant 1/2 chaussée sont ici figurés par les angles θ_1 et θ_2 respectivement pour les sources S_1 et S_2 .

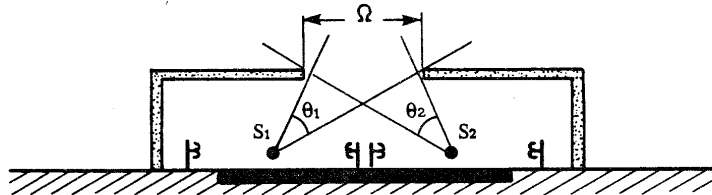


Schéma 4.121 : La route est encore décomposée en deux lignes de sources S_1 et S_2 . Pour deux couvertures partielles laissant une ouverture Ω , les angles de rayonnement direct seront tels que θ_1 et θ_2 figurés sur le schéma, respectivement pour les sources S_1 et S_2 .

On appelle angle de rayonnement direct θ' d'une source image S' l'angle dont le sommet coïncide avec la source image S' (symétrique de la source S par rapport à une paroi), et qui passe par les extrémités de l'ouverture Ω

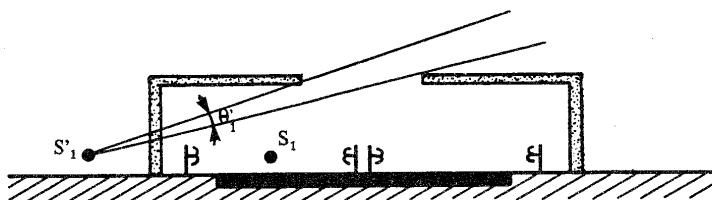


Schéma 4.122 : La source S_1 a une symétrique S'_1 par rapport à la paroi verticale. Pour cette source image S'_1 , l'angle de rayonnement direct est égal à θ'_1 tel que figuré sur le schéma.

b) Calcul du niveau sonore par rayonnement direct

Chaque chaussée, pour une voie de circulation à 2 chaussées séparées, ou chaque sens de circulation pour une voie à une seule chaussée, peut être assimilée à une ligne émettrice située à 0,80 mètre au-dessus du niveau de la chaussée.

Partie IV : Méthode détaillée routes

Pour un récepteur R situé en façade d'un bâtiment protégé par une couverture partielle, le niveau sonore par rayonnement direct sera calculé en considérant que l'énergie émise par les lignes émettrices est diffractée par les bords de la couverture partielle, comme dans les cas d'écrans verticaux (voir paragraphe 5.2).

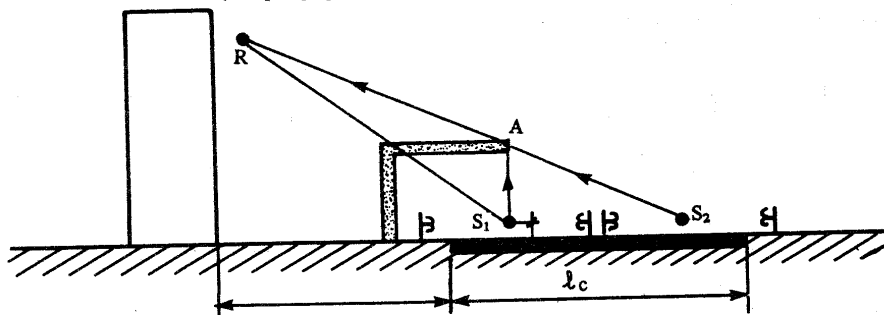


Schéma 4.123 : Diffraction du rayonnement direct par une couverture partielle.

Pour la source S_1 , l'atténuation en diffraction apportée au rayonnement direct (donc à la part d'énergie contenue dans l'angle de rayonnement direct θ_1) est calculée par application de l'abaque de diffraction 4.75, comme pour un écran vertical. La différence de marche utilisée est ici : $\delta_1 = S_1 A + AR - S_1 R$ pour la source S_1 .

Pour la source S_2 , on effectue le même calcul avec une atténuation en diffraction calculée à partir de la différence de marche $\delta_2 = S_2 A + AR - S_2 R$.

Supposons que pour une ligne de sources S_1 , l'atténuation en diffraction lue sur l'abaque 4.75 soit égale à ΔL_1 , le niveau sonore en R dû à cette source peut s'écrire :

$$L_p = L_w + 10 \log \frac{Q}{1000 V} - 12 \log(d + \frac{\lambda_c}{3}) + 10 \log \frac{\beta}{180} - \Delta L_1 + 3 \quad (53)$$

avec :
 L_w = puissance acoustique d'un véhicule moyen,
 d = distance du récepteur au bord de plateforme,
 λ_c = largeur de la chaussée,
 β = angle sous lequel l'énergie parvient à R après diffraction sur le sommet de la couverture,
 ΔL_1 = efficacité en diffraction de la couverture assimilée à un écran vertical et lue sur l'abaque 4.75.

Pour un récepteur en champs libre, il conviendrait de retrancher 3 dB (A) au niveau sonore calculé à l'aide de la formule (53).

Le calcul sera effectué pour la ou les lignes de sources auxquelles on a assimilé la circulation.

Pour un calcul précis, il sera également effectué pour les sources images du premier ordre. Il est en effet souvent inutile d'aller jusqu'à calculer les sources images du second ordre, et ce d'autant plus que dans la suite de la méthode exposée ici, nous prendrons en compte l'existence d'un champ diffus superposé au champ direct.

Pour le calcul du rayonnement direct pour les lignes sources images, si la paroi réfléchissante possède un facteur d'absorption α , on ajoutera algébriquement au niveau sonore calculé pour ces sources la valeur $10 \log(1 - \alpha)$.

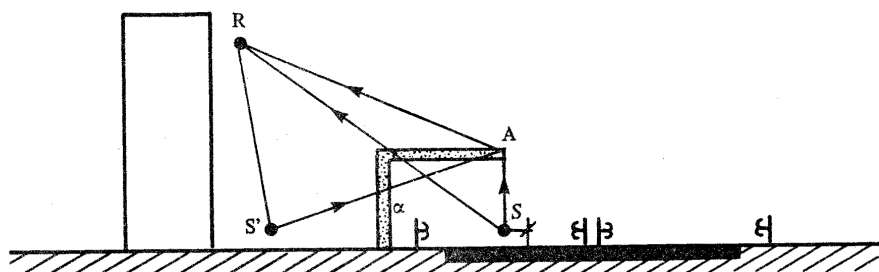


Schéma 4.124 : Niveau sonore correspondant au rayonnement direct.

Dans le schéma 4.124, le rayonnement direct sera calculé pour la source S en considérant une différence de marche $\delta = SA + AR - SR$ et en utilisant l'abaque 4.75.

Ce niveau sonore sera ensuite cumulé avec le niveau issu de S' symétrique de S par rapport à la paroi, dont l'atténuation en diffraction ΔL sera calculé sur la base d'une différence de marche $\delta = S'A + AR - S'R$ et donc le niveau sera :

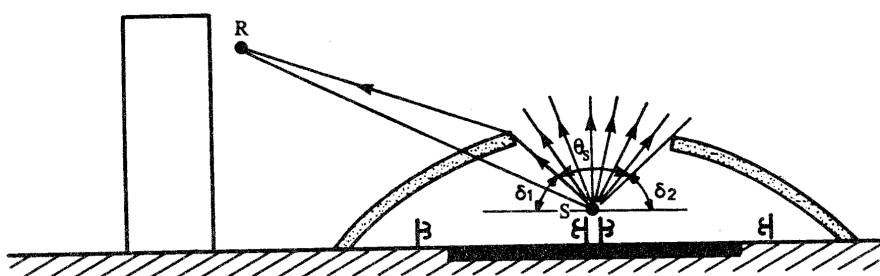
$$L_p = L_W + 10 \log \frac{Q}{1000 V} - 12 \log \left(d + \frac{l_c}{3} \right) + 10 \log \frac{\beta}{180^\circ} - \Delta L + 10 \log (1 - \alpha) + 3 \quad (54)$$

Pour un récepteur en champs libre, il convient de retrancher 3 dB (A) à ce résultat.

avec : β = angle sous lequel on voit la couverture depuis R (voir paragraphe 4.3.2 a ou schéma 4.114).

5.4.3. Calcul du rayonnement diffus

Pour le calcul précédent, indiqué au paragraphe 5.4.2 précédent, la puissance acoustique de l'ensemble des rayons directs issus d'une ligne de sources a été prise en compte, ainsi que la puissance du symétrique de cette ligne émettrice par rapport à la paroi.

Schéma 4.125 : Une partie de l'énergie émise par la source S n'a cependant pas été prise en compte : c'est celle qui se propage depuis S, dans les angles δ_1 et δ_2 .

Partie IV : Méthode détaillée routes

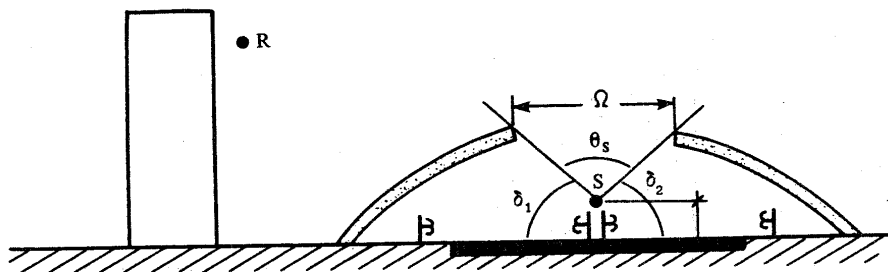


Schéma 4.126 : L'énergie émise par la source S dans les angles δ_1 et δ_2 va se réfléchir un grand nombre de fois avant de « sortir » par l'ouverture Ω et se propager jusqu'au récepteur R . Cette énergie va se répartir sous la couverture et constituer un champ acoustique qui sera, ici, assimilé à un champ diffus.

La proportion d'énergie qui va constituer ce champ diffus sera fonction de $(1 - \frac{\theta_s}{\pi})$.

Le tunnel constitué par l'ensemble « couverture-parois verticales-chaussée » peut être caractérisé par une surface d'absorption équivalente par unité de longueur de voie, qui, comme pour les couvertures complètes, est la somme de trois termes (on ne tiendra pas compte ici de l'ouverture Ω) :

. absorption par les parois (voir paragraphe 5.3.1)

$$A(\text{parois}) = \sum_i [\ell_i \cdot \alpha_i] = \ell_1 \cdot \alpha_1 + \ell_2 \cdot \alpha_2 + 2h \cdot \alpha_3 + \ell \cdot \alpha_4$$

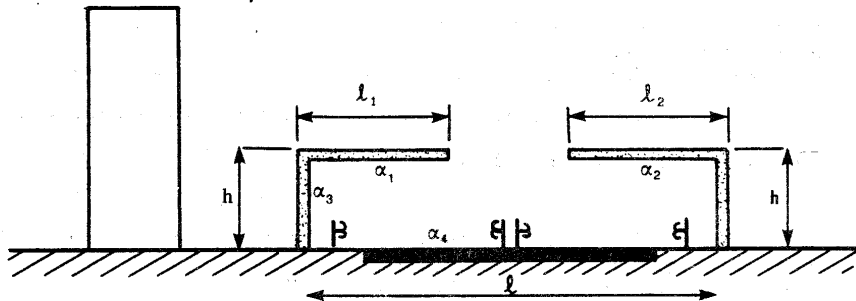


Schéma 4.127 : Absorption par les parois

$$\text{. absorption par les véhicules } A(\text{véhicules}) = \frac{Q}{1000 V} \cdot 1 \text{ m}^2$$

$$\text{. absorption par l'air } A(\text{air}) = 5S \cdot 10^{-3} \text{ m}^2 \quad \text{avec } S = h \cdot \ell$$

La puissance acoustique diffuse sous la couverture s'exprime par la relation suivante :

$$\text{pour } n \text{ lignes de sources : } W = \sum_n \left[W_n \left(1 - \frac{\theta_n + \theta'n}{180^\circ} \right) \right] \left[\frac{\Omega}{A + \Omega} \right] \quad (55)$$

avec : W_n = puissance acoustique à l'émission de la source n , par unité de longueur de voie,

θ_n = angle de rayonnement direct pour la source, n

$\theta'n$ = angle de rayonnement direct pour la source symétrique par rapport à la paroi apportant la réflexion prépondérante parmi toutes les sources réfléchies d'ordre 1,

Ω = surface de l'ouverture, par unité de longueur de voie,

A = surface absorbante équivalente par unité de longueur de voie.

Le niveau de puissance dans ce champ acoustique diffus s'écrit :

$$L_W = 10 \log \frac{\Omega}{A + \Omega} + 10 \log \sum_n \left[10^{10} \left(1 - \frac{\theta_n + \theta'n}{180^\circ} \right) \right] \quad (56)$$

Par extension du théorème de HUYGENS (voir paragraphe 5.3.2 ci-dessus), le champ diffus qui existe sous la couverture est assimilé, pour une longueur unitaire de la voie étudiée, à une source ponctuelle omnidirectionnelle de puissance acoustique égale à celle du champ diffus telle que calculée ci-dessus (pour l'ensemble de la longueur de la couverture, le champ acoustique sera donc assimilé à une ligne ou segment de ligne de sources).

Le calcul du niveau sonore L_p perçu par un récepteur R en façade d'un bâtiment protégé par une couverture partielle, et due au rayonnement diffus, peut donc être assimilé au calcul du niveau sonore dû à une source fictive que l'on place dans l'axe de l'ouverture Ω

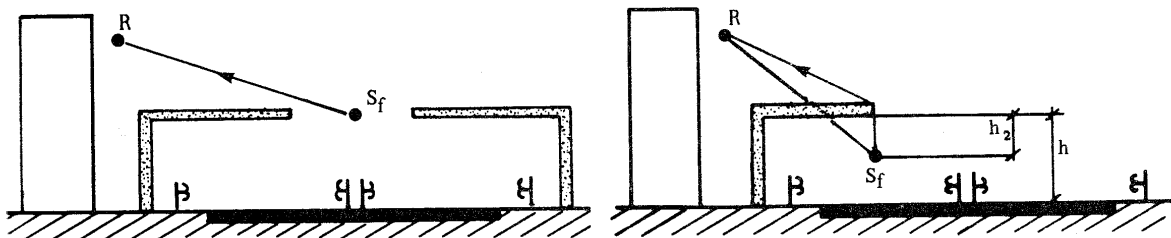


Schéma 4.128 : Situation de la source fictive à laquelle on assimile le champ diffus sous la couverture.

Le niveau sonore L_p dû à ce champ diffus, au point récepteur R s'écrit : pour une couverture partielle infiniment longue.

$$L_p = L_w + 10 \log \frac{Q}{1000 V} + 10 \log \left(1 - \frac{\theta n + \theta'n}{180} \right) + 10 \log \left(\frac{\Omega}{A + \Omega} \right) - 12 \log \left(d + \frac{lc}{3} \right) + 3 \quad (57)$$

S'il existe une diffraction ΔL , on retranchera encore la valeur de ΔL du niveau L_p calculé avec la formule (57). Pour un calcul en champ libre, il conviendrait de plus d'ôter 3 dB (A).

5.4.4. Calcul du niveau sonore global en prévision d'une couverture partielle de longueur limitée.

Le niveau sonore global perçu par le point R en façade d'un bâtiment protégé par une couverture partielle, sera égal au cumul des énergies parvenant en R, soit :

- . énergie se propageant par rayonnement direct, et réfléchie d'ordre 1.
- . énergie diffuse,
- . énergie perçue de façon directe à partir des extrémités de la couverture partielle, par les segments de route non protégés par la couverture.

Dans le plan passant par le point récepteur R, et la ligne de source simulant la route, on peut définir deux zones :

- . sous les angles α et γ l'énergie parvient de façon directe,
- . sous l'angle β l'énergie parvient après diffraction sur la couverture. Elle est la somme de deux termes : énergie rayonnée directement et énergie diffuse.

Le niveau sonore en un point récepteur R en façade sera égale au cumul des niveaux sonores perçus sous les angles α , γ et β

Partie IV : Méthode détaillée routes

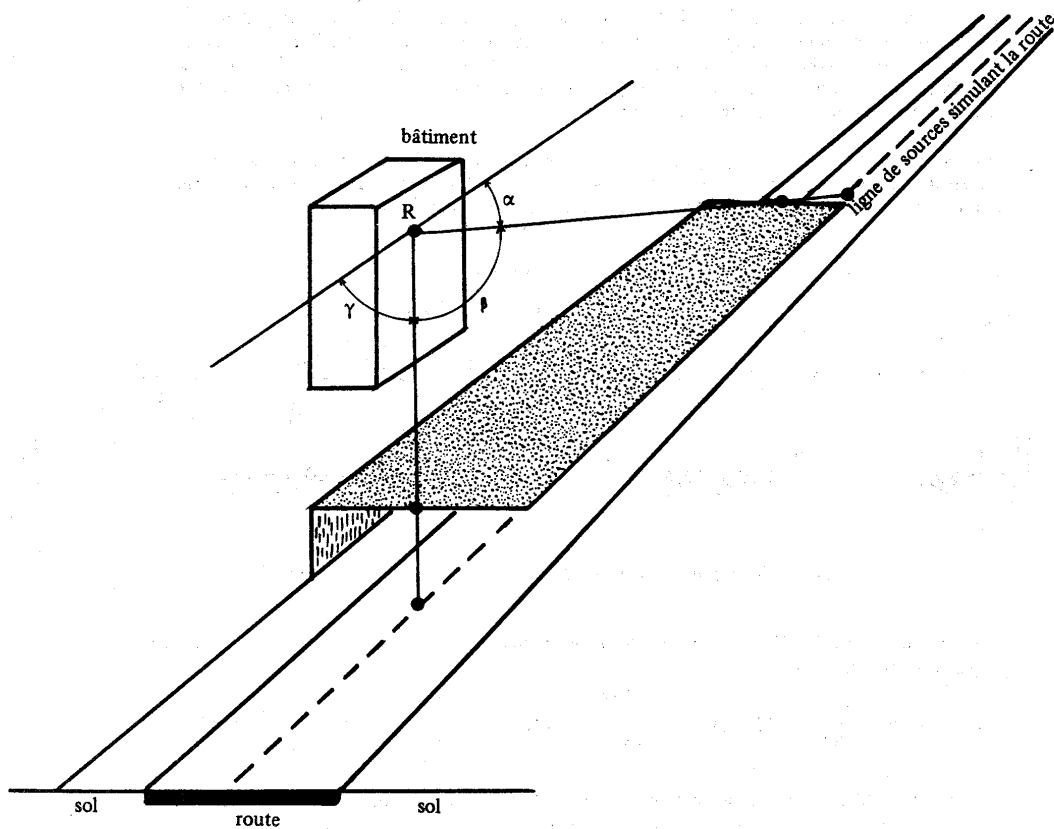


Schéma 4.129 : sous les angles α et γ : énergie directe,
sous l'angle β : énergie rayonnée directement et énergie diffuse sous la couverture.

sous les angles ($\alpha + \gamma$) il est possible d'écrire :

$$L_p = L_w + 10 \log \frac{Q}{1000 V} - 12 \log (d + \frac{l_c}{3}) + 10 \log \frac{\alpha + \beta}{180^\circ} + 3$$

sous l'angle β on peut écrire :

$$L_p = L(\text{direct}) \odot L(\text{réfléchi}) \odot L(\text{diffus})$$

$$\text{avec : } L(\text{direct}) = L_w + 10 \log \frac{Q}{1000 V} - 12 \log (d + \frac{l_c}{3}) + 10 \log \frac{\beta}{180^\circ} - \Delta L + 3$$

$$L(\text{réfléchi}) = L_w + 10 \log \frac{Q}{1000 V} - 12 \log (d + \frac{l_c}{3}) + 10 \log \frac{\beta}{180^\circ} - \Delta L' + 10 \log (1 - \alpha) + 3$$

$$L(\text{diffus}) = L_w + 10 \log \frac{Q}{1000 V} - 10 \log (1 - \frac{\theta + \theta'}{180^\circ}) + 10 \log \frac{\Omega}{A + \Omega} + 3$$

\odot = notation de cumul selon les indications de l'annexe II.

G-Validation elements

The NMPB-Roads-2008 has been validated in two stages. Firstly, every change has been evaluated in academic configurations compared with a reference method. Depending on circumstances, the method using ray-tracing, boundary elements or the parabolic equation has served as a reference (*Cf.* [CSTB2002], [CSTB2007], [LRS2003a], [LRS2003b], [LRS2004]).

Secondly, the entire method has been compared with measurements taken on six actual sites with cross-sections representative of common topographies (*Cf.* [LRS2005][LRS2007]):

- road in cut: sites at Molsheim (67) and Mulhouse (68);
- viaduct road: site at Saint Omer (62);
- road flanking a valley: site at Massiac (15);
- noise barrier: site at Couvron (02);
- hilly terrain: site at Mer (41).

A topographical survey was performed at each site. The sound levels at at least nine points were recorded in short L_{eq} by third-octave band for at least two weeks, at the same time as meteorological measurements. The meteorological readings were used to calculate the rose of occurrences of downward refraction conditions. The extracted noise measurements give attenuation values with respect to a reference microphone for several legal Day (06.00-22.00) or Night (22.00-06.00) periods in L_{Aeq} .

Despite all the care taken with the measuring protocol, obtaining valid measurements beyond 400 m has proved tricky, even in heavy traffic. Once the measurements have been processed, the receivers considered are used to define 310 attenuations compared with a reference receiver, which is the closest to the road. Each attenuation corresponds to a mid-term Day (06.00-22.00) or Night (22.00-06.00) period.

Each site was simulated under both the NMPB-Roads-96 and the NMPB-Roads-2008. The comparison with the measurements gives 310 discrepancies between the measured attenuation and the calculated attenuation. The distribution of discrepancies is represented in Figure G.1 for the NMPB-Roads-96 and Figure G.2 for the NMPB-Roads-2008. The statistical study of these measurement/calculation discrepancies lead to the following conclusions:

- The NMPB-Roads-2008 average of measurement/calculation discrepancies is significantly¹ smaller than in the NMPB-Roads-96. In other words, the NMPB-Roads-2008 is more accurate than the NMPB-Roads-96 (*Cf.* Figure G.1 and Figure G.2);
- There are no significant differences in measurement/calculation discrepancy dispersions² between the two methods: the NMPB-Roads-2008 does not change the accuracy of the noise calculation method compared with the NMPB-Roads-96;
- The NMPB-Roads-2008 measurement/calculation discrepancies follow a normal distribution³, unlike in the NMPB-Roads-96⁴ ;
- Out of 310 measurement/calculation attenuation discrepancy pairings for the NMPB-Roads-2008, 32% are greater than 2 dB in absolute value against 50% with the NMPB-Roads-2008 (*Cf.* Figure G.3).

¹ Student-Welsh statistical test: $p_value < 5\%$ (alternative hypothesis H1: the averages are different). Wilcoxon statistical test: $p_value < 5\%$ (alternative hypothesis H1: the laws of distribution differ).

² Bartlett statistical test: $p_value > 5\%$ (alternative hypothesis H1: the variances are different).

³ Shapiro-Wilk statistical test: $p_value > 5\%$ (alternative hypothesis H1: the discrepancies do not follow a normal distribution).

⁴ Shapiro-Wilk statistical test: $p_value < 5\%$ (alternative hypothesis H1: the discrepancies do not follow a normal distribution).

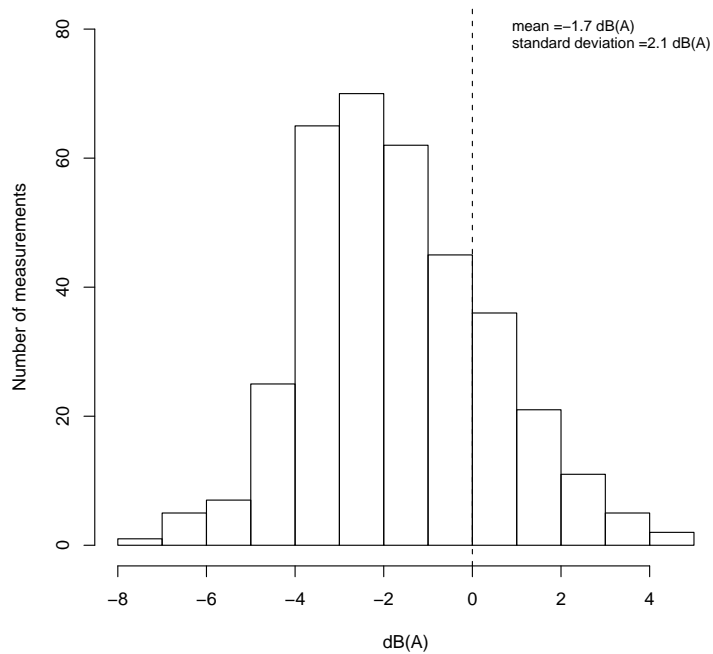


Figure G.1: Histogram of discrepancies between the measured and calculated attenuations for the NMPB-Roads-96.

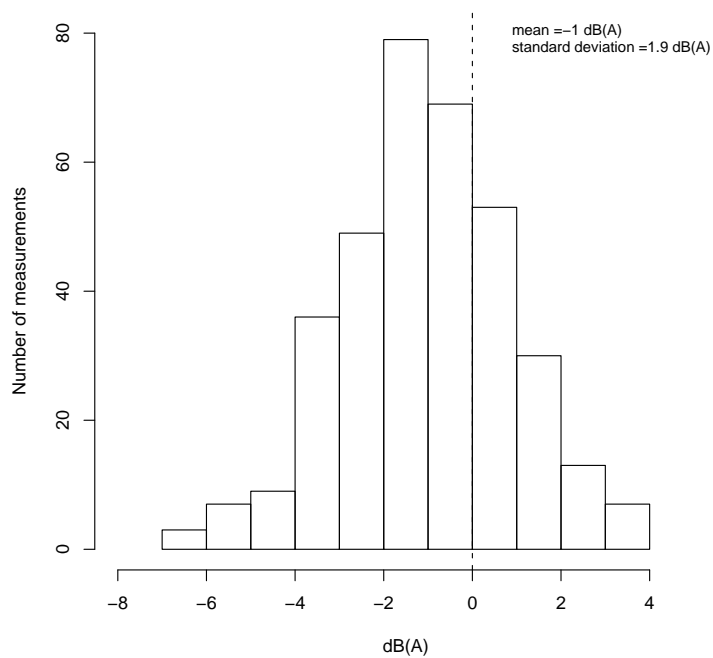


Figure G.2: Histogram of discrepancies between the measured and calculated attenuations for the NMPB-Roads-2008.

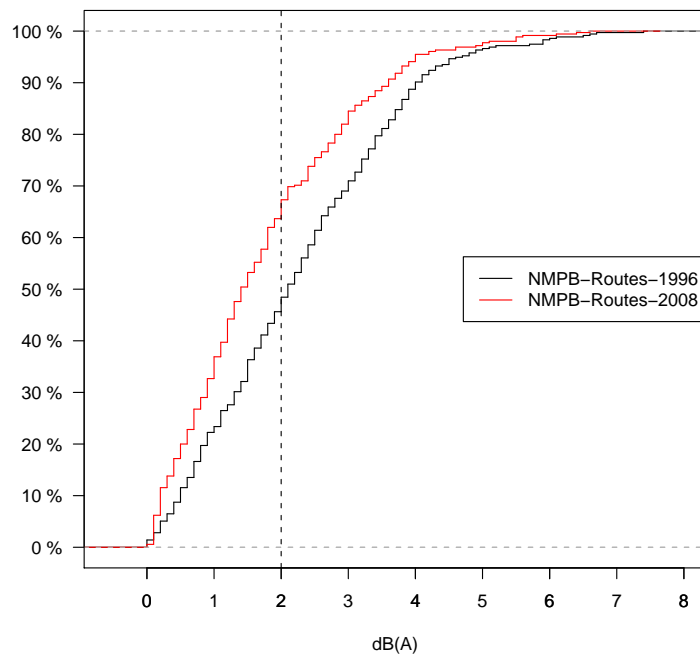


Figure G.3: Measurement/calculation discrepancy distribution function

H - Description of the sites of the experimental campaigns

The results of measurements obtained under the revision and adjustment of new formulae in the noise prediction method come from measurement campaigns on sites representative of situations encountered by the highway engineers. They therefore represent the most typical cases encountered in the national road network. The following figures recall these different configurations.

H.1 - Mulhouse

This site is about ten kilometres north of Mulhouse bordering the A35 motorway between Baldersheim and Battenheim. The A35 has 2x2 lanes with nil slope and a cut about 2 m deep and about 2 km long. Beyond the edge of the cut, the measuring surface is virtually flat and the same type over a width of 500 m (*Cf. Figure H.1*).

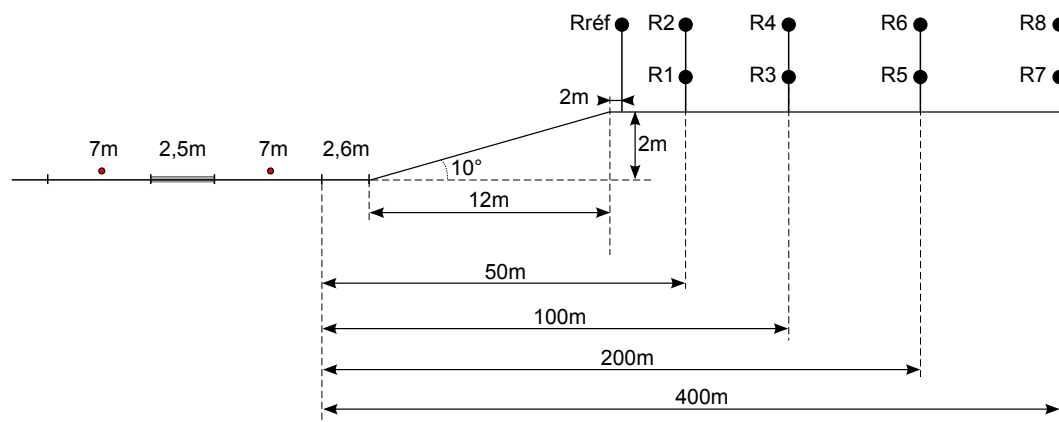


Figure H.1: Cross-section of Mulhouse and location of receivers

The site's meteorological instrumentation requires the installation of three towers, with two near the edge of the cut to analyse disturbances in flow in the area close to the obstacle created by the bank. Behind the cut, the area is homogeneous and perfectly flat (15 cm maximum change in level). The diagram above shows an approximate cross-section of the site passing by each meteorological tower. The figure at each level indicates the position of sensors above the ground.

H.2 - Massiac

The following cross-section shown in Figure H.2 illustrates a measuring campaign located 80 km south of Clermont Ferrand, bordering the A75 motorway 4 km south of Massiac. The receiving points are as previously placed two to five metres above the ground.

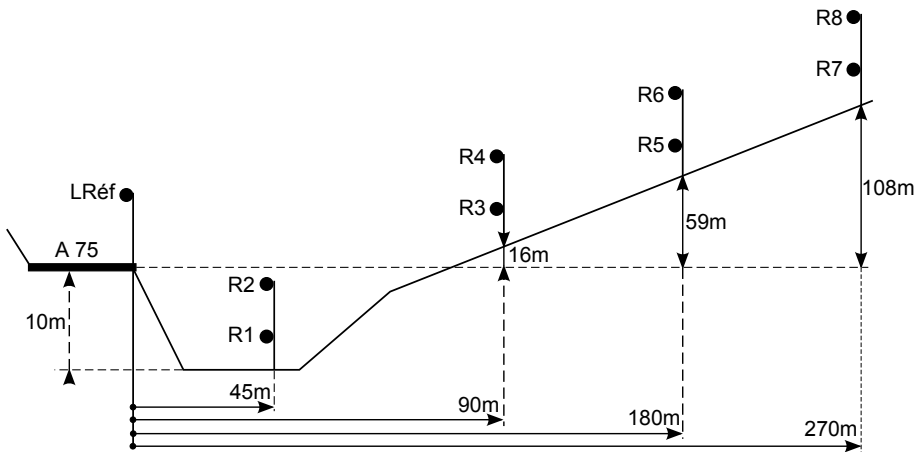


Figure H.2: Cross-section of Massiac and location of receivers

The site's meteorological instrumentation is installed on three towers the length of the acoustic measuring line, to test subsequently the micrometeorological homogeneity of the site. The diagram of Figure H.2 shows an approximate cross-section of the site passing by each meteorological tower. The results obtained for the diffraction via a horizontal platform are summarised in the following table (Receiving point R2):

NMPB-Roads-96	3 dB(A)
NMPB-Roads-2008	<2 dB(A)

H.3-Mer

The third experimental site tested in this document is near the A10 motorway in the municipality of Mer (41). The land is a rounded shape which starts from the motorway, reaches a height of 3 m over the motorway at 150 m then drops down again to motorway level at about 300 m (*Cf.* Figure H.3).

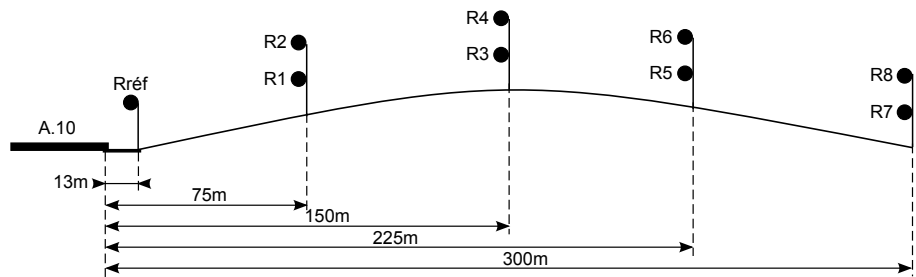


Figure H.3: Cross-section of Mer and location of receivers

The acoustic information is measured at four distances and two different heights (2 m and 5 m above the natural ground). A measuring point right next to the road lane is a reference value, which gives nine measuring points in all.

H.4-Couvron

The campaigns at the fourth site took place bordering the A26 motorway, in the municipality of Couvron. In line with the adopted site, at the level of profile 202+350, the motorway is in cut and a concrete slab screen 2.50 metres high is at the natural level of the ground. The screen is 1120 metres long. The cross-section on Figure H.4 was adopted:

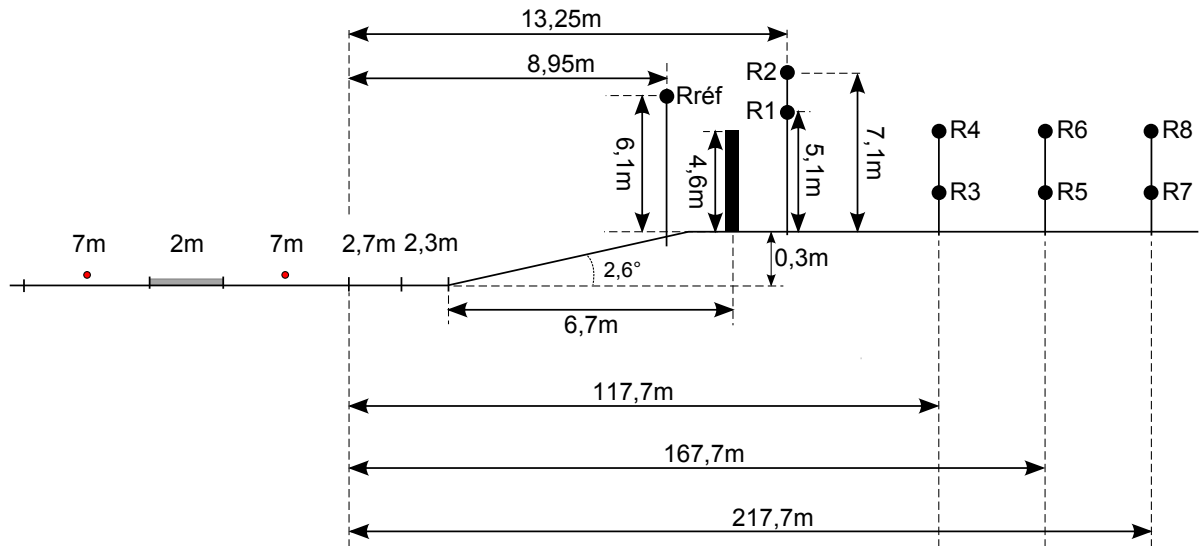


Figure H.4: Cross-section of Couvron and location of receivers

In this site, the microphones are installed to the west of the lane, starting on the edge of the cut (reference point), then at 100 metres, 150 metres and up to 200 metres from the screen. The measuring line is angled at about 123° to the screen and 59° to North. Given the small amount of traffic on the motorway (about 13,500 v/h including 30% heavy goods vehicles) and the presence of the screen, the maximum distance for receiving points from the screen was restricted to 200 metres as the signal/noise ratio was too weak at points further away. Each acoustic tower has two microphones placed at 2 metres and 5 metres respectively above the ground, except for the reference point which only has one microphone 4 metres above the ground and the point just behind the screen with two microphones at 3 metres and 5 metres.

H.5 - Molsheim

The fifth experimentation campaign took place alongside the A352 motorway linking Molsheim to Strasbourg, in the municipality of Altorf. Figure H.5 shows the cross-section of the site.

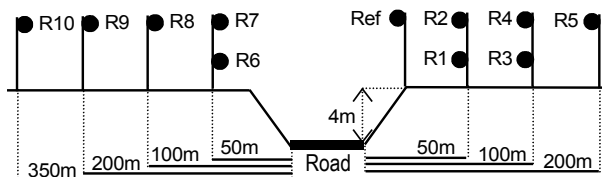


Figure H.5: Cross-section of Molsheim and location of receivers

The angle of view of the lane for each receiver is 180°. The microphones are aligned according to the directions 350° for the South side (direction chosen perpendicular to the lane) and 180° for the North side (direction imposed by the configuration of fields of crops already sown). The meteorological tower was located in a place where the conditions surveyed are representative of average conditions between the road source and the various receiving points.

H.6 - Saint Omer

The sixth and last experimental site is 40 km south-east of Calais, bordering the A26 motorway, 6 km south-west of Saint-Omer. On this site, the A26 is a 2x2 lane motorway and crosses the ravine of Pihem perpendicularly at PR 37+200. The A26 overhangs the bottom of the ravine by about 32 m. The measuring points are installed on the side of the hill parallel to the motorway, with a change in level of 16 to 32 m in

relation to the viaduct. The site is messied around and the ground is absorbent sprinkled with low-growing vegetation. The angle of view of the lane is less than 80°. The measurements were taken at two heights, 2 m and 5 m, above the ground, in free field, either side of the meteorological tower. The positioning of various measuring points and their descriptions are shown in Figure H.6.

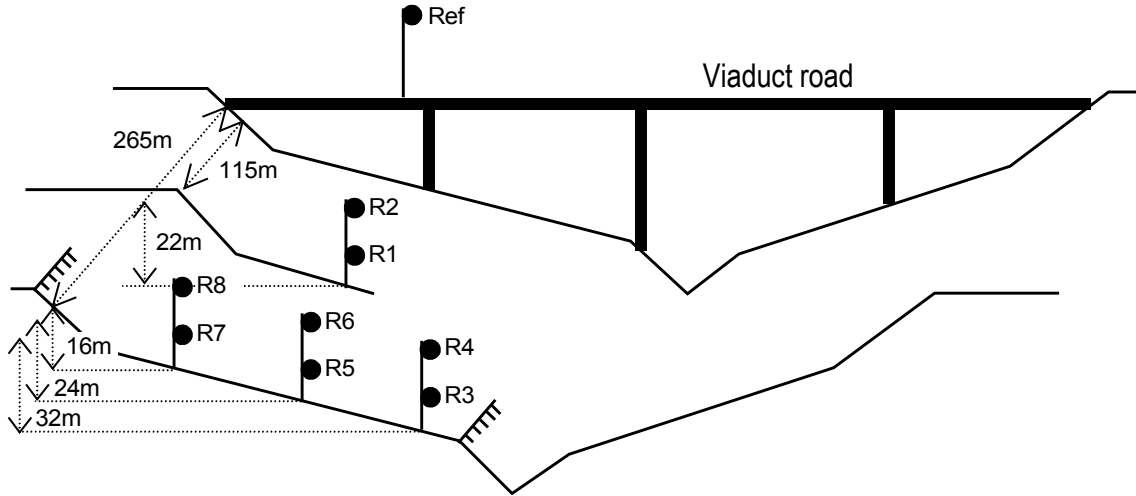


Figure H.6: Cross-section of Saint Omer and location of receivers

The site's meteorological instrumentation is installed on a tower between the acoustic measuring lines. Figure H.6 shows the position of the meteorological tower on the site. The figure at each level indicates the position of sensors above the ground. The results obtained for the diffraction via a horizontal platform are summarised in the following table:

R1 et R2	NMPB-Roads-96	3 dB(A)
	NMPB-Roads-2008	< 2 dB(A)
R5 et R6	NMPB-Roads-96	4-5 dB(A)
	NMPB-Roads-2008	< 2 dB(A)
R7 et R8	NMPB-Roads-96	4-5 dB(A)
	NMPB-Roads-2008	3 dB(A)

I-Sample NMPB-Roads-2008 applications

The aim of this appendix is to illustrate the use of the NMPB-Roads-2008. It should help the reader become familiar with the method, the sequence of the application and its formulae. The method flow chart is available in Appendix A.

It is assumed that the occurrences of Table I.1 apply in the following examples.

Angle (°)	20	40	60	80	100	120	140	160	180	200	220	240	260	280	300	320	340	360
Day (06.00-22.00)	30	28	26	25	27	28	30	32	34	35	36	35	34	32	32	32	32	32
Night (22.00-06.00)	85	85	88	90	92	92	92	92	92	93	94	96	97	96	94	91	88	86

Table I.1: Occurrences of downward refraction conditions as a percentage based on the angle of the source-receiver axis in relation to North (\vec{N}, \vec{RS}).

To measure angles, the horizontal plane is oriented clockwise.

For reasons of readability, the various sections and top views presented in this appendix are traced in non-orthonormal markers. They cannot therefore be used directly to determine whether a source and a receiver are in direct view, or to calculate angles.

I.1 - Site in slight cut

The site in cut represented in Figure I.1 and Figure I.2 is considered. A single traffic lane is studied. The associated source line is placed in the centre of the lane. It is decided to break it down equidistantly. The euclidean distance between the closest receiver and the source line forces a distance interval of less than 8.8 m. For reasons of simplification, the interval is set at 5 m. Only segment S1 centred in line with receivers and S2, 1450 m from S1, are of interest among the source segments. The lane axis defines a 130° angle in relation to North (\vec{N}, \vec{Oy}).

The assumption is that the sound emission has been determined in accordance with [Abaques 2008] and that the power level of a source segment is 80 dB(A). The pavement surface is a BBSG 0/10. The Non-drainage spectrum is therefore the one to use.

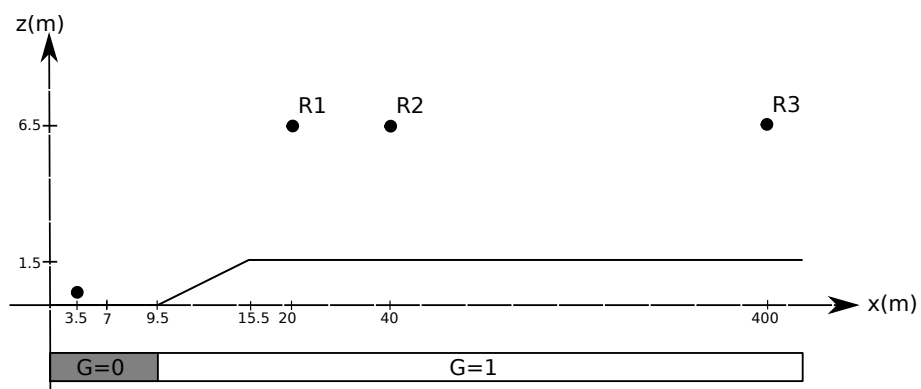


Figure I.1: Vertical section of the site in 1.5 m cut.

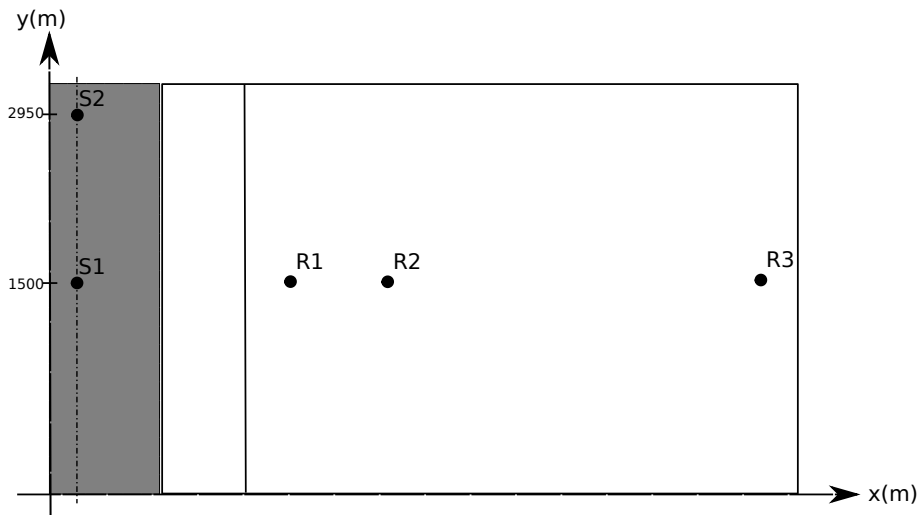


Figure I.2: Top view of the site in 1.5 m cut

I.1.1-Path (S1,R1)

Table I.2 gives the probabilities of occurrence of downward-refraction conditions.

Orientation SR	Sector	Day	Night
40°	40°	0.28	0.85

Table I.2: Occurrences of downward-refraction conditions for path (S1,R1).

I.1.1.1 - Path geometry

SR distance : 17.716 m

The polyline associated to this path is defined in Table I.3.

x (m)	3.5	15.5	20
y (m)	1500	1500	1500
z (m)	0.05	1.5	6.5
z ground (m)	0	1.5	1.5

Table I.3: Path polyline (S1,R1).

I.1.1.2 - Homogeneous conditions

Direct sight: computation of A_{sol}

The related mean ground plane is given in Table I.4.

z_s (m)	d_p (m)	z_r (m)
0.37	17.16	4.77

Table I.4: Mean ground plane for path (S1,R1).

Ground absorption :

- G_{trajet} : 0.64
- G'_{trajet} : 0.07

A_{talus} : no embankment slope detected.

The attenuations in homogeneous conditions are provided in Table I.5.

f	A	100	125	160	200	250	315	400	500	630	800	1000	1250	1600	2000	2500	3150	4000	5000
A_{div}	36.1	36	36	36	36	36	36	36	36	36	36	36	36	36	36	36	36	36	
A_{atm}	0.2	0	0	0	0	0	0	0	0	0.1	0.1	0.1	0.1	0.1	0.2	0.2	0.3	0.5	0.7
A_{sol}	-	2.6	2.8	2.8	2.8	2.8	2.8	2.8	2.8	2.8	2.8	-2.8	-2.8	-2.8	-2.8	-2.8	-2.8	-2.8	
A_{dif}	0.1	0	0	0	0	0	0	0	0	0	0	0	0	0	0	0	0	0	

Table I.5: Attenuations en homogeneous conditions for path (S1,R1).

I.1.1.3 - Downward-refraction conditions

Direct sight: computation of A_{sol}

The related mean ground plane is given in Table I.6.

z_s (m)	d_p (m)	z_r (m)
0.39	17.16	4.81

Table I.6: Mean ground plane for path (S1,R1).

Ground absorption :

- G_{trajet} : 0.64
- G'_{trajet} : 0.07

A_{talus} : no embankment slope detected.

The attenuations in downward-refraction conditions are provided in Table I.7.

f	A	100	125	160	200	250	315	400	500	630	800	1000	1250	1600	2000	2500	3150	4000	5000
A_{div}	36.1	36	36	36	36	36	36	36	36	36	36	36	36	36	36	36	36	36	
A_{atm}	0.2	0	0	0	0	0	0	0	0	0.1	0.1	0.1	0.1	0.1	0.2	0.2	0.3	0.5	0.7
A_{sol}	-	2.6	2.8	2.8	2.8	2.8	2.8	2.8	2.8	2.8	2.8	-2.8	-2.8	-2.8	-2.8	-2.8	-2.8	-2.8	
A_{dif}	0.1	0	0	0	0	0	0	0	0	0	0	0	0	0	0	0	0	0	

Table I.7: Attenuations en downward-refraction conditions for path (S1,R1).

I.1.1.4 - Sound levels

The sound levels in homogeneous conditions are given in Table I.8, in downward-refraction conditions in Table I.9, the long-term sound levels in Table I.10.

I.1.2 - Path (S2,R1)

Ignored: path length larger than $\max(10 \cdot d_{min}, 200)$ m.

I.1.3 - Path (S1,R2)

Table I.11 gives the probabilities of occurrence of downward-refraction conditions.

I.1.3.1 - Path geometry

SR distance : 37.066 m

The polyline associated to this path is defined in Table I.12.

<i>f</i>	A	100	125	160	200	250	315	400	500	630	800	1000	1250	1600	2000	2500	3150	4000	5000
<i>L_w</i>	80	53.1	54.1	56.1	59.1	61.1	64.1	66.1	69.1	69.1	72.1	73.1	72.1	70.1	67.1	64.1	62.1	59.1	57.1
A	33.9	33.2	33.2	33.2	33.2	33.2	33.2	33.2	33.2	33.2	33.3	33.3	33.3	33.3	33.3	33.4	33.5	33.6	33.9
<i>L_{eq}</i>	46.7	19.9	20.9	22.9	25.9	27.9	30.9	32.9	35.9	35.9	38.9	39.9	38.8	36.8	33.8	30.7	28.6	25.5	23.2

Table I.8: Levels in homogeneous conditions for path (S1,R1).

<i>f</i>	A	100	125	160	200	250	315	400	500	630	800	1000	1250	1600	2000	2500	3150	4000	5000
<i>L_w</i>	80	53.1	54.1	56.1	59.1	61.1	64.1	66.1	69.1	69.1	72.1	73.1	72.1	70.1	67.1	64.1	62.1	59.1	57.1
A	33.9	33.2	33.2	33.2	33.2	33.2	33.2	33.2	33.2	33.2	33.3	33.3	33.3	33.3	33.3	33.4	33.5	33.6	33.9
<i>L_{eq}</i>	46.7	19.9	20.9	22.9	25.9	27.9	30.9	32.9	35.9	35.9	38.9	39.9	38.8	36.8	33.8	30.7	28.6	25.5	23.2

Table I.9: Levels in downward-refraction conditions for path (S1,R1).

<i>f</i>	A	100	125	160	200	250	315	400	500	630	800	1000	1250	1600	2000	2500	3150	4000	5000
<i>L_{eq,LT}</i>	46.7	19.9	20.9	22.9	25.9	27.9	30.9	32.9	35.9	35.9	38.9	39.9	38.8	36.8	33.8	30.7	28.6	25.5	23.2

Table I.10: Long-term sound levels for path (S1,R1).

Orientation SR	Sector	Day	Night
40°	40°	0.28	0.85

Table I.11: Occurrences of downward-refraction conditions for path (S1,R2).

x (m)	3.5	15.5	40
y (m)	1500	1500	1500
z (m)	0.05	1.5	6.5
z ground (m)	0	1.5	1.5

Table I.12: Path polyline (S1,R2).

I.1.3.2 - Homogeneous conditions

Single diffraction: computation of A_{dif} and of A_{sol}

Transition frequency : 630 Hz

Direct sight: computation of A_{sol}

The related mean ground plane is given in Table I.13.

z_s (m)	d_p (m)	z_r (m)
0	36. 75	4.56

Table I.13: Mean ground plane for path (S1,R2).

Ground absorption :

- G_{trajet} : 0.84
- G'_{trajet} : 0.23

A_{talus} : no embankment slope detected.

Single diffraction: computation of A_{dif}

- direct sight: YES
- edge of diffraction : [15.5;1500;1.5]
- δ : -0.027 m

The component of A_{dif} are detailed in Table I.14.

f	100	125	160	200	250	315	400	500	630	800	1000	1250	1600	2000	2500	3150	4000	5000	
Δ_{dif}	4.3	4.2	4	3.7	3.4	3	2.4	1.5	0.1	0	0	0	0	0	0	0	0		
$\Delta_{sol(S,O)}$	-	-2	-2	-2	-	1.9	1.8	1.7	1.6	1.3	1.3	-1.3	-1.3	-1	-0.1	1	1.7	1.1	-0.9
$\Delta_{sol(O,R)}$	0	0	0	0	0	0	0	0	0	0	0	0	0	0	0	0	0	0	
$A_{sol(S,O)}$	-	2.2	2.2	2.2	2.2	2.2	2.2	2.2	2.2	2.2	2.2	-2.2	-2.2	-1.6	-0.2	1.6	2.9	1.8	-1.3

Table I.14: Component of A_{dif} for path (S1,R2).

$\Delta_{talus(S,O)}$: no embankment slope detected.

The attenuations in homogeneous conditions are provided in Table I.15.

f	A	100	125	160	200	250	315	400	500	630	800	1000	1250	1600	2000	2500	3150	4000	5000
A_{div}	42.5	42.4	42.4	42.4	42.4	42.4	42.4	42.4	42.4	42.4	42.4	42.4	42.4	42.4	42.4	42.4	42.4	42.4	
A_{atm}	0.3	0	0	0	0	0	0.1	0.1	0.1	0.1	0.1	0.2	0.2	0.2	0.3	0.5	0.7	1	1.5
A_{sol}	0.1	0	0	0	0	0	0	0	0	-2.3	-2.3	-2.3	-2.3	-2.3	-0.9	0.4	1.6	2.7	
A_{dif}	0.1	2.2	2.1	2	1.8	1.6	1.2	0.7	0	-1.3	0	0	0	0	0	0	0	0	

Table I.15: Attenuations en homogeneous conditions for path (S1,R2).

I.1.3.3 - Downward-refraction conditions

Single diffraction: computation of A_{dif} and of A_{sol}

Transition frequency : 500 Hz

Direct sight: computation of A_{sol}

The related mean ground plane is given in Table I.16.

Ground absorption :

z_s (m)	d_p (m)	z_r (m)
0.05	36.75	4.74

Table I.16: Mean ground plane for path (S1,R2).

- G_{trajet} : 0.84
- G'_{trajet} : 0.23

A_{talus} : no embankment slope detected.

Single diffraction: computation of A_{dif}

- direct sight: YES
- edge of diffraction : [15.5;1500;1.5]
- δ : -0.028 m

The component of A_{dif} are detailed in Table I.17.

f	100	125	160	200	250	315	400	500	630	800	1000	1250	1600	2000	2500	3150	4000	5000
Δ_{dif}	4.3	4.1	3.9	3.7	3.4	2.9	2.2	1.3	0	0	0	0	0	0	0	0	0	
$\Delta_{sol(S,O)}$	-	2.1	-2	-2	-2	1.9	1.8	1.7	1.5	1.4	1.3	-0.6	0.5	1.8	2	0.8	-1.6	-1.7
$\Delta_{sol(O,R)}$	0	0	0	0	0	0	0	0	0	0	0	0	0	0	0	0.1	0.1	
$A_{sol(S,O)}$	-	2.2	2.2	2.2	2.2	2.2	2.2	2.2	2.2	2.1	-0.9	0.9	3	3.4	1.2	-2.2	-2.2	-2.2

Table I.17: Component of A_{dif} for path (S1,R2).

$\Delta_{talus(S,O)}$: no embankment slope detected.

The attenuations in downward-refraction conditions are provided in Table I.18.

f	A	100	125	160	200	250	315	400	500	630	800	1000	1250	1600	2000	2500	3150	4000	5000
A_{div}	42.5	42.4	42.4	42.4	42.4	42.4	42.4	42.4	42.4	42.4	42.4	42.4	42.4	42.4	42.4	42.4	42.4	42.4	
A_{atm}	0.3	0	0	0	0	0	0.1	0.1	0.1	0.1	0.1	0.2	0.2	0.2	0.3	0.5	0.7	1	1.5
A_{sol}	0.1	0	0	0	0	0	0	0	-	2.3	-2.3	-2.3	-2.3	-0.8	1.4	3.1	3.3	1.8	
A_{dif}	0.1	2.2	2.1	1.9	1.7	1.5	1.1	0.5	-	0.3	0	0	0	0	0	0	0	0	

Table I.18: Attenuations en downward-refraction conditions for path (S1,R2).

I.1.3.4 - Sound levels

The sound levels in homogeneous conditions are given in Table I.19, in downward-refraction conditions in Table I.20, the long-term sound levels in Table I.21.

I.1.4 - Path (S2,R2)

Ignored: path length larger than $\max(10 \cdot d_{min}, 200)$ m.

I.1.5 - Path (S1,R3)

Table I.22 gives the probabilities of occurrence of downward-refraction conditions.

I.1.5.1 - Path geometry

SR distance : 396.552 m

The polyline associated to this path is defined in Table I.23.

<i>f</i>	A	100	125	160	200	250	315	400	500	630	800	1000	1250	1600	2000	2500	3150	4000	5000
<i>L_w</i>	80	53.1	54.1	56.1	59.1	61.1	64.1	66.1	69.1	69.1	72.1	73.1	72.1	70.1	67.1	64.1	62.1	59.1	57.1
A	43	44.6	44.5	44.4	44.2	44	43.6	43.2	42.4	41.2	40.2	40.2	40.2	40.3	40.4	42	43.4	45	46.5
<i>L_{eq}</i>	39.2	8.5	9.6	11.7	14.9	17.1	20.5	23	26.7	27.9	31.9	32.9	31.9	29.8	26.7	22.2	18.7	14.2	10.6

Table I.19: Levels in homogeneous conditions for path (S1,R2).

<i>f</i>	A	100	125	160	200	250	315	400	500	630	800	1000	1250	1600	2000	2500	3150	4000	5000
<i>L_w</i>	80	53.1	54.1	56.1	59.1	61.1	64.1	66.1	69.1	69.1	72.1	73.1	72.1	70.1	67.1	64.1	62.1	59.1	57.1
A	43	44.6	44.5	44.3	44.1	43.9	43.5	43	42.2	40.2	40.2	40.2	40.2	40.3	41.9	44.2	46.1	46.7	45.7
<i>L_{eq}</i>	39.2	8.5	9.6	11.8	15	17.2	20.6	23.1	26.9	29	31.9	32.9	31.9	29.8	25.3	19.9	16	12.5	11.5

Table I.20: Levels in downward-refraction conditions for path (S1,R2).

<i>f</i>	A	100	125	160	200	250	315	400	500	630	800	1000	1250	1600	2000	2500	3150	4000	5000
<i>L_{eq,LT}</i>	39.2	8.5	9.6	11.8	14.9	17.2	20.5	23	26.7	28.2	31.9	32.9	31.9	29.8	26.4	21.6	18.1	13.7	10.9

Table I.21: Long-term sound levels for path (S1,R2).

Orientation SR	Sector	Day	Night
40°	40°	0.28	0.85

Table I.22: Occurrences of downward-refraction conditions for path (S1,R3).

x (m)	3.5	15.5	400
y (m)	1500	1500	1500
z (m)	0.05	1.5	6.5
z ground (m)	0	1.5	1.5

Table I.23: Path polyline (S1,R3).

I.1.5.2 - Homogeneous conditions

Single diffraction: computation of A_{dif}

- direct sight: NO
- edge of diffraction : [15.5;1500;1.5]
- δ : 0.067 m

The component of A_{dif} are detailed in Table I.24.

f	100	125	160	200	250	315	400	500	630	800	1000	1250	1600	2000	2500	3150	4000	5000
Δ_{dif}	5.8	6	6.3	6.6	7	7.4	7.9	8.4	9	9.7	10.4	11.1	12	12.8	13.6	14.5	15.4	16.3
$\Delta_{sol(S,O)}$	-	-	-	-	-	-	-	-	-	-	-1.5	-1.5	-1.1	-0.1	1	1.8	1.1	-0.8
$\Delta_{sol(O,R)}$	1.9	1.9	1.8	1.8	1.7	1.7	1.7	1.6	1.6	1.6	10.7	11	11.4	11.6	11.9	12.1	12.3	12.5
$A_{sol(S,O)}$	0	0	0	1.1	4.4	6.7	7.9	8.8	9.7	10.3	-2.2	-2.2	-1.6	-0.2	1.6	2.9	1.8	-1.3
$A_{sol(O,R)}$	2.2	2.2	2.2	2.2	2.2	2.2	2.2	2.2	2.2	2.2	-2.2	-2.2	-1.6	-0.2	1.6	2.9	1.8	-1.3

Table I.24: Component of A_{dif} for path (S1,R3).

$\Delta_{talus(S,O)}$: no embankment slope detected.

The attenuations in homogeneous conditions are provided in Table I.25.

f	A	100	125	160	200	250	315	400	500	630	800	1000	1250	1600	2000	2500	3150	4000	5000
A_{div}	63.1	63	63	63	63	63	63	63	63	63	63	63	63	63	63	63	63	63	
A_{atm}	1.9	0.1	0.2	0.2	0.3	0.4	0.6	0.8	0.9	1.1	1.3	1.6	2	2.6	3.5	4.8	7	10.5	15.8
A_{sol}	0.1	0	0	0	0	0	0	0	0	0	0	0	0	0	0	0	0	0	
A_{dif}	18.6	3.9	4.1	4.5	5.9	9.6	12.4	14.2	15.6	17.1	18.4	19.5	20.6	22.2	24.3	26.5	28.3	28.8	27.9

Table I.25: Attenuations en homogeneous conditions for path (S1,R3).

I.1.5.3 - Downward-refraction conditions

Single diffraction: computation of A_{dif}

- direct sight: NO
- edge of diffraction : [15.5;1500;1.5]
- δ : 0.045 m

The component of A_{dif} are detailed in Table I.26.

f	100	125	160	200	250	315	400	500	630	800	1000	1250	1600	2000	2500	3150	4000	5000
Δ_{dif}	5.5	5.6	5.8	6.1	6.3	6.7	7.1	7.5	8	8.6	9.2	9.8	10.6	11.3	12.1	12.9	13.8	14.7
$\Delta_{sol(S,O)}$	-	-	-	-	-	-	-	-	-	-	-0.6	0.5	1.7	1.8	0.7	-1.3	-1.3	-1.3
$\Delta_{sol(O,R)}$	1.9	1.8	1.8	1.7	1.7	1.6	1.6	1.5	1.5	1.4	1.4	1.4	1.4	1.4	1.4	1.4	1.4	1.4
$A_{sol(S,O)}$	0	0	0	0	0	0	0	0	0	0	0	0	0	0	0	0	0	0
$A_{sol(O,R)}$	2.2	2.2	2.2	2.2	2.2	2.2	2.2	2.2	2.2	2.2	-0.9	0.9	3	3.4	1.2	-2.2	-2.2	-2.2

Table I.26: Component of A_{dif} for path (S1,R3).

$\Delta_{talus(S,O)}$: no embankment slope detected.

The attenuations in downward-refraction conditions are provided in Table I.27.

I.1.5.4 - Sound levels

The sound levels in homogeneous conditions are given in Table I.28, in downward-refraction conditions in Table I.29, the long-term sound levels in Table I.30.

<i>f</i>	A	100	125	160	200	250	315	400	500	630	800	1000	1250	1600	2000	2500	3150	4000	5000
A_{div}	63.1	63	63	63	63	63	63	63	63	63	63	63	63	63	63	63	63	63	
A_{atm}	1.9	0.1	0.2	0.2	0.3	0.4	0.6	0.8	0.9	1.1	1.3	1.6	2	2.6	3.5	4.8	7	10.5	15.8
A_{sol}	0.1	0	0	0	0	0	0	0	0	0	0	0	0	0	0	0	0	0	
A_{dif}	10.2	3.6	3.8	4	4.3	4.6	5	5.5	6	8.9	10.8	11.6	11.8	12.3	13.1	12.7	11.6	12.5	13.4

Table I.27: Attenuations en downward-refraction conditions for path (S1,R3).

<i>f</i>	A	100	125	160	200	250	315	400	500	630	800	1000	1250	1600	2000	2500	3150	4000	5000
L_w	80	53.1	54.1	56.1	59.1	61.1	64.1	66.1	69.1	69.1	72.1	73.1	72.1	70.1	67.1	64.1	62.1	59.1	57.1
A	83.7	66.9	67.3	67.7	69.2	73	76	77.9	79.5	81.2	82.7	84.1	85.6	87.8	90.7	94.3	98.3	102	107
L_{eq}	-	-	-	-	-	-	-	-	-	-	-	-11	-	-	-	-	-	-	
	0.8	13.8	13.1	11.6	10.1	11.9	11.9	11.8	10.4	12.1	10.6	13.5	17.7	23.6	30.2	36.2	43.1	49.6	

Table I.28: Levels in homogeneous conditions for path (S1,R3).

<i>f</i>	A	100	125	160	200	250	315	400	500	630	800	1000	1250	1600	2000	2500	3150	4000	5000
L_w	80	53.1	54.1	56.1	59.1	61.1	64.1	66.1	69.1	69.1	72.1	73.1	72.1	70.1	67.1	64.1	62.1	59.1	57.1
A	75.3	66.6	66.9	67.2	67.6	68.1	68.6	69.2	69.9	73	75.1	76.2	76.8	77.8	79.6	80.5	81.6	85.9	92.1
L_{eq}	6.2	-	-	-	-	-	-	-	-	-	-3.1	-4.6	-7.7	-	-	-	-	-35	
		13.5	12.8	11.1	8.5	6.9	4.5	3.1	0.8	3.9	2.9								

Table I.29: Levels in downward-refraction conditions for path (S1,R3).

<i>f</i>	A	100	125	160	200	250	315	400	500	630	800	1000	1250	1600	2000	2500	3150	4000	5000		
$L_{eq,LT}$	2.5	-	13.7	13	11.4	9.6	9.9	8.3	7.3	5.2	-8	6.9	-7.1	-8.9	-	12.2	17.2	21.5	24.8	32.1	40.2

Table I.30: Long-term sound levels for path (S1,R3).

I.1.6 - Path (S2,R3)

Table I.31 gives the probabilities of occurrence of downward-refraction conditions.

Orientation SR 114.7°	Sector 120°	Day 0.28	Night 0.92
--------------------------	----------------	-------------	---------------

Table I.31: Occurrences of downward-refraction conditions for path (S2,R3).

I.1.6.1 - Path geometry

SR distance : 1503.248 m

The polyline associated to this path is defined in Table I.32.

x (m)	3.5	15.5	400
y (m)	2950	2906.116	1500
z (m)	0.05	1.5	6.5
z ground (m)	0	1.5	1.5

Table I.32: Path polyline (S2,R3).

I.1.6.2 - Homogeneous conditions

Single diffraction: computation of A_{dif}

- direct sight: NO
- edge of diffraction : [15.5;2906.116;1.5]
- δ : 0.018 m

The component of A_{dif} are detailed in Table I.33.

f	100	125	160	200	250	315	400	500	630	800	1000	1250	1600	2000	2500	3150	4000	5000
Δ_{dif}	5.1	5.1	5.2	5.3	5.5	5.6	5.8	6.1	6.4	6.7	7.1	7.5	8	8.6	9.2	9.8	10.6	11.3
$\Delta_{sol(S,O)}$	-	-	-	-	-	-	-	-	-	-1	1.9	5.1	7.8	8.3	7.5	6.1	4.7	3.4
$\Delta_{sol(O,R)}$	0	1	6.4	12.1	16.6	18.2	18.4	18.2	18	17.7	17.4	17	16.6	16.3	16	15.6	15.3	15.1
$A_{sol(S,O)}$	-	-	-	-	-	-	-	-	-	1.3	2.5	7.8	14.6	17.8	15.6	11.9	8.6	5.9

Table I.33: Component of A_{dif} for path (S2,R3).

$\Delta_{talus(S,O)}$: no embankment slope detected.

The attenuations in homogeneous conditions are provided in Table I.34.

I.1.6.3 - Downward-refraction conditions

Single diffraction: computation of A_{dif} and of A_{sol}

Transition frequency : 200 Hz

Direct sight: computation of A_{sol}

The related mean ground plane is given in Table I.35.

Ground absorption :

- G_{trajet} : 0.98
- G'_{trajet} : 0.98

f	A	100	125	160	200	250	315	400	500	630	800	1000	1250	1600	2000	2500	3150	4000	5000
A_{div}	74.7	74.5	74.5	74.5	74.5	74.5	74.5	74.5	74.5	74.5	74.5	74.5	74.5	74.5	74.5	74.5	74.5	74.5	
A_{atm}	5.8	0.4	0.6	0.9	1.2	1.7	2.3	2.9	3.5	4.3	5.1	6.1	7.6	9.8	13.2	18.3	26.6	39.7	60
A_{sol}	0.1	0	0	0	0	0	0	0	0	0	0	0	0	0	0	0	0	0	
A_{dif}	24.8	3.6	4.7	10.2	16.1	20.7	22.5	22.9	23	23.1	23.4	26.3	29.6	32.5	33.2	32.6	31.6	30.6	29.8

Table I.34: Attenuations en homogeneous conditions for path (S2,R3).

z_s (m)	d_p (m)	z_r (m)
1.83	1503.23	232.73

Table I.35: Mean ground plane for path (S2,R3).

A_{talus} : no embankment slope detected.

Single diffraction: computation of A_{dif}

- direct sight: NO
- edge of diffraction : [15.5;2906.116;1.5]
- δ : -0.069 m

The component of A_{dif} are detailed in Table I.36.

f	100	125	160	200	250	315	400	500	630	800	1000	1250	1600	2000	2500	3150	4000	5000
Δ_{dif}	3.4	3	2.3	1.4	0	0	0	0	0	0	0	0	0	0	0	0	0	0
$\Delta_{sol(S,O)}$	-	-	-	-	-	-	-	-	-	-	-	-	-	-	-	-	-	-
$\Delta_{sol(O,R)}$	2.8	2.7	2.6	2.5	2.2	2.4	2.7	2.9	1.7	1.1	4.7	7.9	7.8	4.5	0.9	-2.2	-2.9	-2.9
$A_{sol(S,O)}$	0	0	0	0	0	0	0	0	0	0	0	0	0	0	0	0	0	0
$A_{sol(O,R)}$	0	0	0	0	0	0	0	0	0	0	0	0	0	0	0	0	0	0
$A_{sol(S,R)}$	2.9	2.9	2.9	2.9	2.9	2.9	2.9	2.9	1.7	1.1	4.7	7.9	7.8	4.5	0.9	-2.2	-2.9	-2.9

Table I.36: Component of A_{dif} for path (S2,R3).

$\Delta_{talus(S,O)}$: no embankment slope detected.

The attenuations in downward-refraction conditions are provided in Table I.37.

I.1.6.4 - Sound levels

The sound levels in homogeneous conditions are given in Table I.38, in downward-refraction conditions in Table I.39, the long-term sound levels in Table I.40.

<i>f</i>	A	100	125	160	200	250	315	400	500	630	800	1000	1250	1600	2000	2500	3150	4000	5000
A_{div}	74.7	74.5	74.5	74.5	74.5	74.5	74.5	74.5	74.5	74.5	74.5	74.5	74.5	74.5	74.5	74.5	74.5	74.5	
A_{atm}	5.8	0.4	0.6	0.9	1.2	1.7	2.3	2.9	3.5	4.3	5.1	6.1	7.6	9.8	13.2	18.3	26.6	39.7	60
A_{sol}	0.1	0	0	0	0	-0.1	0.1	0.1	0.1	0.1	0.1	-0.1	-0.1	-0.1	-0.1	-0.1	-0.1	-0.1	
A_{dif}	0.1	0.6	0.3	-0.3	-1	0	0	0	0	0	0	0	0	0	0	0	0	0	

Table I.37: Attenuations en downward-refraction conditions for path (S2,R3).

<i>f</i>	A	100	125	160	200	250	315	400	500	630	800	1000	1250	1600	2000	2500	3150	4000	5000
L_w	80	53.1	54.1	56.1	59.1	61.1	64.1	66.1	69.1	69.1	72.1	73.1	72.1	70.1	67.1	64.1	62.1	59.1	57.1
A	105	78.6	79.8	85.6	91.9	97	99.3	100	101	102	103	107	112	117	121	125	133	145	164
L_{eq}	-	-	-	-	-	-	-	-	-	-	-	-	-	-	-	-	-	-	

Table I.38: Levels in homogeneous conditions for path (S2,R3).

<i>f</i>	A	100	125	160	200	250	315	400	500	630	800	1000	1250	1600	2000	2500	3150	4000	5000
L_w	80	53.1	54.1	56.1	59.1	61.1	64.1	66.1	69.1	69.1	72.1	73.1	72.1	70.1	67.1	64.1	62.1	59.1	57.1
A	80.7	75.6	75.4	75.1	74.7	76.1	76.7	77.3	78	78.7	79.5	80.5	82	84.2	87.6	92.8	101	114	134
L_{eq}	0.1	22.4	21.3	19	15.6	15	12.6	11.2	8.8	9.6	7.4	-7.4	-9.9	14.1	20.5	28.6	38.9	-55	77.3

Table I.39: Levels in downward-refraction conditions for path (S2,R3).

<i>f</i>	A	100	125	160	200	250	315	400	500	630	800	1000	1250	1600	2000	2500	3150	4000	5000
$L_{eq,LT}$	-	-	-	-	-	-	-	-	-	-	-	-	-	-26	-	-	-	-	
	5.5	24.4	24	23.6	20.9	20.4	18	16.7	14.3	15	12.9	12.9	15.4	19.6	34.2	44.4	60.5	82.8	

Table I.40: Long-term sound levels for path (S2,R3).

I.2 - Site in large cut

The studied site here is identical to the one in Section I.1, except that the cut is 4 m instead of 1.5 m. This site illustrates taking into account the reflection on an embankment slope, in the ground effect and in the diffraction. The vertical section of the site is given in Figure I.3.

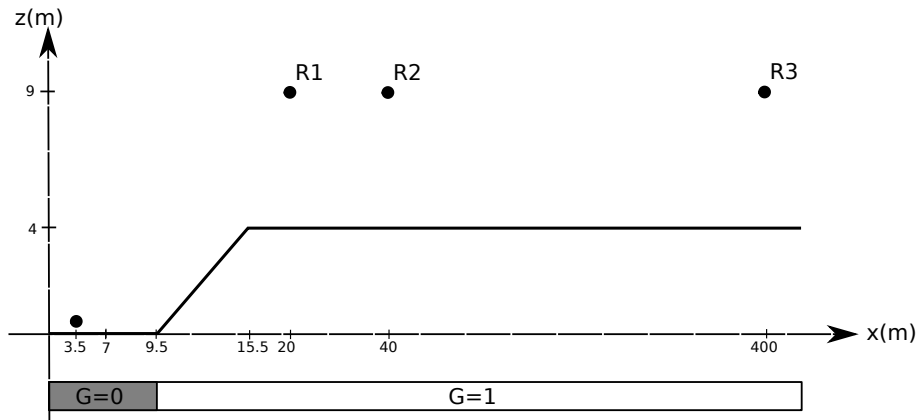


Figure I.3: Vertical section of the site in 4 m cut.

I.2.1 - Path (S1,R1)

Table I.41 gives the probabilities of occurrence of downward-refraction conditions.

Orientation SR	Sector	Day	Night
40°	40°	0.28	0.85

Table I.41: Occurrences of downward-refraction conditions for path (S1,R1).

I.2.1.1 - Path geometry

SR distance : 18.771 m

The polyline associated to this path is defined in Table I.42.

x (m)	3.5	15.5	20
y (m)	1500	1500	1500
z (m)	0.05	4	9
z ground (m)	0	4	4

Table I.42: Path polyline (S1,R1).

I.2.1.2 - Homogeneous conditions

Direct sight: computation of A_{sol}

The related mean ground plane is given in Table I.43.

z_s (m)	d_p (m)	z_r (m)
0.87	18.46	4.25

Table I.43: Mean ground plane for path (S1,R1).

Ground absorption :

- G_{trajet} : 0.64

- G'_{trajet} : 0.08

The computation of A_{talus} are given in Table I.44.

f (Hz)	100	125	160	200	250	315	400	500	630	800	1000	1250	1600	2000	2500	3150	4000	5000
A_{talus}	-0.5	-0.6	-0.6	-0.7	-0.7	-0.7	-0.7	-0.7	-0.7	-0.7	-0.7	-0.7	-0.6	-0.6	-0.6	-0.6	-0.6	

Table I.44: Components of A_{talus} .

The attenuations in homogeneous conditions are provided in Table I.45.

f	A	100	125	160	200	250	315	400	500	630	800	1000	1250	1600	2000	2500	3150	4000	5000
A_{div}	36.6	36.5	36.5	36.5	36.5	36.5	36.5	36.5	36.5	36.5	36.5	36.5	36.5	36.5	36.5	36.5	36.5	36.5	
A_{atm}	0.2	0	0	0	0	0	0	0	0.1	0.1	0.1	0.1	0.1	0.2	0.2	0.3	0.5	0.7	
A_{sol}	-3.2	-3.3	-3.3	-3.4	-3.5	-3.5	-3.5	-3.5	-3.5	-3.5	-3.4	-3.4	-3.4	-3.4	-3.4	-3.4	-3.4	-3.3	
A_{dif}	0.1	0	0	0	0	0	0	0	0	0	0	0	0	0	0	0	0	0	

Table I.45: Attenuations en homogeneous conditions for path (S1,R1).

I.2.1.3 - Downward-refraction conditions

Direct sight: computation of A_{sol}

The related mean ground plane is given in Table I.46.

z_s (m)	d_p (m)	z_r (m)
0.9	1 8.46	4.3

Table I.46: Mean ground plane for path (S1,R1).

Ground absorption :

- G_{trajet} : 0.64
- G'_{trajet} : 0.08

The computation of A_{talus} are given in Table I.47.

The attenuations in downward-refraction conditions are provided in Table I.48.

I.2.1.4 - Sound levels

The sound levels in homogeneous conditions are given in Table I.49, in downward-refraction conditions in Table I.50, the long-term sound levels in Table I.51.

I.2.2 - Path (S2,R1)

Ignored: path length larger than $\max(10 \cdot d_{min}, 200)$ m.

I.2.3 - Path (S1,R2)

Table I.52 gives the probabilities of occurrence of downward-refraction conditions.

I.2.3.1 - Path geometry

SR distance : 37.581 m

The polyline associated to this path is defined in Table I.53.

f (Hz)	100	125	160	200	250	315	400	500	630	800	1000	1250	1600	2000	2500	3150	4000	5000
A_{talus}	-0.5	-0.6	-0.6	-0.7	-0.7	-0.7	-0.7	-0.7	-0.7	-0.7	-0.7	-0.7	-0.7	-0.6	-0.6	-0.6	-0.6	

Table I.47: Components of A_{talus} .

f	A	100	125	160	200	250	315	400	500	630	800	1000	1250	1600	2000	2500	3150	4000	5000
A_{div}	36.6	36.5	36.5	36.5	36.5	36.5	36.5	36.5	36.5	36.5	36.5	36.5	36.5	36.5	36.5	36.5	36.5	36.5	
A_{atm}	0.2	0	0	0	0	0	0	0	0	0.1	0.1	0.1	0.1	0.1	0.2	0.2	0.3	0.5	0.7
A_{sol}	3.2	3.3	3.3	3.4	3.5	3.5	3.5	3.5	3.5	3.5	3.5	-3.4	-3.4	-3.4	-3.4	-3.4	-3.4	-3.3	
A_{dif}	0.1	0	0	0	0	0	0	0	0	0	0	0	0	0	0	0	0	0	

Table I.48: Attenuations en downward-refraction conditions for path (S1,R1).

f	A	100	125	160	200	250	315	400	500	630	800	1000	1250	1600	2000	2500	3150	4000	5000
L_w	80	53.1	54.1	56.1	59.1	61.1	64.1	66.1	69.1	69.1	72.1	73.1	72.1	70.1	67.1	64.1	62.1	59.1	57.1
A	33.7	33.2	33.1	33.1	33	33	33	33	33	33.1	33.1	33.1	33.1	33.2	33.2	33.3	33.4	33.6	33.9
L_{eq}	46.9	19.9	21	23	26.1	28.1	31.1	33.1	36.1	36.1	39	40	39	36.9	33.9	30.8	28.7	25.5	23.2

Table I.49: Levels in homogeneous conditions for path (S1,R1).

f	A	100	125	160	200	250	315	400	500	630	800	1000	1250	1600	2000	2500	3150	4000	5000
L_w	80	53.1	54.1	56.1	59.1	61.1	64.1	66.1	69.1	69.1	72.1	73.1	72.1	70.1	67.1	64.1	62.1	59.1	57.1
A	33.7	33.2	33.1	33.1	33	33	33	33	33	33.1	33.1	33.1	33.1	33.2	33.2	33.3	33.4	33.6	33.9
L_{eq}	46.9	19.9	21	23	26.1	28.1	31.1	33.1	36.1	36.1	39	40	39	36.9	33.9	30.8	28.7	25.5	23.2

Table I.50: Levels in downward-refraction conditions for path (S1,R1).

f	A	100	125	160	200	250	315	400	500	630	800	1000	1250	1600	2000	2500	3150	4000	5000
$L_{eq,LT}$	46.9	19.9	21	23	26.1	28.1	31.1	33.1	36.1	36.1	39	40	39	36.9	33.9	30.8	28.7	25.5	23.2

Table I.51: Long-term sound levels for path (S1,R1).

Orientation SR	Sector	Day	Night
40°	40°	0.28	0.85

Table I.52: Occurrences of downward-refraction conditions for path (S1,R2).

x (m)	3.5	15.5	40
y (m)	1500	1500	1500
z (m)	0.05	4	9
z ground (m)	0	4	4

Table I.53: Path polyline (S1,R2).

I.2.3.2 - Homogeneous conditions

Single diffraction: computation of A_{dif}

- direct sight: NO
- edge of diffraction : [15.5;1500;4]
- δ : 0.057 m

The component of A_{dif} are detailed in Table I.54.

f	100	125	160	200	250	315	400	500	630	800	1000	1250	1600	2000	2500	3150	4000	5000
Δ_{dif}	5.6	5.8	6.1	6.4	6.7	7.1	7.5	8	8.6	9.2	9.9	10.6	11.4	12.2	13	13.8	14.8	15.6
$\Delta_{sol(S,O)}$	-	-	-	-	-	-	0	-	-	-	-1.2	-1.4	-1.4	-1.4	-1.4	-1.3	-1.3	-1.3
$\Delta_{sol(O,R)}$	1.6	1.3	0.9	0.6	0.3	0.1	0.1	0.1	0.3	0.6	-	-	-	-	-	-	-	-
$A_{sol(S,O)}$	0	0	0	0	0	0	0	0	0	0	0	0	0	0	0	0	0	0
$\Delta_{talus(S,O)}$	-	-	-	-	-	-	-	-	-	-	-2.2	-2.6	-2.6	-2.6	-2.6	-2.6	-2.6	-2.6
	2.1	1.7	1.3	0.9	0.5	0.2	0.1	0.1	0.5	1.2	-	-	-	-	-	-	-	-
	0.3	0.3	0.3	0.2	0.2	0.2	0.2	0.2	0.2	0.2	-0.2	-0.2	-0.2	-0.2	-0.2	-0.1	-0.1	-0.1

Table I.54: Component of A_{dif} for path (S1,R2).

The attenuations in homogeneous conditions are provided in Table I.55.

f	A	100	125	160	200	250	315	400	500	630	800	1000	1250	1600	2000	2500	3150	4000	5000
A_{div}	42.6	42.5	42.5	42.5	42.5	42.5	42.5	42.5	42.5	42.5	42.5	42.5	42.5	42.5	42.5	42.5	42.5	42.5	
A_{atm}	0.3	0	0	0	0	0	0.1	0.1	0.1	0.1	0.1	0.2	0.2	0.2	0.3	0.5	0.7	1	1.5
A_{sol}	0.1	0	0	0	0	0	0	0	0	0	0	0	0	0	0	0	0	0	
A_{dif}	8.9	3.7	4.3	4.9	5.5	6.1	6.7	7.3	7.8	8.2	8.4	8.5	9	9.8	10.6	11.5	12.3	13.3	14.2

Table I.55: Attenuations en homogeneous conditions for path (S1,R2).

I.2.3.3 - Downward-refraction conditions

Single diffraction: computation of A_{dif}

- direct sight: NO
- edge of diffraction : [15.5;1500;4]
- δ : 0.056 m

The component of A_{dif} are detailed in Table I.56.

f	100	125	160	200	250	315	400	500	630	800	1000	1250	1600	2000	2500	3150	4000	5000
Δ_{dif}	5.6	5.8	6.1	6.3	6.7	7	7.5	8	8.5	9.2	9.8	10.5	11.3	12.1	12.9	13.7	14.7	15.5
$\Delta_{sol(S,O)}$	-	-	-	-	-	-	-	-	-	-	-1.5	-1.4	-1.4	-1.4	-1.4	-1.3	-1.3	-1.3
$\Delta_{sol(O,R)}$	1.5	1.2	0.9	0.7	0.5	0.5	0.6	0.7	0.9	1.2	-	-	-	-	-	-	-	-
$A_{sol(S,O)}$	0	0	0	0	0	0	0	0	0	0	0	0	0	0	0	0	0	0
$\Delta_{talus(S,O)}$	-2	-1.6	-1.3	-1	-0.8	-0.8	-0.9	-1.2	-1.6	-2.1	-2.6	-2.6	-2.6	-2.6	-2.6	-2.6	-2.6	-2.6
	0.3	0.3	0.3	0.2	0.2	0.2	0.2	0.2	0.2	0.2	-0.2	-0.2	-0.2	-0.2	-0.1	-0.1	-0.1	-0.1

Table I.56: Component of A_{dif} for path (S1,R2).

The attenuations in downward-refraction conditions are provided in Table I.57.

I.2.3.4 - Sound levels

The sound levels in homogeneous conditions are given in Table I.58, in downward-refraction conditions in Table I.59, the long-term sound levels in Table I.60.

<i>f</i>	A	100	125	160	200	250	315	400	500	630	800	1000	1250	1600	2000	2500	3150	4000	5000
<i>A_{div}</i>	42.6	42.5	42.5	42.5	42.5	42.5	42.5	42.5	42.5	42.5	42.5	42.5	42.5	42.5	42.5	42.5	42.5	42.5	
<i>A_{atm}</i>	0.3	0	0	0	0	0	0.1	0.1	0.1	0.1	0.1	0.2	0.2	0.2	0.3	0.5	0.7	1	1.5
<i>A_{sot}</i>	0.1	0	0	0	0	0	0	0	0	0	0	0	0	0	0	0	0	0	
<i>A_{dif}</i>	8.6	3.8	4.3	4.9	5.4	5.9	6.3	6.7	7.1	7.4	7.8	8.2	8.9	9.7	10.5	11.4	12.3	13.5	14.4

Table I.57: Attenuations en downward-refraction conditions for path (S1,R2).

<i>f</i>	A	100	125	160	200	250	315	400	500	630	800	1000	1250	1600	2000	2500	3150	4000	5000
<i>L_w</i>	80	53.1	54.1	56.1	59.1	61.1	64.1	66.1	69.1	69.1	72.1	73.1	72.1	70.1	67.1	64.1	62.1	59.1	57.1
A	51.9	46.2	46.8	47.5	48.1	48.7	49.3	49.9	50.4	50.8	51	51.2	51.7	52.6	53.5	54.4	55.5	56.8	58.2
<i>L_{eq}</i>	28.8	6.9	7.3	8.7	11	12.4	14.8	16.2	18.7	18.3	21.1	22	20.5	17.5	13.7	9.7	6.6	2.4	-1

Table I.58: Levels in homogeneous conditions for path (S1,R2).

<i>f</i>	A	100	125	160	200	250	315	400	500	630	800	1000	1250	1600	2000	2500	3150	4000	5000
<i>L_w</i>	80	53.1	54.1	56.1	59.1	61.1	64.1	66.1	69.1	69.1	72.1	73.1	72.1	70.1	67.1	64.1	62.1	59.1	57.1
A	51.6	46.3	46.8	47.4	48	48.4	48.9	49.3	49.7	50	50.4	50.8	51.6	52.5	53.4	54.3	55.5	57	58.4
<i>L_{eq}</i>	29.2	6.8	7.3	8.7	11.2	12.7	15.2	16.8	19.5	19.1	21.7	22.3	20.5	17.6	13.7	9.8	6.7	2.1	-1.3

Table I.59: Levels in downward-refraction conditions for path (S1,R2).

<i>f</i>	A	100	125	160	200	250	315	400	500	630	800	1000	1250	1600	2000	2500	3150	4000	5000
<i>L_{eq,LT}</i>	28.9	6.9	7.3	8.7	11.1	12.5	14.9	16.4	19	18.6	21.2	22	20.5	17.6	13.7	9.7	6.6	2.3	-1.1

Table I.60: Long-term sound levels for path (S1,R2).

I.2.4 - Path (S2,R2)

Ignored: path length larger than $\max(10^*d_{min}, 200)$ m.

I.2.5 - Path (S1,R3)

Table I.61 gives the probabilities of occurrence of downward-refraction conditions.

Orientation SR	Sector	Day	Night
40°	40°	0.28	0.85

Table I.61: Occurrences of downward-refraction conditions for path (S1,R3).

I.2.5.1 - Path geometry

SR distance : 396.601 m

The polyline associated to this path is defined in Table I.62.

x (m)	3.5	15.5	400
y (m)	1500	1500	1500
z (m)	0.05	4	9
z ground (m)	0	4	4

Table I.62: Path polyline (S1,R3).

I.2.5.2 - Homogeneous conditions

Single diffraction: computation of A_{dif}

- direct sight: NO
- edge of diffraction : [15.5;1500;4]
- δ : 0.565 m

The component of A_{dif} are detailed in Table I.63.

f	100	125	160	200	250	315	400	500	630	800	1000	1250	1600	2000	2500	3150	4000	5000
Δ_{dif}	9.8	10.5	11.3	12.1	12.9	13.8	14.7	15.6	16.5	17.5	18.4	19.3	20.4	21.3	22.3	23.3	24.3	25
$\Delta_{sol(S,O)}$	-	-	-	-	-	0.2	0	-	-	-	-1.6	-1.9	-1.9	-1.9	-1.9	-1.9	-1.9	-1.9
$\Delta_{sol(O,R)}$	1.6	1.3	0.9	0.6	0.4	-	-	0.1	0.3	0.8	-	-	-	-	-	-	-	-
$A_{sol(S,O)}$	0	0	0	1.1	4.5	7.1	8.6	9.8	11.1	12.1	12.8	13.6	14.4	15	15.6	16.2	16.7	17.2
$\Delta_{talus(S,O)}$	-	-	-	-	-	-	-	-	-	-	-2.2	-2.6	-2.6	-2.6	-2.6	-2.6	-2.6	-2.6
$A_{sol(O,R)}$	2.1	1.7	1.3	0.9	0.5	0.2	0.1	0.1	0.5	1.2	-	-	-	-	-	-	-	-
$\Delta_{talus(O,R)}$	0.3	0.3	0.3	0.3	0.3	0.3	0.3	0.3	0.3	0.3	-0.3	-0.3	-0.3	-0.3	-0.3	-0.3	-0.3	-0.3

Table I.63: Component of A_{dif} for path (S1,R3).

The attenuations in homogeneous conditions are provided in Table I.64.

I.2.5.3 - Downward-refraction conditions

Single diffraction: computation of A_{dif}

- direct sight: NO
- edge of diffraction : [15.5;1500;4]
- δ : 0.542 m

f	A	100	125	160	200	250	315	400	500	630	800	1000	1250	1600	2000	2500	3150	4000	5000
A_{div}	63.1	63	63	63	63	63	63	63	63	63	63	63	63	63	63	63	63	63	
A_{atm}	1.9	0.1	0.2	0.2	0.3	0.4	0.6	0.8	0.9	1.1	1.3	1.6	2	2.6	3.5	4.8	7	10.5	15.8
A_{sol}	0.1	0	0	0	0	0	0	0	0	0	0	0	0	0	0	0	0	0	
A_{dif}	27.4	7.9	8.9	10.1	12.3	16.8	20.5	23	25.1	27	28.5	29.4	30.7	32.6	34.2	35.7	37.3	38.9	40

Table I.64: Attenuations en homogeneous conditions for path (S1,R3).

f	100	125	160	200	250	315	400	500	630	800	1000	1250	1600	2000	2500	3150	4000	5000
Δ_{dif}	9.7	10.4	11.2	12	12.8	13.6	14.5	15.4	16.4	17.3	18.2	19.2	20.2	21.2	22.1	23.1	24.1	25
$\Delta_{sol(S,O)}$	-	-	-	-	-	-	-	-	-	-	-1.9	-1.9	-1.9	-1.9	-1.9	-1.9	-1.9	-1.9
$\Delta_{sol(O,R)}$	0	0	0	0	0	0	0	0	2.7	4.2	3.6	1.7	0	0	0	0	0	0
$A_{sol(S,O)}$	-2	-	-	-1	-	-	-	-	-	-	-2.6	-2.6	-2.6	-2.6	-2.6	-2.6	-2.6	-2.6
$\Delta_{talus(S,O)}$	0.3	0.3	0.3	0.3	0.3	0.3	0.3	0.3	0.3	0.3	-0.3	-0.3	-0.3	-0.3	-0.3	-0.3	-0.3	-0.3

Table I.65: Component of A_{dif} for path (S1,R3).

The component of A_{dif} are detailed in Table I.65.

The attenuations in downward-refraction conditions are provided in Table I.66.

f	A	100	125	160	200	250	315	400	500	630	800	1000	1250	1600	2000	2500	3150	4000	5000
A_{div}	63.1	63	63	63	63	63	63	63	63	63	63	63	63	63	63	63	63	63	
A_{atm}	1.9	0.1	0.2	0.2	0.3	0.4	0.6	0.8	0.9	1.1	1.3	1.6	2	2.6	3.5	4.8	7	10.5	15.8
A_{sol}	0.1	0	0	0	0	0	0	0	0	0	0	0	0	0	0	0	0	0	
A_{dif}	17.5	7.9	8.9	10	11	11.9	12.8	13.6	14.3	17.6	19.7	19.7	18.7	18.1	19	20	20.9	22	22.9

Table I.66: Attenuations en downward-refraction conditions for path (S1,R3).

I.2.5.4 - Sound levels

The sound levels in homogeneous conditions are given in Table I.67, in downward-refraction conditions in Table I.68, the long-term sound levels in Table I.69.

I.2.6 - Path (S2,R3)

Table I.70 gives the probabilities of occurrence of downward-refraction conditions.

I.2.6.1 - Path geometry

SR distance : 1503.261 m

The polyline associated to this path is defined in Table I.71.

I.2.6.2 - Homogeneous conditions

Single diffraction: computation of A_{dif}

- direct sight: NO
- edge of diffraction : [15.5;2906.116;4]
- δ : 0.153 m

The component of A_{dif} are detailed in Table I.72.

$\Delta_{talus(S,O)}$: no embankment slope detected.

The attenuations in homogeneous conditions are provided in Table I.73.

I.2.6.3 - Downward-refraction conditions

Single diffraction: computation of A_{dif}

<i>f</i>	A	100	125	160	200	250	315	400	500	630	800	1000	1250	1600	2000	2500	3150	4000	5000
<i>L_w</i>	80	53.1	54.1	56.1	59.1	61.1	64.1	66.1	69.1	69.1	72.1	73.1	72.1	70.1	67.1	64.1	62.1	59.1	57.1
A	92.5	71	72	73.3	75.6	80.2	84	86.7	89	91.1	92.8	94	95.7	98.1	101	104	107	112	119
<i>L_{eq}</i>	-	-	-	-	-	-	-	-	-	-	-	-	-	-28	-	-	-	-	-
	8.4	17.9	17.9	17.2	16.5	19.1	19.9	20.6	19.8	22	20.6	20.9	23.6	33.5	39.4	45.2	53.2	61.7	

Table I.67: Levels in homogeneous conditions for path (S1,R3).

<i>f</i>	A	100	125	160	200	250	315	400	500	630	800	1000	1250	1600	2000	2500	3150	4000	5000
<i>L_w</i>	80	53.1	54.1	56.1	59.1	61.1	64.1	66.1	69.1	69.1	72.1	73.1	72.1	70.1	67.1	64.1	62.1	59.1	57.1
A	82.6	71	72	73.2	74.2	75.3	76.3	77.3	78.2	81.7	84	84.3	83.7	83.6	85.4	87.8	90.9	95.4	102
<i>L_{eq}</i>	-	-	-	-	-	-	-	-	-	-	-	-	-	-	-	-	-	-	
	1.5	17.8	17.9	17	15.1	14.2	12.2	11.2	9.1	12.6	11.9	11.2	11.6	13.5	18.3	23.6	28.8	36.3	44.5

Table I.68: Levels in downward-refraction conditions for path (S1,R3).

<i>f</i>	A	100	125	160	200	250	315	400	500	630	800	1000	1250	1600	2000	2500	3150	4000	5000
<i>L_{eq,LT}</i>	-	5.2	17.9	17.9	17.1	16.1	17.1	16.2	15.6	13.8	17	16.1	15.6	16.4	18.6	23.5	28.9	34.1	41.6

Table I.69: Long-term sound levels for path (S1,R3).

Orientation SR	Sector	Day	Night
114.7°	120°	0.28	0.92

Table I.70: Occurrences of downward-refraction conditions for path (S2,R3).

x (m)	3.5	15.5	400
y (m)	2950	2906.116	1500
z (m)	0.05	4	9
z ground (m)	0	4	4

Table I.71: Path polyline (S2,R3).

<i>f</i>	100	125	160	200	250	315	400	500	630	800	1000	1250	1600	2000	2500	3150	4000	5000
Δ_{dif}	6.8	7.2	7.7	8.2	8.8	9.4	10.1	10.8	11.6	12.4	13.2	14.1	15	15.9	16.8	17.8	18.8	19.7
$\Delta_{sol(S,O)}$	1.5	1.5	1.5	1.4	1.4	1.4	1.4	1.3	1.3	0.5	0.8	2.1	2.3	0.8	-1.3	-1.3	-1.3	-1.3
$\Delta_{sol(O,R)}$	0	1	6.2	11.8	16.1	17.8	18.3	18.6	18.8	19.1	19.4	19.7	20	20.2	20.4	20.6	20.8	20.9
$A_{sol(S,O)}$	-	-	-	-	-	-	-	-	-	-	1.2	3.3	3.7	1.2	-1.9	-1.9	-1.9	-1.9
	1.9	1.9	1.9	1.9	1.9	1.9	1.9	1.9	1.9	0.8								

Table I.72: Component of A_{dif} for path (S2,R3).

<i>f</i>	A	100	125	160	200	250	315	400	500	630	800	1000	1250	1600	2000	2500	3150	4000	5000
A_{div}	74.7	74.5	74.5	74.5	74.5	74.5	74.5	74.5	74.5	74.5	74.5	74.5	74.5	74.5	74.5	74.5	74.5	74.5	
A_{atm}	5.8	0.4	0.6	0.9	1.2	1.7	2.3	2.9	3.5	4.3	5.1	6.1	7.6	9.8	13.2	18.3	26.6	39.7	60
A_{sol}	0.1	0	0	0	0	0	0	0	0	0	0	0	0	0	0	0	0	0	0
A_{dif}	30.7	5.3	6.7	12.5	18.6	23.5	25.8	27	28	29.1	31	33.5	35.9	37.3	36.9	36	37.1	38.3	39.3

Table I.73: Attenuations en homogeneous conditions for path (S2,R3).

- direct sight: NO
- edge of diffraction : [15.5;2906.116;4]
- δ : 0.067 m

The component of A_{dif} are detailed in Table I.74.

f	100	125	160	200	250	315	400	500	630	800	1000	1250	1600	2000	2500	3150	4000	5000
Δ_{dif}	5.8	6	6.3	6.6	7	7.4	7.9	8.4	9	9.7	10.4	11.1	11.9	12.7	13.5	14.4	15.4	16.3
$\Delta_{sol(S,O)}$	-	-	-	-	-	-	-	-	-	1	1.7	1.5	-0.2	-1	-1	-1	-1	-1
$\Delta_{sol(O,R)}$	0	0	0	0	0	0	0	0	0	0	0	0	0	0	0	0	0	0
$A_{sol(S,O)}$	-	-	-	-	-	-	-	-	-	0.4	1.8	3.4	2.9	-0.3	-1.9	-1.9	-1.9	-1.9
$A_{sol(O,R)}$	1.9	1.9	1.9	1.9	1.9	1.9	1.9	1.8	1.8	1.8	1.8	1.8	1.8	1.8	1.8	1.8	1.8	1.8

Table I.74: Component of A_{dif} for path (S2,R3).

$\Delta_{talus(S,O)}$: no embankment slope detected.

The attenuations in downward-refraction conditions are provided in Table I.75.

f	A	100	125	160	200	250	315	400	500	630	800	1000	1250	1600	2000	2500	3150	4000	5000
A_{div}	74.7	74.5	74.5	74.5	74.5	74.5	74.5	74.5	74.5	74.5	74.5	74.5	74.5	74.5	74.5	74.5	74.5	74.5	
A_{atm}	5.8	0.4	0.6	0.9	1.2	1.7	2.3	2.9	3.5	4.3	5.1	6.1	7.6	9.8	13.2	18.3	26.6	39.7	60
A_{sol}	0.1	0	0	0	0	0	0	0	0	0	0	0	0	0	0	0	0	0	
A_{dif}	10.7	4.3	4.6	4.9	5.3	5.7	6.1	6.7	7.3	8.8	10.6	12.1	12.5	11.7	11.7	12.5	13.4	14.4	15.3

Table I.75: Attenuations en downward-refraction conditions for path (S2,R3).

I.2.6.4 - Sound levels

The sound levels in homogeneous conditions are given in Table I.76, in downward-refraction conditions in Table I.77, the long-term sound levels in Table I.78.

f	A	100	125	160	200	250	315	400	500	630	800	1000	1250	1600	2000	2500	3150	4000	5000
L_w	80	53.1	54.1	56.1	59.1	61.1	64.1	66.1	69.1	69.1	72.1	73.1	72.1	70.1	67.1	64.1	62.1	59.1	57.1
A	111	80.2	81.8	87.9	94.3	99.7	103	104	106	108	111	114	118	122	125	129	138	152	174
L_{eq}	-	-	-	-	-	-	-	-	-	-	-	-41	-	-	-	-	-	-	
	22.5	27.1	27.7	31.7	35.2	38.6	38.5	38.3	37	38.8	38.5	45.9	51.5	57.5	64.7	76.1	93.4	116.7	

Table I.76: Levels in homogeneous conditions for path (S2,R3).

I.3-Site in fill with low screen

The site in fill represented in Figure I.4 is now considered. The top view is not necessary here as only the propagation in the cut plane is studied. A screen 0.80 m high is placed at the edge of the platform. The lane axis defines a 10° angle in relation to North (\vec{N}, \vec{Oy}).

f	A	100	125	160	200	250	315	400	500	630	800	1000	1250	1600	2000	2500	3150	4000	5000
L_w	80	53.1	54.1	56.1	59.1	61.1	64.1	66.1	69.1	69.1	72.1	73.1	72.1	70.1	67.1	64.1	62.1	59.1	57.1
A	91.3	79.2	79.7	80.3	81	81.9	83	84.1	85.4	87.6	90.3	92.7	94.7	96.1	99.4	105	115	129	150
L_{eq}	-9	-	-	-	-	-	-	-	-	-	-	-	-26	-	-	-	-	-	-92.7

Table I.77: Levels in downward-refraction conditions for path (S2,R3).

f	A	100	125	160	200	250	315	400	500	630	800	1000	1250	1600	2000	2500	3150	4000	5000
$L_{eq,LT}$	-	-	-	-	-	-	-	-	-	-	-	-	-28	-	-	-	-75	-	
		14.1	26.8	27	28.1	27	26.1	24.2	23.4	21.7	23.9	23.6	25.1	31.5	37.8	46.8	57.9	98.2	

Table I.78: Long-term sound levels for path (S2,R3).

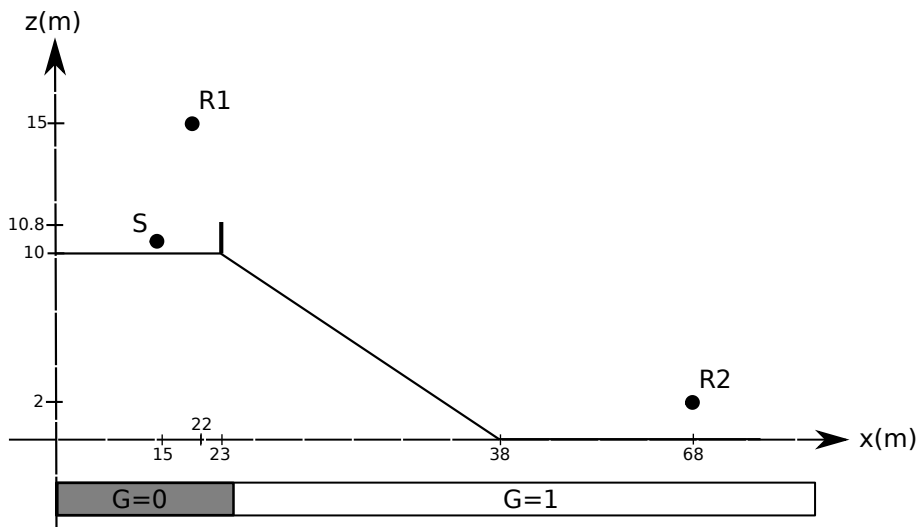


Figure I.4: Vertical section of the site in fill.

I.3.1 - Path (S,R1)

Table I.79 gives the probabilities of occurrence of downward-refraction conditions.

Orientation SR	Sector	Day	Night
280°	280°	0.32	0.96

Table I.79: Occurrences of downward-refraction conditions for path (S,R1).

I.3.1.1 - Path geometry

SR distance : 8.573 m

The polyline associated to this path is defined in Table I.80.

I.3.1.2 - Homogeneous conditions

Direct sight: computation of A_{sol}

The related mean ground plane is given in Table I.81.

Ground absorption :

- $G_{trajet} : 0$
- $G'_{trajet} : 0$

x (m)	15	22
y (m)	50	50
z (m)	10.05	15
z ground (m)	10	10

Table I.80: Path polyline (S,R1).

z_s (m)	d_p (m)	z_r (m)
0.05	7	5

Table I.81: Mean ground plane for path (S,R1).

A_{talus} : no embankment slope detected.

The attenuations in homogeneous conditions are provided in Table I.82.

f	A	100	125	160	200	250	315	400	500	630	800	1000	1250	1600	2000	2500	3150	4000	5000
A_{div}	29.8	29.7	29.7	29.7	29.7	29.7	29.7	29.7	29.7	29.7	29.7	29.7	29.7	29.7	29.7	29.7	29.7	29.7	
A_{atm}	0.2	0	0	0	0	0	0	0	0	0	0	0	0	0.1	0.1	0.1	0.2	0.3	
A_{sol}	- 2.8	-3	-3	-3	-3	-3	-3	-3	-3	-3	-3	-3	-3	-3	-3	-3	-3	-3	
A_{dif}	0.1	0	0	0	0	0	0	0	0	0	0	0	0	0	0	0	0	0	

Table I.82: Attenuations en homogeneous conditions for path (S,R1).

I.3.1.3 - Downward-refraction conditions

Direct sight: computation of A_{sol}

The related mean ground plane is given in Table I.83.

Ground absorption :

- G_{trajet} : 0
- G'_{trajet} : 0

A_{talus} : no embankment slope detected.

The attenuations in downward-refraction conditions are provided in Table I.84.

I.3.1.4 - Sound levels

The sound levels in homogeneous conditions are given in Table I.85, in downward-refraction conditions in Table I.86, the long-term sound levels in Table I.87.

I.3.2 - Path (S,R2)

Table I.88 gives the probabilities of occurrence of downward-refraction conditions.

I.3.2.1 - Path geometry

SR distance : 53.608 m

The polyline associated to this path is defined in Table I.89.

I.3.2.2 - Homogeneous conditions

Single diffraction: computation of A_{dif}

- direct sight: NO
- edge of diffraction : [23;50;10.8]

z_s (m)	d_p (m)	z_r (m)
0.06	7	5.01

Table I.83: Mean ground plane for path (S,R1).

f	A	100	125	160	200	250	315	400	500	630	800	1000	1250	1600	2000	2500	3150	4000	5000
A_{div}	29.8	29.7	29.7	29.7	29.7	29.7	29.7	29.7	29.7	29.7	29.7	29.7	29.7	29.7	29.7	29.7	29.7	29.7	
A_{atm}	0.2	0	0	0	0	0	0	0	0	0	0	0	0	0.1	0.1	0.1	0.2	0.2	0.3
A_{sol}	- 2.8	-3	-3	-3	-3	-3	-3	-3	-3	-3	-3	-3	-3	-3	-3	-3	-3	-3	
A_{dif}	0.1	0	0	0	0	0	0	0	0	0	0	0	0	0	0	0	0	0	

Table I.84: Attenuations en downward-refraction conditions for path (S,R1).

f	A	100	125	160	200	250	315	400	500	630	800	1000	1250	1600	2000	2500	3150	4000	5000
L_w	80	53.1	54.1	56.1	59.1	61.1	64.1	66.1	69.1	69.1	72.1	73.1	72.1	70.1	67.1	64.1	62.1	59.1	57.1
A	27.3	26.7	26.7	26.7	26.7	26.7	26.7	26.7	26.7	26.7	26.7	26.7	26.7	26.7	26.7	26.8	26.8	26.9	27
L_{eq}	53.3	26.5	27.5	29.4	32.4	34.4	37.4	39.4	42.4	42.4	45.4	46.4	45.4	43.4	40.4	37.3	35.3	32.2	30.1

Table I.85: Levels in homogeneous conditions for path (S,R1).

f	A	100	125	160	200	250	315	400	500	630	800	1000	1250	1600	2000	2500	3150	4000	5000
L_w	80	53.1	54.1	56.1	59.1	61.1	64.1	66.1	69.1	69.1	72.1	73.1	72.1	70.1	67.1	64.1	62.1	59.1	57.1
A	27.3	26.7	26.7	26.7	26.7	26.7	26.7	26.7	26.7	26.7	26.7	26.7	26.7	26.7	26.8	26.8	26.9	27	
L_{eq}	53.3	26.5	27.5	29.4	32.4	34.4	37.4	39.4	42.4	42.4	45.4	46.4	45.4	43.4	40.4	37.3	35.3	32.2	30.1

Table I.86: Levels in downward-refraction conditions for path (S,R1).

f	A	100	125	160	200	250	315	400	500	630	800	1000	1250	1600	2000	2500	3150	4000	5000
$L_{eq,LT}$	53.3	26.5	27.5	29.4	32.4	34.4	37.4	39.4	42.4	42.4	45.4	46.4	45.4	43.4	40.4	37.3	35.3	32.2	30.1

Table I.87: Long-term sound levels for path (S,R1).

Orientation SR	Sector	Day	Night
280°	280°	0.32	0.96

Table I.88: Occurrences of downward-refraction conditions for path (S,R2).

x (m)	15	23	68
y (m)	50	50	50
z (m)	10.05	10.8	2
z ground (m)	10	10	0

Table I.89: Path polyline (S,R2).

- δ : 0.28 m

The component of A_{dif} are detailed in Table I.90.

f	100	125	160	200	250	315	400	500	630	800	1000	1250	1600	2000	2500	3150	4000	5000
Δ_{dif}	8	8.5	9.2	9.8	10.5	11.3	12.1	12.9	13.8	14.7	15.6	16.4	17.5	18.4	19.3	20.3	21.3	22.2
$\Delta_{sol(S,O)}$	-	-	-	-	-	-	-	-	-	-2.9	-2.9	-2.9	-2.9	-2.9	-2.9	-2.9	-2.9	-2.9
$\Delta_{sol(O,R)}$	2.9	2.9	2.9	2.9	2.9	2.9	2.9	2.9	2.9	0	0	0	0	0	0	0	0	0
$A_{sol(S,O)}$	0	0	0	0	0	0	0	0	0	0	0	0	0	0	0	0	0	0
$A_{sol(O,R)}$	-3	-3	-3	-3	-3	-3	-3	-3	-3	-3	-3	-3	-3	-3	-3	-3	-3	-3

Table I.90: Component of A_{dif} for path (S,R2).

$\Delta_{talus}(S,O)$: no embankment slope detected.

The attenuations in homogeneous conditions are provided in Table I.91.

f	A	100	125	160	200	250	315	400	500	630	800	1000	1250	1600	2000	2500	3150	4000	5000
A_{div}	45.7	45.6	45.6	45.6	45.6	45.6	45.6	45.6	45.6	45.6	45.6	45.6	45.6	45.6	45.6	45.6	45.6	45.6	
A_{atm}	0.4	0	0	0	0	0.1	0.1	0.1	0.1	0.2	0.2	0.2	0.3	0.3	0.5	0.7	0.9	1.4	2.1
A_{sol}	0.1	0	0	0	0	0	0	0	0	0	0	0	0	0	0	0	0	0	
A_{dif}	12.3	5	5.6	6.2	6.9	7.6	8.3	9.2	10	10.8	11.8	12.6	13.5	14.6	15.5	16.4	17.4	18.4	19.3

Table I.91: Attenuations en homogeneous conditions for path (S,R2).

I.3.2.3 - Downward-refraction conditions

Single diffraction: computation of A_{dif}

- direct sight: NO
- edge of diffraction : [23;50;10.8]
- δ : 0.277 m

The component of A_{dif} are detailed in Table I.92.

f	100	125	160	200	250	315	400	500	630	800	1000	1250	1600	2000	2500	3150	4000	5000
Δ_{dif}	8	8.5	9.1	9.8	10.5	11.2	12.1	12.9	13.7	14.6	15.5	16.4	17.4	18.3	19.3	20.2	21.3	22.2
$\Delta_{sol(S,O)}$	-	-	-	-	-	-	-	-	-	-2.9	-2.9	-2.9	-2.9	-2.9	-2.9	-2.9	-2.9	-2.9
$\Delta_{sol(O,R)}$	2.9	2.9	2.9	2.9	2.9	2.9	2.9	2.9	2.9	0	0	0	0	0	0	0	0	0
$A_{sol(S,O)}$	0	0	0	0	0	0	0	0	0	0	0	0	0	0	0	0	0	0
$A_{sol(O,R)}$	-3	-3	-3	-3	-3	-3	-3	-3	-3	-3	-3	-3	-3	-3	-3	-3	-3	-3

Table I.92: Component of A_{dif} for path (S,R2).

$\Delta_{talus}(S,O)$: no embankment slope detected.

The attenuations in downward-refraction conditions are provided in Table I.93.

I.3.2.4 - Sound levels

The sound levels in homogeneous conditions are given in Table I.94, in downward-refraction conditions in Table I.95, the long-term sound levels in Table I.96.

<i>f</i>	A	100	125	160	200	250	315	400	500	630	800	1000	1250	1600	2000	2500	3150	4000	5000
A_{div}	45.7	45.6	45.6	45.6	45.6	45.6	45.6	45.6	45.6	45.6	45.6	45.6	45.6	45.6	45.6	45.6	45.6	45.6	
A_{atm}	0.4	0	0	0	0	0.1	0.1	0.1	0.1	0.2	0.2	0.2	0.3	0.3	0.5	0.7	0.9	1.4	2.1
A_{sol}	0.1	0	0	0	0	0	0	0	0	0	0	0	0	0	0	0	0	0	
A_{dif}	12.3	5	5.6	6.2	6.9	7.6	8.3	9.1	9.9	10.8	11.7	12.6	13.5	14.5	15.4	16.4	17.3	18.4	19.3

Table I.93: Attenuations en downward-refraction conditions for path (S,R2).

<i>f</i>	A	100	125	160	200	250	315	400	500	630	800	1000	1250	1600	2000	2500	3150	4000	5000
L_w	80	53.1	54.1	56.1	59.1	61.1	64.1	66.1	69.1	69.1	72.1	73.1	72.1	70.1	67.1	64.1	62.1	59.1	57.1
A	58.5	50.6	51.2	51.9	52.5	53.2	54	54.9	55.7	56.6	57.5	58.5	59.4	60.5	61.5	62.6	63.9	65.4	67.1
L_{eq}	22.4	2.5	2.9	4.3	6.6	7.9	10.1	11.3	13.4	12.5	14.6	14.7	12.7	9.6	5.6	1.5	-1.8	-6.3	-10

Table I.94: Levels in homogeneous conditions for path (S,R2).

<i>f</i>	A	100	125	160	200	250	315	400	500	630	800	1000	1250	1600	2000	2500	3150	4000	5000
L_w	80	53.1	54.1	56.1	59.1	61.1	64.1	66.1	69.1	69.1	72.1	73.1	72.1	70.1	67.1	64.1	62.1	59.1	57.1
A	58.5	50.6	51.2	51.8	52.5	53.2	54	54.8	55.7	56.6	57.5	58.4	59.4	60.5	61.5	62.6	63.9	65.4	67
L_{eq}	22.4	2.5	3	4.3	6.6	7.9	10.1	11.3	13.5	12.6	14.6	14.7	12.8	9.7	5.6	1.5	-1.8	-6.2	-9.9

Table I.95: Levels in downward-refraction conditions for path (S,R2).

<i>f</i>	A	100	125	160	200	250	315	400	500	630	800	1000	1250	1600	2000	2500	3150	4000	5000
$L_{eq,LT}$	22.4	2.5	2.9	4.3	6.6	7.9	10.1	11.3	13.4	12.5	14.6	14.7	12.7	9.6	5.6	1.5	-1.8	-6.3	-9.9

Table I.96: Long-term sound levels for path (S,R2).

I.4 - Site with multiple diffraction

The last example in this appendix covers the site with multiple diffraction whose cross-section is represented in Figure I.5. The road pass through fill, 6 m above the natural land. The road platform is edged with a 4 m-high screen. Near the fill is an 8 m-high building, which is assumed to be sufficiently large according to $\vec{O}y$ that the contribution from side diffractions is negligible.

The lane axis defines a 100° angle in relation to North ($\vec{N}, \vec{O}y$).

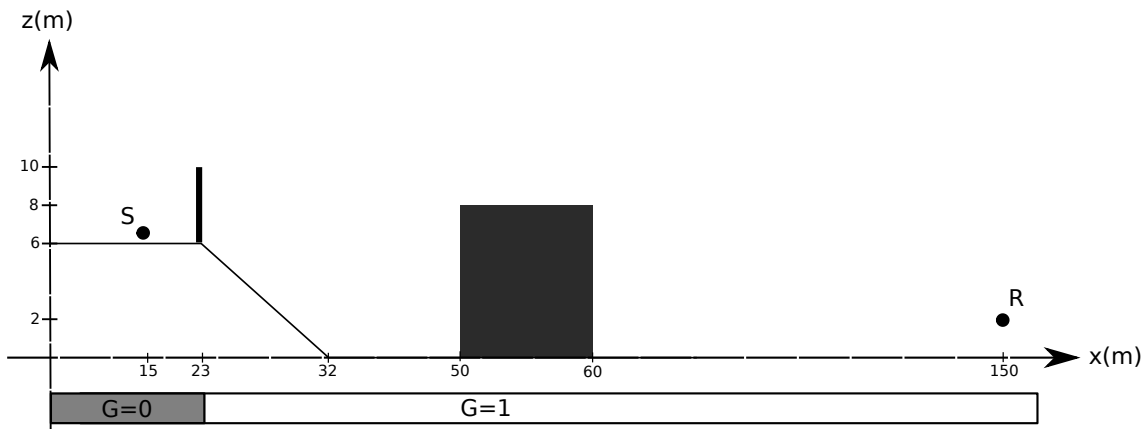


Figure I.5: Vertical section of the site with multiple diffraction.

Three edges on this site prevent the direct view between S and R . Only two are to be considered in accordance with the rule defined in Section 7.4.3. On the building, the roof edge closest to the road is not in the convex envelope between S and R .

I.4.1 - Path (S,R)

Table I.97 gives the probabilities of occurrence of downward-refraction conditions.

Orientation SR	Sector	Day	Night
100°	100°	0.27	0.92

Table I.97: Occurrences of downward-refraction conditions for path (S,R).

I.4.1.1 - Path geometry

SR distance : 135.061 m

The polyline associated to this path is defined in Table I.98.

x (m)	15	23	60	150
y (m)	50	50	50	50
z (m)	6.05	10	8	2
z ground (m)	6	6	8	0

Table I.98: Path polyline (S,R).

I.4.1.2 - Homogeneous conditions

Multiple diffraction: computation of A_{dif}

- direct sight: NO

- First edge of diffraction: [23;50;10]
- Last edge of diffraction: [60;50;8]
- δ : 1.115 m

The components of A_{dif} are detailed in Table I.99.

f	100	125	160	200	250	315	400	500	630	800	1000	1250	1600	2000	2500	3150	4000	5000
Δ_{dif}	15.1	16.3	17.6	18.7	19.8	20.9	21.9	22.9	23.9	25	25	25	25	25	25	25	25	25
$\Delta_{sol(S,O)}$	-3	-3	-2.9	2.9	2.9	2.9	2.9	2.9	2.9	-2.9	-2.9	-2.9	-2.9	-2.9	-2.9	-2.9	-2.9	-2.9
$\Delta_{sol(O,R)}$	0	0	0	0	0	0	0	0	0	0	0	0	0	0	0	0	0	0
$A_{sol(S,O)}$	-3	-3	-3	-3	-3	-3	-3	-3	-3	-3	-3	-3	-3	-3	-3	-3	-3	-3

Table I.99: Components of A_{dif} .

$\Delta_{talus(S,O)}$: no embankment slope detected.

The attenuations in homogeneous conditions are provided in Table I.100.

f	A	100	125	160	200	250	315	400	500	630	800	1000	1250	1600	2000	2500	3150	4000	5000
A_{div}	53.7	53.6	53.6	53.6	53.6	53.6	53.6	53.6	53.6	53.6	53.6	53.6	53.6	53.6	53.6	53.6	53.6	53.6	
A_{atm}	0.8	0	0.1	0.1	0.1	0.2	0.2	0.3	0.3	0.4	0.5	0.6	0.7	0.9	1.2	1.6	2.4	3.6	5.4
A_{sol}	0.1	0	0	0	0	0	0	0	0	0	0	0	0	0	0	0	0	0	
A_{dif}	21.5	12.1	13.4	14.7	15.8	16.8	17.9	19	20	21	22	22.1	22.1	22.1	22.1	22.1	22.1	22.1	

Table I.100: Attenuations en homogeneous conditions for path (S,R).

I.4.1.3 - Downward-refraction conditions

Multiple diffraction: computation of A_{dif}

- direct sight: NO
- First edge of diffraction: [23;50;10]
- Last edge of diffraction: [60;50;8]
- δ : 1.055 m

The components of A_{dif} are detailed in Table I.101.

f	100	125	160	200	250	315	400	500	630	800	1000	1250	1600	2000	2500	3150	4000	5000
Δ_{dif}	15	16.2	17.5	18.7	19.7	20.8	21.9	22.9	23.9	24.9	25	25	25	25	25	25	25	25
$\Delta_{sol(S,O)}$	-3	-3	-2.9	2.9	2.9	2.9	2.9	2.9	2.9	-2.9	-2.9	-2.9	-2.9	-2.9	-2.9	-2.9	-2.9	-2.9
$\Delta_{sol(O,R)}$	0	0	0	0	0	0	0	0	0	0	0	0	0	0	0	0	0	0
$A_{sol(S,O)}$	-3	-3	-3	-3	-3	-3	-3	-3	-3	-3	-3	-3	-3	-3	-3	-3	-3	-3

Table I.101: Components of A_{dif} .

$\Delta_{talus(S,O)}$: no embankment slope detected.

The attenuations in downward-refraction conditions are provided in Table I.102.

I.4.1.4 - Sound levels

The sound levels in homogeneous conditions are given in Table I.103, in downward-refraction conditions in Table I.104, the long-term sound levels in Table I.105.

<i>f</i>	A	100	125	160	200	250	315	400	500	630	800	1000	1250	1600	2000	2500	3150	4000	5000
A_{div}	53.7	53.6	53.6	53.6	53.6	53.6	53.6	53.6	53.6	53.6	53.6	53.6	53.6	53.6	53.6	53.6	53.6	53.6	
A_{atm}	0.8	0	0.1	0.1	0.1	0.2	0.2	0.3	0.3	0.4	0.5	0.6	0.7	0.9	1.2	1.6	2.4	3.6	5.4
A_{sol}	0.1	0	0	0	0	0	0	0	0	0	0	0	0	0	0	0	0	0	
A_{dif}	21.5	12.1	13.3	14.6	15.7	16.8	17.9	18.9	19.9	20.9	22	22.1	22.1	22.1	22.1	22.1	22.1	22.1	

Table I.102: Attenuations en downward-refraction conditions for path (S,R).

<i>f</i>	A	100	125	160	200	250	315	400	500	630	800	1000	1250	1600	2000	2500	3150	4000	5000
L_w	80	53.1	54.1	56.1	59.1	61.1	64.1	66.1	69.1	69.1	72.1	73.1	72.1	70.1	67.1	64.1	62.1	59.1	57.1
A	76.1	65.8	67	68.3	69.5	70.6	71.7	72.9	73.9	75	76.1	76.2	76.3	76.5	76.8	77.3	78.1	79.2	81.1
L_{eq}	4.8	-	-	-	-	-	-	-	-	-	-4	-3.1	-4.2	-6.4	-9.7	-	-	-	

Table I.103: Levels in homogeneous conditions for path (S,R).

<i>f</i>	A	100	125	160	200	250	315	400	500	630	800	1000	1250	1600	2000	2500	3150	4000	5000
L_w	80	53.1	54.1	56.1	59.1	61.1	64.1	66.1	69.1	69.1	72.1	73.1	72.1	70.1	67.1	64.1	62.1	59.1	57.1
A	76.1	65.7	67	68.3	69.4	70.5	71.7	72.8	73.9	74.9	76.1	76.2	76.3	76.5	76.8	77.3	78.1	79.2	81.1
L_{eq}	4.9	-	-	-	-	-	-	-	-	-	-3.1	-4.2	-6.4	-9.7	-	-	-	-	

Table I.104: Levels in downward-refraction conditions for path (S,R).

<i>f</i>	A	100	125	160	200	250	315	400	500	630	800	1000	1250	1600	2000	2500	3150	4000	5000
$L_{eq,LT}$	4.8	-	-	-	-	-	-	-	-	-	-4	-3.1	-4.2	-6.4	-9.7	-	-	-	

Table I.105: Long-term sound levels for path (S,R).

J-From the NMPB-Roads-96 to the NMPB-Roads-2008

Table J.1 summarises the changes introduced into the NMPB-Roads-2008 compared with the NMPB-Roads-96. The reader will find the justification for these changes in the bibliography.

Aspect	NMPB-Roads-96	NMPB-Roads-2008
Scope (altitude, site, etc.)	[[NMPB96],1 and 3.3.1]	Unchanged
Occurrences of downward refraction conditions	Quantitative UiTi grid [LRA1995]	Calculation of $Grad_c$ with the MAGRET software program (INRA) [LRS2008]
Resolution	Octaves (125-4000 Hz)	Third-octave (100-5000 Hz)
Source height	0.5 m	0.05 m [Gaulin2000]
Emission spectrum	Unique [EN1793p3]	Drainage/Non-drainage [Abaques 2008]
Discretisation	[[NMPB96],5.1.3]	Restrictive writing. Several cases for equiangular discretisation [LRS2007]
Minimum extent of the source line	Not specified	Distance ratios, the longest minimum length of the direct ray [CSTB2007]
Maximum path length	None	2,000 m [CSTB2007]
Ground factor G	0 or 1	Values of G based on the type of ground [Emb1997] deduced from the air flow resistivity σ by $G = \min((300/\sigma)^{0.57}, 1)$
Ground effect in downward-refraction conditions	Derived from [ISO9613p2]	Derived from $A_{sol,H}$ NMPB-Roads-96 [CSTB2002]
Embankment slope	Taken into account in the mean ground plane	A_{talus} or Δ_{talus} [CSTB2002]
A_{sol}/A_{dif} transition	Test at 500 Hz [[NMPB96],7.4]	Test for each third-octave band [LRS2005]
Taking low screens into account	No	Yes [CSTB2007]
Upper limit of Δ_{dif}	25 dB on horizontal edge [[NMPB96],7.4.2]	Only in Δ_{dif} figuring in the calculation of A_{dif} [SETRA07]
Path difference in downward-refraction conditions	Raising in line with diffraction edges [[NMPB96],7.4.3]	Calculation of the length of ray curves [SETRA04]
Standardisation of $A_{sol(S,O)}$	Possible in some cases [[NMPB96],7.4.4]	Possibility deleted

Table J.1: Summary of changes.

The NMPB-Roads-2008 is the French road noise prediction method leading on from the NMPB-Roads-1996. It is designed for both road project impact studies and for noise mapping in application of Directive 2002/49/EC.

This method takes into account the effect of micrometeorology on the propagation of sound. To achieve this, it stipulates for each source-receiver trajectory a sound level calculation in conditions favourable to sound propagation and a calculation in homogeneous conditions. The second calculation provides an upper bound for the sound level in unfavourable conditions. The sum of levels in favourable conditions and homogeneous conditions weighted by the probability of occurrence of favourable conditions and its supplement provide the long-term sound level.

This document is intended for both users (design offices, State departments) and software program publishers. It specifies the breakdown of a linear infrastructure into point sources, the micrometeorological characterisation of a site, the search for elementary trajectories and the calculation of the attenuation in an elementary trajectory. The probabilities of occurrence of favourable conditions are tabulated for 41 stations spread across France.

The NMPB-Roads-2008 is an in-depth revision of the initial method. Experience has shown that the NMPB-Roads-2008 improves the accuracy of the road noise prediction significantly. For the user, the revised method is far more perceptive both in its consideration of the topography and in the study of means of protecting against noise without a major increase in calculation times.

Service d'études sur les transports, les routes et leurs aménagements
46 avenue Aristide Briand – BP 100 – 92225 Bagneux Cedex – France
téléphone : 33(0)1 46 31 53 – télécopie : 33 (0)1 46 11 33 55

This document can be consulted at, and downloaded from, the Sétra website:
• <http://www.setra.developpement-durable.gouv.fr/>

Reference : 0957-2A
Sétra authorisation is strictly required for even partial reproduction of this document.
© 2009 Sétra – N° ISRN : EQ-SETRA-09-ED32-FR+ENG

Le Sétra appartient
au Réseau Scientifique
et Technique
du MEEDDM

